NASA/TP—2011–216456

Design of Refractory Metal Heat Pipe Life Test Environment Chamber, Cooling System, and Radio Frequency Heating System

J.J. Martin, S.M. Bragg-Sitton, R.S. Reid, E.T. Stewart, and J.D. Davis
Marshall Space Flight Center, Marshall Space Flight Center, Alabama

February 2011

The NASA STI Program…in Profile

Since its founding, NASA has been dedicated to the advancement of aeronautics and space science. The NASA Scientific and Technical Information (STI) Program Office plays a key part in helping NASA maintain this important role.

The NASA STI Program Office is operated by Langley Research Center, the lead center for NASA's scientific and technical information. The NASA STI Program Office provides access to the NASA STI Database, the largest collection of aeronautical and space science STI in the world. The Program Office is also NASA's institutional mechanism for disseminating the results of its research and development activities. These results are published by NASA in the NASA STI Report Series, which includes the following report types:

- TECHNICAL PUBLICATION. Reports of completed research or a major significant phase of research that present the results of NASA programs and include extensive data or theoretical analysis. Includes compilations of significant scientific and technical data and information deemed to be of continuing reference value. NASA's counterpart of peer-reviewed formal professional papers but has less stringent limitations on manuscript length and extent of graphic presentations.

- TECHNICAL MEMORANDUM. Scientific and technical findings that are preliminary or of specialized interest, e.g., quick release reports, working papers, and bibliographies that contain minimal annotation. Does not contain extensive analysis.

- CONTRACTOR REPORT. Scientific and technical findings by NASA-sponsored contractors and grantees.

- CONFERENCE PUBLICATION. Collected papers from scientific and technical conferences, symposia, seminars, or other meetings sponsored or cosponsored by NASA.

- SPECIAL PUBLICATION. Scientific, technical, or historical information from NASA programs, projects, and mission, often concerned with subjects having substantial public interest.

- TECHNICAL TRANSLATION. English-language translations of foreign scientific and technical material pertinent to NASA's mission.

Specialized services that complement the STI Program Office's diverse offerings include creating custom thesauri, building customized databases, organizing and publishing research results…even providing videos.

For more information about the NASA STI Program Office, see the following:

- Access the NASA STI program home page at <http://www.sti.nasa.gov>

- E-mail your question via the Internet to <help@sti.nasa.gov>

- Fax your question to the NASA STI Help Desk at 443–757–5803

- Phone the NASA STI Help Desk at 443–757–5802

- Write to:
  NASA STI Help Desk
  NASA Center for AeroSpace Information
  7115 Standard Drive
  Hanover, MD 21076–1320

NASA/TP—2011–216456

Design of Refractory Metal Heat Pipe Life Test Environment Chamber, Cooling System, and Radio Frequency Heating System

J.J. Martin, S.M. Bragg-Sitton, R.S. Reid, E.T. Stewart, and J.D. Davis
Marshall Space Flight Center, Marshall Space Flight Center, Alabama

National Aeronautics and
Space Administration

Marshall Space Flight Center • MSFC, Alabama 35812

February 2011

TRADEMARKS

Available from:

NASA Center for AeroSpace Information
7115 Standard Drive
Hanover, MD 21076–1320
443–757–5802

This report is also available in electronic form at
<https://www2.sti.nasa.gov>

TABLE OF CONTENTS

1. INTRODUCTION 1

2. ENVIRONMENTAL TEST CHAMBERS 3

2.1 General Layout and Components 3
2.2 Engineering Design 6
2.3 General Procurement Specifications 6

3. WATER COOLING 8

3.1 General Requirements Layout Description: Calorimeter Assemblies 8
3.2 Coolant Water Quality 9
3.3 Sizing and Performance 12
3.4 General Fill and Test Procedures 19
3.5 General Procurement Specifications 23

4. RADIO FREQUENCY HEATING SYSTEM 24

4.1 General Heat Pipe Test Arrangement 24
4.2 General Inductive Coil Geometry 26
4.3 Inductive Coil Sizing and Performance Parameters 28
4.4 Overall Radio Frequency Power System Layout 38
4.5 General Procurement Specifications 40

5. PURIFIED INERT GAS CONDITIONING SYSTEM 42

5.1 Sizing and Performance 42
5.2 General Procurement Specifications 56

6. INSTRUMENTATION 58

6.1 Data Acquisition and Control Methodology 58
6.2 Instrumentation Components and Procurement Specifications 61
6.3 Data Quality 65

7. SUMMARY 67

APPENDIX A—ENVIRONMENTAL TEST CHAMBER ENGINEERING DRAWINGS 68

TABLE OF CONTENTS (Continued)

APPENDIX B—HEAT PIPE CLUSTER SUPPORT ENGINEERING DRAWINGS 71

APPENDIX C—CALORIMETER ENGINEERING DRAWINGS 74

APPENDIX D—ENVIRONMENTAL TEST CHAMBER PROCUREMENTS 76

APPENDIX E—CALORIMETER COOLING SUBSYSTEM PROCUREMENTS 77

APPENDIX F—RADIO FREQUENCY INDUCTIVE COIL THERMAL LOAD WORKSHEET 78

APPENDIX G—MOLYBDENUM-RHENIUM AND SODIUM RESISTIVITY PROPERTIES 80

APPENDIX H—RADIO FREQUENCY INDUCTIVE COIL ONE-DIMENSIONAL SIMULATION RESULTS 82

APPENDIX I— RADIO FREQUENCY INDUCTIVE COIL TWO-DIMENSIONAL SIMULATION RESULTS 84

APPENDIX J—RADIO FREQUENCY INDUCTIVE COIL ASSEMBLY DESIGN AND FABRICATION WITH ASSOCIATED BUSSWORK SPECIFICATIONS 85

J.1 Integrated Financial Management Program Procurement 85
J.2 Radio Frequency Coil and Network Specifications 86

APPENDIX K—GAS PURIFICATION SUBSYSTEM PROCUREMENTS 90

APPENDIX L—WATER-COOLING SUBSYSTEM INSTRUMENTATION 92

APPENDIX M—MASS AND VOLUMETRIC FLOW METERS FOR LOW-PRESSURE HELIUM/ARGON MIXTURES 95

M.1 Thermal Mass Flow-Type Meters 95
M.2 Laminar Volumetric-Type Flow Meters 96

APPENDIX N—TWO-BAND OPTICAL PYROMETER SPECIFICATIONS 97

APPENDIX O—VACUUM GAUGING SPECIFICATIONS 98

APPENDIX P— DISTRIBUTED FIELDPOINT INPUT/OUTPUT COMPONENT SPECIFICATIONS 99

REFERENCES 100

LIST OF FIGURES

1.	General configuration of large environmental test chambers	4
2.	Heat pipe and calorimeter mounting support structure	5
3.	Heat pipe and calorimeter attachment bracket	5
4.	General calorimeter water-cooling system layout (one calorimeter illustrated)	9
5.	Computed system pressure-flow curves for water-cooling system	18
6.	General test chamber layout showing the typical five-position RF coil cluster	25
7.	Sample RF inductive coil layout	27
8.	General test chamber section/RF inductive coil configuration	27
9.	Direct current breakdown voltages in pure He, Ar, and He-Ar mixtures (Paschen curves)	28
10.	Breakdown voltage range with a total operating pressure of 76 torr	29
11.	Radio frequency inductor to heat pipe geometry	30
12.	Heat pipe to RF inductive coil heat loss versus standoff distance (pressure = 76 torr)	31
13.	Radio frequency inductive coil cluster (five coils) power loss due to internal RF losses and thermal transport from heat pipe	32
14.	Radio frequency inductive coil cluster (five coils) required coolant water flow rate	33
15.	One-dimensional simulation results for inductive coil efficiency	34
16.	One-dimensional simulation results RF power supply output requirement (five coils)	35
17.	One-dimensional simulation results—coil assembly required voltage (five coils)	35
18.	Radio frequency coil with flux concentrator in open space	37
19.	Radio frequency coil without flux concentrator in open space	37

LIST OF FIGURES (Continued)

20. Radio frequency coil with flux concentrator; close to neighboring inductor 38

21. Radio frequency coil without flux concentrator; close to neighbor inductor 38

22. General RF power subsystem hardware layout 39

23. Oxygen concentration (ppmv) in the heat pipe test chambers following successive dilutions with (a) UHP He or (b) UHP Ar fill gas 43

24. Test chamber gas mixture and purification system 44

25. Final oxygen concentration in the heat pipe test chambers with UHP gas, purified using an inline SAES microtorr ambient gas purifier to 1 ppb O_2 prior to chamber inlet 45

26. Simplified test loop for pressure drop calculation 48

27. Residual gas analyzer sampling system 52

28. General data acquisition and control system subsystems 60

29. Test chamber assembly (three segments integrated) (Dwg. No. 90M11906) 68

30. Detail test chamber shell (Dwg. No. 90M11906) 69

31. Detail test chamber support structure (Dwg. No. 90M11906) 70

32. Heat pipe and calorimeter cluster attachment support and bracket assembly (Dwg. No. 90M11911) 71

33. Attachment support structure details (Dwg. No. 90M11911) 72

34. Heat pipe and calorimeter mounting bracket detail (Dwg. No. 90M11911) 73

35. Heat pipe calorimeter assembly (Dwg. No. 90M11898) 74

36. Calorimeter design detail (Dwg. No. 90M11898) 75

37. Electrical resistivity curves for Na and Mo-50%Re 81

38. General dimensional layout of a single RF inductive coil position 86

39. Direct current breakdown voltages in pure He, Ar, and mixtures (Paschen curves) 88

LIST OF TABLES

1. Baseline heat pipe life test matrix conditions 2

2. Water grades from the ASTM standard specification for reagent water 11

3. Comparisons for water and solutions of water and DOWTHERM 4000 (concentrations given in percent volume) for F(-4) (all properties assumed constant) 11

4. Flow element descriptions for the water-cooling system spreadsheet model 13

5. Key parameters for the calorimeter section spreadsheet model for test case F(-4) 14

6. Calculated pressure drops for each of the 16 heat pipe test cases 16

7. Key parameters for the calorimeter and supply section spreadsheet model 17

8. Proposed heat pipe life test matrix 24

9. Position of heat pipes within test chamber clusters 26

10. SAES monotorr phase II 3000 performance guarantee for rare gases 46

11. Loss coefficients for system pressure drop calculation 48

12. Approximate outgassing rates of stainless steel as reported in Roth 49

13. Approximate volume and mass of water vapor emanating from the three large test chamber surfaces per unit time 50

14. Thermocouple to pyrometer comparison 63

15. General hardware needed for fabrication of environmental test chambers 76

16. General hardware list for assembly of the heat pipe water-cooling subsystem 77

17. Heat transfer loss estimates between RF inductive coil and heat pipe surface 79

18. Sodium resistivity 80

19. Mo-50%Re resistivity 80

LIST OF TABLES (Continued)

20. Radio frequency inductive coil one-dimensional simulation results using one- and five-coil calculations 83

21. Radio frequency inductive coil two-dimensional simulation results using one- and five-coil calculations 84

22. Required RF power induced in the part without thermal losses 87

23. General hardware for gas purification subsystems (large/small chambers) 91

24. General instrumentation options for water-cooling system 92

25. Optical pyrometer specifications 97

26. Kurt J. Lesker multigauge box system with control boards 98

27. Vacuum pressure sensors for the multigauge box 98

28. FieldPoint I/O components 99

LIST OF ACRONYMS AND SYMBOLS

AI	aperture inlet
Ar	argon
ASME	American Society of Mechanical Engineers
ASTM	American Society for Testing and Materials
BPVC	Boiler and Pressure Vessel Code
CH_4	methane
CO	carbon monoxide
CO_2	carbon dioxide
CTI	capillary tube inlet
DC	direct current
DI	deionized
DO	dissolved oxygen
ELTA	Electro-Thermal Analysis (marketed by BNV Corp)
FP	FieldPoint
GFSSP	Generalized Fluid System Simulation Program
H_2	hydrogen
H_2O	water
HCI	high-conductance inlet
He	helium
IAPWS	International Association for the Properties of Water and Steam
ID	inside diameter
I/O	inlet/outlet
Mo	molybdenum
MSFC	Marshall Space Flight Center
N	nitrogen
N_2	nitrogen

LIST OF ACRONYMS AND SYMBOLS (Continued)

Na	sodium
NDE	nondestructive evaluation
NI	National Instruments
NIST	National Institute of Standards and Technology
O_2	oxygen
OD	outside diameter
PLC	programmable logic controller
Re	rhenium
RF	radio frequency
RGA	residual gas analyzer
RT	real time
RTC	real-time controller
SA	surface area
SS	stainless steel
TBD	to be determined
TC	thermocouple
TP	Technical Publication
UHP	ultra-high purity
UV	ultraviolet
VCR	type of metal seal

NOMENCLATURE

A	area
A_c	cross-sectional area normal to flow (m^2)
A_i	surface area inner wall (m^2)
A_o	surface area outer wall (m^2)
B	test chamber acceptable operating stress (psi)
c_p	specific heat (kJ/kg-K)
D	diameter of cooling system piping outlet manifold to inlet manifold (m)
D_o	test chamber diameter (in)
d	outer (larger) diameter of an annular gap (m)
d_h	hydraulic diameter (m)
d_i	inner (smaller) diameter of an annular gap (m)
d_o	outer (larger) diameter of an annular gap (m)
f	friction factor
f_T	friction factor in zone of complete turbulence
Gr	Grashof number
g	gravity (m/s^2)
H	height (m)
h	convective heat transfer coefficient
h_l	head loss (m^2/s^2)
I	current (amps)
ID	inside diameter (m)
I_{gap}	inductive coil as a function of the gap width
K	resistance coefficient – $K = fL/d_h$
k	effective thermal conductivity (W/m-K)
L	length (m)

NOMENCLATURE (Continued)

L_c	inductor length (cm)
L_e	equivalent length
$\dot{m}$	mass flow rate (kg/s)
$\dot{m}_{coolant}$	RF inductor system mass flow rate (kg/s)
$\dot{m}_{tot}$	total mass flow rate through the water cooling system (kg/s)
n	viscosity correction exponent
Nu	Nusselt number
P	pressure (MPa)
P_1	static pressure at the inlet
P_2	static pressure at the outlet
P_a	test chamber pressure (psi)
Pr	Prandtl number
p	pressure (Pa)
Q	flow rate (m^3/s)
$\dot{Q}_{cond}$	conductive heat transfer (W)
$\dot{Q}_{losses}$	total power absorbed by inductive coil (thermal and electrical) (W)
$\dot{Q}_{rad}$	radiation heat transfer (W)
$\dot{Q}_{total}$	total heat transfer (W)
q_D	outgassing rate (torr-l/s-cm^2)
Ra	Rayleigh number
Re	Reynolds number – $\mathrm{Re} = \rho V d_h / \mu$
Re^*	critical Reynolds number for annular friction factor correlation
r	radius of the restriction
T	temperature (K)
T_{in}	coolant inlet temperature (K)
T_{ind}	inductor temperature (K)
T_{out}	coolant outlet temperature (K)

NOMENCLATURE (Continued)

T_{hp}	heat pipe temperature (K)
T_s	surface temperature (K)
T_w	wall temperature (K)
T_∞	fluid temperature far from wall (K)
t	test chamber wall thickness (in)
V	volume (m^3); voltage
V_h	dynamic pressure – $V_h = \rho V^2/2$ (MPa)
$\bar{v}$	mean velocity of flow (m/s)
β	coefficient of expansion
ΔH	change in elevation (m)
ΔP	change in pressure (MPa)
Γ	viscosity ratio – $\Gamma = \mu_b/\mu_w$
ε	pipe diameter ratio – d_i/d_o; emissivity
ε_i	inner surface emissivity
ε_o	outer surface emissivity
μ	absolute (dynamic) viscosity (Pa-s or kg/m-s)
μ_b	absolute (dynamic) viscosity at the mean fluid bulk temperature (Pa-s or kg/m-s)
μ_w	absolute (dynamic) viscosity at the mean wall temp (Pa-s or kg/m-s)
ρ	density (kg/m^3)
σ	Stefan-Boltzmann constant (W/m^2-K^4)
η	absolute viscosity of the fluid (kg/m-s)
ψ	annular friction factor correction

TECHNICAL PUBLICATION

DESIGN OF REFRACTORY METAL HEAT PIPE LIFE TEST ENVIRONMENT CHAMBER, COOLING SYSTEM, AND RADIO FREQUENCY HEATING SYSTEM

1. INTRODUCTION

A proposed approach to evaluate molybdenum- (Mo-) 44.5% rhenium (Re) alloy/sodium (Na) heat pipes for life-limiting effects was reported by Martin et al.[1] The baseline test matrix includes 16 heat pipes (12 in long with a diameter of 5/8 in) operated at various power levels, temperatures, and durations. Tests are planned to proceed around the clock with removal, examination, and test resumption at 6-mo intervals. A combination of nondestructive and destructive evaluations will be made to determine aging effects within the heat pipe during removal. Heat pipe testing will include a series following the guidelines specified in American Society for Testing and Materials (ASTM) G68-80 (referred to as the G-series) in which all heat pipes will be operated at the same temperature and power but for variable operational exposure to control the total mass fluence.[2] A second set of tests based on a central composite structure test design will be evaluated to examine cross correlations between mass fluence, temperature, and power.[3] A summary of the baseline test conditions for this evaluation is provided in table 1. The required test conditions are achieved with a series of subsystems, including the following:

• Environmental test chambers—Provide containment and mounting support for the heat pipes; flooded with a purified inert gas atmosphere (helium (He)/argon (Ar) mixture).

• Gas conditioning—Provides an actively purified inert He/Ar mixture to conductively couple the heat pipe condenser and calorimeter by means of a gas gap.

• Radio frequency (RF) power/inductive coils—Provide a clean, noncontact and reliable method of imposing a well-defined mass transfer boundary at the heat pipe evaporator.

• Water cooling—Provides primary method for monitoring heat pipe throughput with a condenser-mounted calorimeter.

Typical operations and procedures to govern the expected use of the hardware subsystems have been outlined and will serve as a guide during buildup and checkout testing. It is expected that a number of checkout tests will be required to adequately verify that subsystems meet the design goals. These procedures and process descriptions represent a growing document that will be updated with findings accumulated throughout the project.

Table 1. Baseline heat pipe life test matrix conditions.

Test Identifier	Power Level (W)	Heat Pipe Temperature (K)	Gas Gap Mixture	Gas Gap Width (in)	Coolant Flow (gpm)	Coolant Delta Temperature (K)	Number of Heat Pipes
G-Series	3,000	1,273	He-32%Ar	0.025	0.61	18.8	7
F(-4)	5,000	1,273	He-6%Ar	0.025	0.77	24.6	1
F(-3)	1,000	1,273	He-32%Ar	0.103	0.11	35.2	1
F(-2)	3,000	1,373	He-32%Ar	0.031	0.56	21.1	1
F(-1)	3,000	1,173	He-32%Ar	0.021	0.65	17.6	1
F(0)	3,000	1,273	He-32%Ar	0.025	0.61	18.8	1
F(1)	2,000	1,223	He-32%Ar	0.037	0.54	13.9	1
F(2)	4,000	1,223	He-32%Ar	0.017	0.67	22.8	1
F(3)	2,000	1,323	He-32%Ar	0.046	0.50	15.2	1
F(4)	4,000	1,323	He-32%Ar	0.020	0.63	24.0	1

Budgetary limitations and material availability allow for comparatively few tests to study a few key variables. Tests would employ the best available processing procedures, incorporating contamination getters in each pipe. This approach would also provide margins typical of flight heat pipe designs. The heat pipe life test matrix considers a relevant range of operating temperatures and evaporator mass fluences. To avoid random introduction of external impurities, isolating boundary conditions will be imposed on the heat pipes. Life tests that compress operating time may approach boiling limits; therefore, initial performance tests would be required to determine the achievable compression. The proposed test series reflects constraints, yet permits the scope to be expanded in a modular fashion comensurate with changing design and material system requirements.

2. ENVIRONMENTAL TEST CHAMBERS

The evaluation of 16 heat pipes will require a series of environmental test chambers containing controlled purity, inert gas environments to provide sufficient thermal coupling between the heat pipe condenser sections, and water flow calorimeters. The high-purity gas is necessary to avoid random introduction of external contamination. Two types of environmental test chambers have been outlined to satisfy the test requirement. These include several large chambers, each containing a cluster of five heat pipe/calorimeter assemblies (arranged in a pentagonal configuration) and a small test chamber that contains a single, high-power heat pipe. The large test chambers require a more stringent design cycle due to their size (account for applied pressure loads); therefore, the primary design emphasis for this effort was directed toward the larger test chambers. The shell and flange arrangement on the smaller chamber will allow use of commercial off-the-shelf vacuum-rated items. To mount heat pipes and calorimeters, a common mounting bracket and support structure will be used in all test chambers. In general, commonality will be maintained (to the extent possible) with respect to the designs, selection of hardware items, and overall construction to allow flexibility in the final hardware setup.

2.1 General Layout and Components

To support operations anticipated over the course of this project, the environmental test chambers have been designed for flexible use (operated individually or integrated into a single unit). The final design is sized with sufficient internal volume to ease access for installation and maintenance and uses similar components in all test chambers for commonality. Figure 1 illustrates the general layout with two test chambers integrated into a single assembly and the third unit separated—all three share a common gas system. The chambers are constructed of stainless steel, which is well suited for operating in both vacuum and in low-pressure, high-purity internal environments. The large chambers will have a cylindrical barrel diameter of 24 in with a length of 36 in. The chamber diameter was set based on the largest commercial off-the-shelf metal seal flange available (27-in diameter). A number of penetrations provide access for RF power feeds, water coolant inlet/outlet (I/O) flow, vacuum source, purified circulation gas, thermocouples, and optical access for pyrometers. These penetrations will be a combination of 2- and 6-in-diameter tube half-nipples, sealed with knife-edge seal flanges (Conflat and VCR type).

The calorimeter water feed lines present a more challenging situation since the current baseline uses copper tubing. Two methods are available to seal these tubes at the test chamber stainless steel interface flange. The first requires a copper to stainless steel transition. (The use of mechanical fittings on the water lines inside the test chamber is to be avoided at all costs.) Initial investigations indicate that these transition pieces—produced by explosive bonding a sheet of stainless steel to a sheet of copper and then machining the required fittings—are commercially available. Unfortunately, they have an unacceptably high cost per fitting and vendors require a minimum purchase. The second alternative is to weld a stainless steel metal compression ring-type fitting to the chamber flange interface and to extend the calorimeter copper feed lines through these fittings. The compression fittings would then be tightened

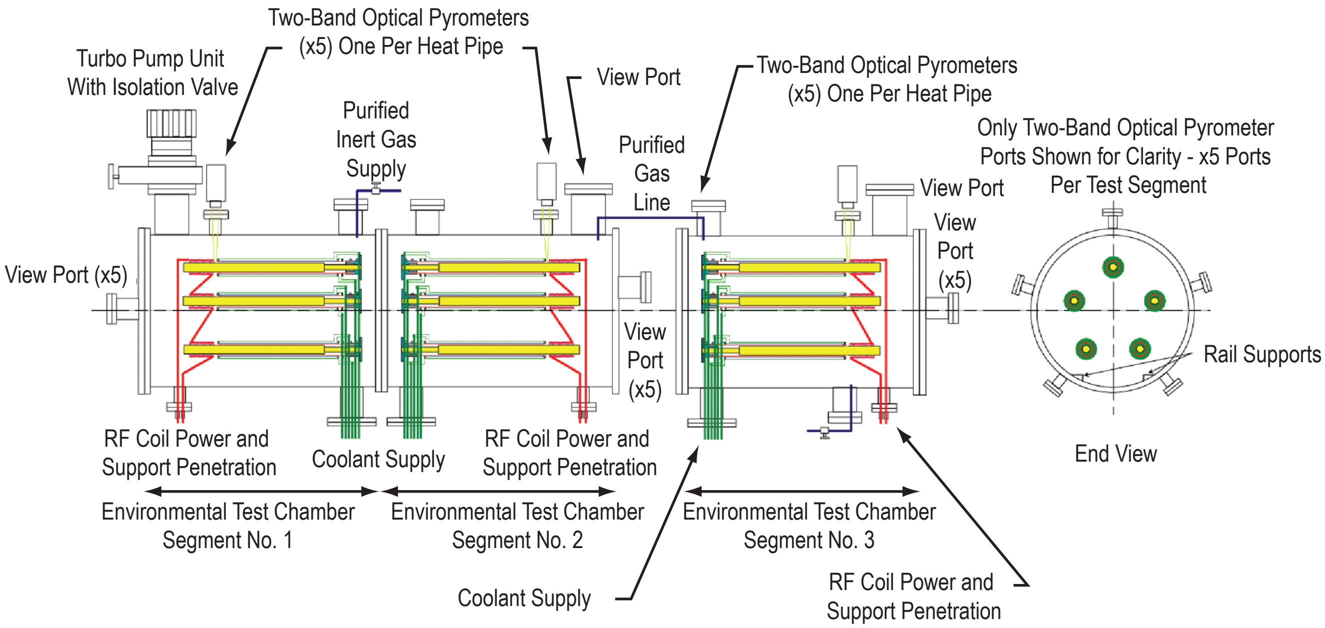

Figure 1. General configuration of large environmental test chambers.

on the outside of the chamber, biting into the copper feed line to provide a seal against atmospheric pressure. The copper calorimeter feed line that extends beyond the chamber-mounted compression fitting (external to the chamber) can now be hooked into the cooling water subsystem. Compression-type fittings are typically avoided for vacuum applications because it is difficult to maintain seal consistency; however, for this application, there are few cost-effective alternatives. Engineering drawings for the environmental test chamber and its support stand are provided in appendix A.

Mechanical support for the heat pipe and calorimeter clusters contained within the large test chambers is provided by a support structure and frame clamped to internal rails. These rails are drilled and tapped to provide a number of tie-down locations that allow freedom in positioning and alignment of the heat pipes. This support structure is illustrated in figure 2.

The calorimeter and heat pipe attachment bracket are attached to the internal support structure using a tight tolerance concentric arrangement as shown in figure 3. The central bore is machined slightly larger than the heat pipe support tube, allowing for insertion of an insulating material for final heat pipe centering. The insulator would allow continuity measurements to be made between the heat pipe and the calorimeter to monitor for the possibility of contact during testing. The use of an insulator, however, introduces a number of issues, such as potential contamination and a loss in dimension tolerance due to the difference in materials and ability to machine. Tight dimensional constraints are mandatory due to the small gas conduction gap separating the heat pipe and calorimeter. Before pursuing this option in earnest, a detailed examination will be performed to justify its need and to identify available alternatives. At present, a metallic insert can be placed at this location to allow the insulator to be incorporated later. In the baseline approach, the heat pipe is supported in cantilever fashion at the condenser end of the support tube (shown in fig. 3). If it becomes necessary to support the heat pipe from the evaporator end, due to alignment issues or potential vibration, an additional bracket can be mounted on the

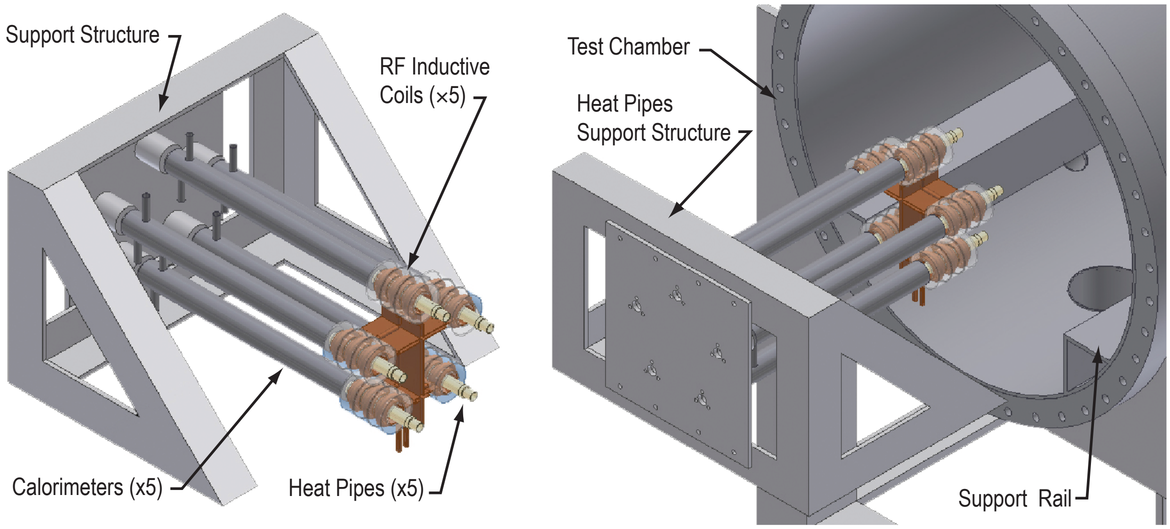

Figure 2. Heat pipe and calorimeter mounting support structure.

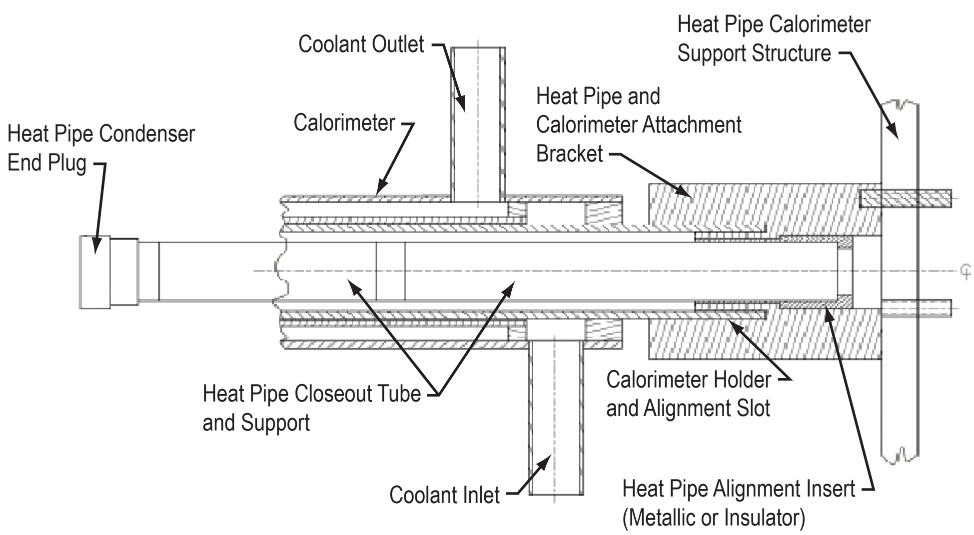

Figure 3. Heat pipe and calorimeter attachment bracket.

support structure's lower frame that makes contact on the evaporator end plug extension. The engineering drawings for the support structure/attachment bracket and calorimeters are provided in appendices B and C.

External test chamber cooling, if needed, would be provided by forced convection generated by high-velocity electric fans placed around the chambers. Even though there is significant power dissipated into each of the heat pipe clusters, the majority of this power is absorbed by the calorimeter and RF inductor water-cooling systems. In the final test configuration, very little of the active heat pipe surface is exposed to the test chamber walls. If the test chamber becomes unacceptably hot during test, copper tubing connected to the facility water system can be wrapped snugly around the chamber external wall, covering the affected areas. For flange surfaces, stainless steel tubing can be coiled around the desired region and tack welded in place to provide additional cooling.

2.2 Engineering Design

Large environmental test chamber designs are governed by the American Soiciety of Mechanical Engineers (ASME) Boiler and Pressure Vessel Code (BPVC).[4] ASME code applies for vacuum system applications since primary operation of the test chambers will be at significantly reduced pressure. The software used in producing engineering drawings is Microstation Version 7.0 (marketed by Bentley Systems). The vacuum chamber design is performed in accordance with the ASME BPVC, section VIII, division I, part UG-28 for thickness of shells and tubes under external pressure. The calculations performed for the test chamber are based on the following approach:

(1) Establish initial geometric conditions, including the outside diameter of the pressure shell ($D_o = 24$ in), shell thickness ($t = 0.188$ in), and an overall length between flanges ($L = 33.75$ in).

(2) Verify ratio of $D_o/t > 10 \quad \rightarrow \quad 24.0/0.188 = 128$

(3) Assess ratio of $L/D_o \quad \rightarrow \quad 33.75/24.0 = 1.41$

(4) An acceptable operating stress of $B = 6{,}800$ psi is calculated using the above factors and the appropriate figures within the ASME BPVC, subpart III of section II to determine the operating stress with the following applied inputs:

- Material properties for stainless steel 316.
- Material average operating temperature (set to 375 ºC, conservative estimate).

(5) The maximum allowable external pressure can then be assessed:

$$P_a = 4B/3(D_o/t) \quad \rightarrow \quad P_a = (4*6{,}800)/(3*(24/0.188)) = 71.0 \text{ psi.}$$

(6) The calculated value of P_a is compared to the actual value of external pressure of 14.7 psi. Because the calculated maximum allowable pressure is much greater than 14.7 psi, the selected wall thickness is acceptable per the ASME BPVC.

All vacuum flanges in the proposed design are standard vacuum components and require no further analysis; however, additional analysis can be performed if nonstandard hardware is required. Structural loads on the designed chamber external support stand are minimal and standard materials and welding practices are sufficient, requiring no additional analysis.

2.3 General Procurement Specifications

Hardware procurements necessary to complete the fabrication and assembly of the baseline environmental test chamber assembly have been identified. Hardware purchases were planned to be completed as solicitations issued by Marshall Space Flight Center (MSFC) using full and open competition. The final evaluation of vendor quotes will be based on the lowest cost technically acceptable approach. The current baseline requires sufficient material to fabricate three large chambers and one small chamber. The primary components within the test systems include the following:

(1) Three large chamber cylindrical pressure shells (24-in-diameter pipe segments or rolled plate) with electropolished inner surface suitable for vacuum application. These are commercial off-the-shelf items; current vendor cost is estimated at $2.5K each with a delivery of 4 to 6 wk.

(2) Six large chamber flange sets (metal wire seal type), including the chamber mounted flange (bored) and blank end plate. These flanges are commercial off-the-shelf items; current vendor cost is estimated at $5K per set (bored and blank) with a delivery of 4 to 6 wk.

(3) Small chamber pressure shell with attached flanges (typical 12-in-diameter vacuum full-nipple section). These are commercial off-the-shelf components with an estimated price in the $5K to $7K range, available from a variety of vendors with typical delivery of 4 to 6 wk.

(4) Variety of 2- and 6-in tube, half-nipple flange penetrations with associated blank flanges, optical view ports, fluid feedthroughs, valves, and bolt/nut hardware. These items are available from a number of vacuum vendors, with availability estimated at 4 to 6 wk. The cost of these components is expected to be on the order of $12K to $15K.

(5) Structural material to fabricate support stands, internal frames, and mounting brackets from stainless steel and refractory metals. Also includes mechanical positioners to accurately control placement of the heat pipes and calorimeters. This material is commercial off-the-shelf with cost estimated at approximately $15K to $20K and a delivery of 4 to 6 wk.

(6) Part fabrication and assembly at machine shops, as required to complete test chambers. On-demand basis with estimated cost in the $10K to $15K range.

Appendix D provides a partial listing of primary components selected for assembly of the environmental test chambers. Additional details and possible substitutions will be added when the design is finalized.

3. WATER COOLING

To support test operations, water cooling is necessary for several hardware subsystems, including the heat pipe calorimeter assemblies, the environmental test chamber walls, if required, and the RF power supplies/induction coils. Each of these is serviced by a closed recirculation loop that rejects waste heat to a common facility coolant system using water-water heat exchangers. The sophistication of each loop is dependent on materials selection (corrosion potential) and the minimum flow passage size (small sizes are more likely to be blocked). The chamber cooling traces are of the lowest concern since they will be 0.25-in-diameter tubes or larger located external to the environmental test chamber. Because leakage and service present minimal concern for chamber cooling, they can make use of coolant water directly from the facility system—no intermediate conditioning system. The RF power supplies and inductive coil assemblies are of moderate concern since coil cooling traces penetrate the environmental test chamber and must carry a significant amount of waste heat. The coil traces will be constructed from 0.25-in-diameter tubing or larger to minimize the risk of plugging. The current baseline is to use a commercial circulation unit to process the coolant water for this system.

The calorimeter assemblies serve a critical test role and are of high concern since they are positioned in very close proximity to the heat pipes and extract large amounts of power. The calorimeter makes use of a small water flow annulus (width of 0.01 to 0.015 in) to absorb power, placing increased emphasis on the control of particulates and corrosion to minimize the potential for blockage. This subsystem will be the focus of the following discussion.

3.1 General Requirements Layout Description: Calorimeter Assemblies

The conceptual layout for the calorimeter coolant system is illustrated in figure 4. The coolant system is divided into two sections—the calorimeter and the supply. The calorimeter section is composed of all flow elements between the inlet and outlet manifolds on the test chamber side of the loop: the manifolds, calorimeter, copper tubing, stainless steel tubing, control valves, thermocouples, flow meters, thermal switches, and flow switches. Water for each calorimeter is routed between a common inlet manifold and outlet manifold adequately sized to eliminate pressure or flow restrictions. The specific calorimeter mass flow rate, selected to meet test requirements, is regulated by a hand valve located at the calorimeter exit; temperature and flow rate measurements are also taken at this location so that calorimeter power can be determined.

By definition, the supply contains everything that is not a part of the calorimeter and includes the recirculation components and connections to the facility coolant/electrical supply. This section maintains the required bulk water flow rate, temperature, filtration, and purity requirements. The current baseline is to make use of a single supply loop and set of manifolds to service all 16 calorimeters; however, this may be subdivided, depending on the final configuration of the environmental test chambers. Purified and/or treated water is loaded and maintained by the supply section using appropriate filters, deionizers,

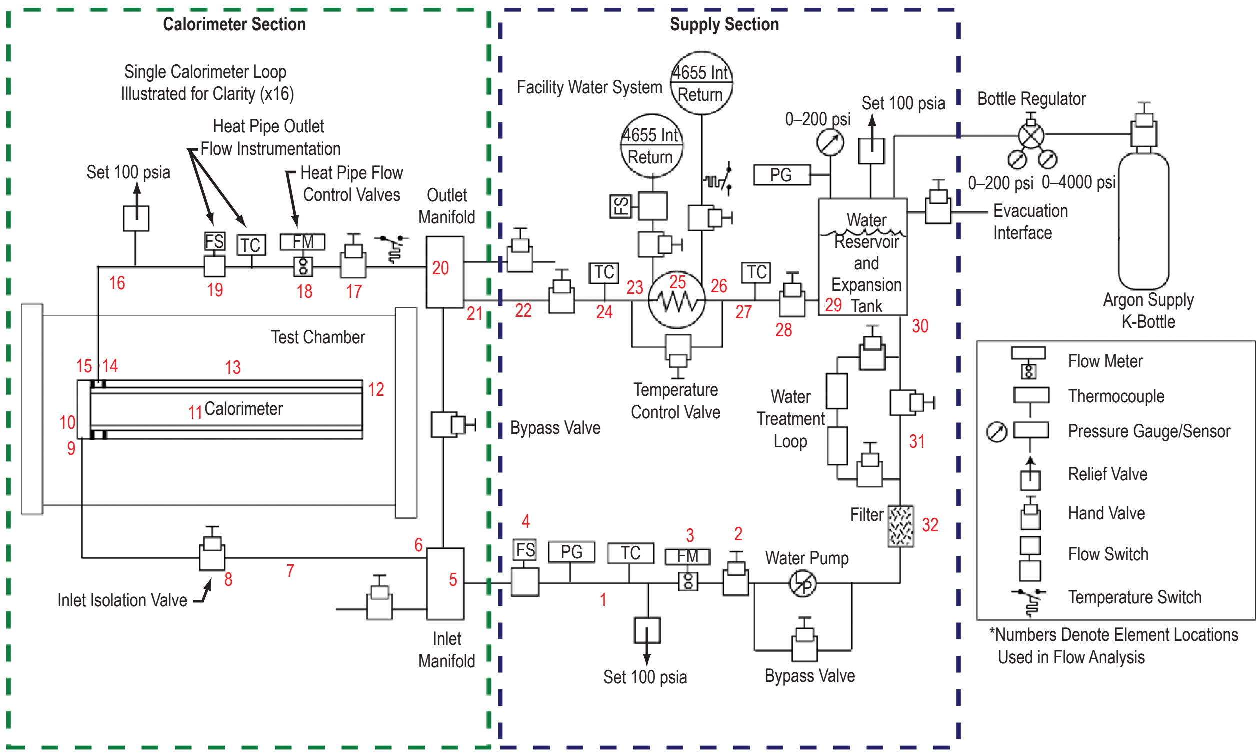

Figure 4. General calorimeter water-cooling system layout (one calorimeter illustrated).

etc. to provide stable, long-term operation. To conservatively satisfy estimated cooling requirements, the selected supply section will be required to operate at an absolute pressure of ≈65 psia and to provide pure water at a minimum of 20 gpm at a pressure rise of 45 psi with a temperature of 300 K. Additional capacity will be built into the supply system to account for uncertainties. A complete flow analysis of the supply system will be used to determine final hardware requirements necessary for the procurement of a commercial turnkey coolant recirculation unit. Both the calorimeter and supply sections have initially been laid out with flow and temperature switches to interrupt the RF power supplies in the event of coolant circulation failure or an over-temperature condition. However, these switches are redundant to the flow and temperature measurements already located in the lines and may be dropped from the system, depending on the final data/control system used to monitor operations.

3.2 Coolant Water Quality

To maintain long-term reliable operation of the water-cooling system it is mandatory that issues such as scaling and corrosion be kept in check, leading to consideration of deionized (DI) water in the coolant loop. As the coolant system design matured, further investigation indicated that DI water creates problems when used with copper, the selected material for use in the calorimeter assemblies. Dortwegt and Pellegrino provide a good discussion of the potential issues and recommended practices.[5,6] Suggested system values for water include conductivity <0.2 µS/cm, dissolved oxygen (DO) < 20 ppb, and a pH range of 6.8 to 7.2. The DO concentration appears to be a major concern throughout. However, with the low pH range—driven by the resistivity requirement—copper corrosion is an unavoidable drawback. Several recommended practices that are pertinent to the current design include the following:

- Avoid the use of small (<1/8-in diameter) orifices for regulation of water flow rate.

- Employ ≈0.5-µm, point-of-use filtration in the primary loop; routine filter changes should be avoided to minimize the ingress of oxygen.

- Employ a branch treatment loop, if possible, with 0.05- to 0.1-µm filtration (≈5% of total throughput).

- Introduce all makeup water at a vacuum deaerator to remove all but trace DO.

- Maintain branch lines that are not used regularly with a continuous minimum flow to avoid DO accumulation.

- Flush pump seals to avoid direct impingement of copper particles on seal faces.

- Avoid use of flow-measuring equipment with moving parts, if economically possible.

- It is imperative that the source water for initial system filling and for makeup be free of bacterial contamination. Once filled, continuously circulate the system water; an additional ultraviolet (UV) treatment may be beneficial.

A significant driver for the systems described by Dortwegt and Pellegrino that led to the recommended practices above was the lower limit of resistivity, which in effect restricts the upper limit on pH.[5,6] The water-cooling system application within this TP is not as sensitive to resistivity, so operation with water at a higher pH is a viable approach to alleviating concerns over copper corrosion. With this in mind, the above recommendations may be viewed as practices to follow if economically feasible, but not as strict requirements to be placed on the current calorimeter coolant system design.

Table 2 provides the ASTM standard specification for reagent water (D1193-99$^{\varepsilon 1}$).[7] While these grades may be too stringent for the current application and too costly to maintain, type IV water with a pH at the upper bound (≈8) would be a good target for the initial fill and any makeup water. At a minimum, the supply section should contain a 0.5-µm filter, a deionizing cartridge, and a UV purification unit. If it is found that tighter control of water pH and DO content is required, then a purification loop may be added to the supply section, where a percentage (≈5 percent) of the total flow would be circulated and continuously purified.

Another coolant option that was investigated would employ a 30% to 50% mixture, by volume, of DOWTHERM 4000 and water.[8,9] This approach is advantageous in that the fluid contains corrosion inhibitors that offer increased system protection without the needed expense for ancillary purifiers. DOWTHERM 4000 is an inhibited ethylene glycol-based heat transfer fluid manufactured by the Dow Chemical Company. Dow recommends using good quality water for dilution, containing only minute traces of calcium (<50 ppm), magnesium (<50 ppm), chloride (<25 ppm), and sulfate (<25 ppm), and <100 ppm of total hardness as $CaCO_3$ (type III water). Dow also provides prediluted solutions, AMBITROL, if good quality water is not available. To date, the calorimeter and water system design have been

Table 2. Water grades from the ASTM standard specification for reagent water.[7]

	Type I	Type II	Type III	Type IV
Electrical conductivity, maximum µS/cm at 298 K (25 °C)	0.056	1	0.25	5
Electrical resistivity, minimum MΩ•cm at 298 K (25 °C)	18	1	4	0.2
pH at 298 K (25 °C)	*	*	*	5 to 8
Total organic carbon, maximum (µg/L)	50	50	200	No limit
Sodium, maximum (µg/L)	1	5	10	50
Chlorides, maximum (µg/L)	1	5	10	50
Total silica, maximum (µg/L)	3	3	500	No limit
Microbiological contamination—When bacterial levels need to be controlled, reagent grade types should be further classified as follows:				
		Type A	Type B	Type C
Maximum heterotrophic bacterial count		10/1,000 mL	10/100 mL	100/10 mL
Endotoxin, EU/mL**		<0.03	0.25	NA

*The measurement of pH in type I, II, and III reagent waters has been eliminated from the specification because these grades of water do not contain constituents in sufficient quantity to significantly alter the pH.
**EU=Endotoxin units.

sized assuming the use of pure water as the heat transfer fluid. The addition of DOWTHERM 4000 to the water alters the fluid properties, the effects of which are presented in table 3. The computed flow rates and pressure drops are based on the listed constant fluid properties applied to heat pipe test case F(-4) (the 5,000-W test condition).

Table 3. Comparisons for water and solutions of water and DOWTHERM 4000 (concentrations given in percent volume) for F(-4) (all properties assumed constant).

Parameter	Water	30% DOWTHERM 4000	50% DOWTHERM 4000
ρ (kg/m^3)	992	1,044	1,075
c_p (kJ/kg-K)	4.2	3.7	3.3
k (W/m-K)	0.63	0.47	0.39
μ (Pa-s)	0.00065	0.0013	0.0023
Re	2,329	2,678	2,816
Q (gpm)	0.78	1.7	3.1
ΔP (psi)	4.2	19.6	64.3

The flow rates and pressure drops resulting from the addition of DOWTHERM 4000 represent a substantial increase over that of pure water and are unacceptable. Vendor discussions indicate that it is also possible to tailor a fluid, e.g., the antifreeze protection afforded by DOWTHERM 4000 is not needed, consisting of water and corrosion inhibiters that provide heat transfer properties nearer that of pure water. This possibility will be investigated further and system design/performance impacts assessed; however, water will remain the baseline coolant. The final coolant selection will be based on recommendations from the commercial vendor selected (through open procurement) to supply the heat removal water recirculation systems.

3.3 Sizing and Performance

Spreadsheet-level analyses have assessed the performance of the water-cooling system. Simplifying assumptions were necessary due to the preliminary status of the design. However, the intent was to provide a conservative estimate with sufficient fidelity to facilitate component sizing. As the design matures, so will the spreadsheet analyses. In addition, a more detailed model could be developed with the Generalized Fluid System Simulation Program (GFSSP) to accurately predict system performance.[10] More detailed multidimensional, e.g., finite element, etc., analyses will be performed as required to assess any design issues or to guide optimization of component-level performance.

The properties for water are generated with software that incorporates the IAPWS-95 formulation for the thermodynamic properties of pure water into an ActiveX component in Visual Basic 6.0.[11] The ActiveX component is called by Microsoft Excel, which is used to create the current cooling system model.

Table 4 provides a general description of each flow element modeled. It includes both the calorimeter section (elements 6–20) and those components of the supply section (elements 1–5 and 21–32) that are a part of the closed recirculation cooling system. While purchasing of a commercial turnkey system for the supply section is the preferred option, modeling of the supply section assists in determining specifications for the turnkey system and provides an initial baseline design should it become an MSFC-built supply section.

3.3.1 Calorimeter Section

Table 5 provides a listing of the primary model parameter values and the predicted pressure drops. The flow elements are consistent with figure 4 and are in order beginning at the pump exit. The pressure drops are computed using either of the following equations:

$$\Delta P = f\left(\frac{L}{d_h}\right)\frac{\rho\bar{v}^2}{2}\Gamma^n \tag{1}$$

or

$$\Delta P = K\,\frac{\rho\bar{v}^2}{2}\Gamma^n \ , \tag{2}$$

where the hydraulic diameter, d_h, is given by the tube diameter for a circular tube; for an annular gap, $d_h = d_o - d_i$. The viscosity ratio, Γ, is used to account for temperature-induced variations in viscosity whenever heat is transferred to or from the fluid. The value of n used in all results is that recommended by Furukawa, $n = -0.25$.[12] (Note that other references suggest different values.) All calculations assume that the thin flow annulus, i.e., flow element 11, is the only element that transfers heat, with all other elements being adiabatic, i.e., $T_w = T_{in} = T_{out}$. Friction factors are computed using formulas given by Furukawa.[12] For a circular tube or pipe,

Table 4. Flow element descriptions for the water-cooling system spreadsheet model.

Flow Element	Flow Element Description	
1	Pipe from pump exit to inlet manifold	Supply Section
2	Ball valve	
3	Turbine flow meter	
4	Flow switch	
5	Pipe exit into inlet manifold	
6	Tube entrance from inlet manifold to calorimeter	Calorimeter Section
7	Tube from inlet manifold to calorimeter	
8	Ball valve	
9	Tube exit into calorimeter	
10	Calorimeter entrance into thin annulus	
11	Calorimeter thin annulus	
12	Calorimeter turnaround	
13	Calorimeter thick annulus	
14	Calorimeter exit out of thick annulus	
15	Tube entrance from calorimeter to outlet manifold	
16	Tube from calorimeter to exit manifold	
17	Ball valve	
18	Turbine flow meter	
19	Flow switch	
20	Tube exit into outlet manifold	
21	Pipe entrance from outlet manifold to heat exchanger	Supply Section
22	Pipe from outlet manifold to heat exchanger	
23	Pipe exit into heat exchanger	
24	Ball valve	
25	Heat exchanger	
26	Pipe entrance from heat exchanger to expansion tank	
27	Pipe from heat exchanger to expansion tank	
28	Ball valve	
29	Pipe exit into expansion tank	
30	Pipe entrance from expansion tank to pump inlet	
31	Pipe from expansion tank to pump inlet	
32	Filter	

$$f = \frac{64}{Re} \quad \text{if} \quad Re \le 2{,}000 \quad , \tag{3}$$

$$f = 0.2088 - 0.1868\left(\frac{Re}{1{,}000}\right) + 0.0624\left(\frac{Re}{1{,}000}\right)^2 - 0.00656\left(\frac{Re}{1{,}000}\right)^3 \quad \text{if} \ 2{,}000 < Re < 4{,}000 \quad , \tag{4}$$

Table 5. Key parameters for the calorimeter section spreadsheet model for test case F(-4).

Flow Element	Inputs								Outputs			
	Type	T_w (K)	T_{in} (K)	T_{out} (K)	d or d_i (m)	d_o (m)	L (m)	ΔH (m)	Re	f	K	ΔP (psi)
6	0	300	300	300	0.00775			0	9,321	0.0322	0.5	0.038
7	0	300	300	300	0.00775		1.219	0.762	9,321	0.0322	5.1	1.469
8	0	300	300	300	0.00775		0.023	0	9,321	0.0322	0.1	0.007
9	0	300	300	300	0.00775			0	9,321	0.0322	1	0.077
10	1	300	300	300	0.02019	0.02096		0	1,755	0.0547	0.5	0.141
11	1	396	300	324.4	0.02019	0.02096	0.330	0	2,254	0.0336	14.6	4.109
12	1	324.4	324.4	324.4	0.02019	0.02096	0.038	0	2,797	0.0416	2.1	0.591
13	1	324.4	324.4	324.4	0.02396	0.03026	0.330	0	2,123	0.0452	2.4	0.006
14	1	324.4	324.4	324.4	0.02396	0.03026		0	2,123	0.0452	1	0.002
15	0	324.4	324.4	324.4	0.00775			0	14,857	0.0287	0.5	0.039
16	0	324.4	324.4	324.4	0.00775		1.829	–0.762	14,857	0.0287	6.8	–0.546
17	0	324.4	324.4	324.4	0.00775		0.023	0	14,857	0.0287	0.1	0.007
18	0	324.4	324.4	324.4	0.00775		1.549	0	14,857	0.0287	5.7	0.444
19	0	324.4	324.4	324.4	0.00775		0.054	0	14,857	0.0287	0.2	0.016
20	0	324.4	324.4	324.4	0.00775			0	14,857	0.0287	1	0.077
												6.48

and

$$f = 0.3164\, Re^{-0.25} \text{ if } Re \geq 4{,}000 \quad , \tag{5}$$

while for an annular gap,

$$f = \frac{64}{Re}\psi \text{ if } Re < Re^{*} \quad , \tag{6}$$

and

$$f = 0.304\varepsilon^{0.1} Re^{-0.25} \text{ if } Re \geq Re^{*} \quad , \tag{7}$$

where

$$\varepsilon = \frac{d_i}{d_o} \quad , \tag{8}$$

$$\psi = \frac{(1-\varepsilon)^2}{\left[1 + \varepsilon^2 + \frac{\left(1-\varepsilon^2\right)}{\ln(\varepsilon)}\right]} \quad , \tag{9}$$

and

$$Re^* = 1{,}250\,\psi^{1.33}\,\varepsilon^{-0.133} \quad . \tag{10}$$

To account for secondary losses, e.g., entrance effects, exit effects, etc., and flow elements that are not tubes or annular gaps, e.g., valves, flow meters, etc., the Crane Report is used to approximate the appropriate resistance coefficients, $K=f\,(L/d_h)$.[13] Table 5 lists K for all flow elements in the cooling system design.

For the tube and annular gap elements, K is computed using equations (3) through (10). All entrance effects are approximated with $K=0.5$, i.e., treated as a sharp-edged pipe entrance, while $K=1$, i.e., treated as a pipe exit, is used to account for exit effects. All valves are treated as ball valves where $K=3\,f_T$ and the friction factor in the fully turbulent zone, f_T, is calculated with the previous relations for a circular tube at the appropriate flow rate and diameter. Defining K as a function of f_T effectively defines an effective (L/d_h), which is how these values are input into the spreadsheet model. For example, while (L/d_h) is calculated for the tube and annular gaps, for the ball valves, the value of L is input as 3 d_h. In a similar manner, the constant K values defining entrance and exit effects are input into the spreadsheet by replacing the computed K with the appropriate constant values. The resistance coefficients for the transition from the thin annular gap of the calorimeter to the thicker annular gap is treated as a closed pattern return bend ($K=50\,f_T$). The resistance coefficients for the flow meters ($K=200\,f_T$), the flow switches ($K=7\,f_T$), the heat exchanger ($K=500\,f_T$), and the filter ($K=200\,f_T$) are all rough estimates at this point and will need refinement as the design matures. In addition, the calculation assumes that there is no significant pressure drop in the inlet and outlet manifolds. The manifold diameters will be relatively large to minimize any effects they might have on flow distribution between the calorimeters. As a result, there will be very little dynamic pressure and very little change in static pressure. The current baseline is a 4-in-diameter manifold. There are 16 units, i.e., heat pipes, to be tested, resulting in unique operating conditions through each of the 16 calorimeters. Table 5 represents the conditions corresponding to unit F(-4), which yields the largest pressure drop. Table 6 gives the pressure drops through each of the 16 defined test conditions. Note that there are seven G-series heat pipes to be tested, all of which yield the same calculated pressure drop.

The maximum pressure drop occurs through the F(-4) calorimeter; this value will be used to size the remaining water subsystem. The appropriate flow splits will be obtained through the other calorimeters by adjustment of the individual flow control valves.

3.3.2 Supply Section

Table 7 provides a listing of the primary model parameter values along with the predicted pressure drops for both the calorimeter and supply sections of the recirculating coolant loop. The pressure drops are computed at the operational conditions for test case F(-4) since these represent the largest pressure drop. The flow element pressure drop calculations utilize equations (1) through (10).

Figure 5 illustrates the system pressure-flow curves for two cases with primary feed system piping diameters of 1 and 2 in (with wall thickness of 0.083 in). The calorimeter inlet and outlet manifolds are set at 4-in diameters to eliminate potential flow restrictions. The tubing for each calorimeter, i.e., from inlet

Table 6. Calculated pressure drops for each of the 16 heat pipe test cases.

Units	ΔP (psi)
G series	5.11
F(-4)	6.48
F(-3)	0.74
F(-2)	4.67
F(-1)	5.66
F(1)	4.89
F(2)	5.50
F(3)	4.44
F(4)	5.06
F(0)	5.11

manifold to outlet manifold, has a diameter of 0.375 in, with a wall thickness of 0.035 in. In the actual installation, the supply section piping may very well have some combination of diameters—and reduction at fittings and components—but in bounding the problem, the assumption is made that the diameter will reside between 1 and 2 in.

In summary, the water-cooling system has been characterized through spreadsheet-level analyses, making use of simplifications and assumptions that are believed to be suitable for the preliminary status of the design. The intent was to establish a simple model incorporating representative flow components with a conservative treatment and additional margin added to account for calculation uncertainty and the addition of unanticipated ancillary cooling requirements. The results of this assessment shall be used to set procurement specifications for the supply side recirculation system. The final pump selection should be capable of delivering a minimum of 20 gpm at a supply pressure of 45 psi.

3.3.3 Calorimeter Exit Flow Temperature Measurement

To minimize the risk of water leakage inside the environmental test chambers, all temperature probes in contact with water, using mechanical connections, will be located outside of the chamber. This introduces an unknown regarding measurement of the calorimeter outlet water temperature, since it would be positioned outside the test chamber (≈18 in downstream of the calorimeter). To analyze possible heat loss from the calorimeter tubes, an assessment is made using convection and radiation heat transfer relations and properties obtained from Incropera.[14] It is assumed that the primary source of heat transfer will be between the 300 K supply tubes/chamber surfaces and the warmer return tubes. The heat loss from the return tubes between the calorimeter exit and the measurement location external to the test chamber is assessed using appropriate parameters. The distance between the exit and measurement locations is assumed to be ≈18 in, the emissivity of copper is 0.45, the outside diameter of the copper tube is 0.375 in, and all other surfaces are assumed to be at a temperature of 300 K. Test setup F(-3) has the maximum outlet temperature condition of 335 K, which will result in the greatest heat loss. Under these conditions, 1.75 W of heat is radiated from the tube surface between the calorimeter exit and external measurement location. For the natural convection contribution to heat loss, due to a He environment, the Nusselt, Rayleigh, and Grashof numbers are given by equations (11) through (13):

Table 7. Key parameters for the calorimeter and supply section spreadsheet model.

Flow Element	Inputs								Outputs			
	Type	T_w (K)	T_{in} (K)	T_{out} (K)	d or d_i (m)	d_o (m)	L (m)	ΔH (m)	Re	f	K	ΔP (psi)
1	0	300	300	300	0.02118		1.829	0	40,862	0.0223	1.92	0.379
2	0	300	300	300	0.02118		0.064	0	40,862	0.0223	0.07	0.013
3	0	300	300	300	0.02118		4.237	0	40,862	0.0223	4.45	0.878
4	0	300	300	300	0.02118		0.148	0	40,862	0.0223	0.16	0.031
5	0	300	300	300	0.02118			0	40,862	0.0223	1	0.197
6	0	300	300	300	0.00775			0	9,321	0.0322	0.5	0.038
7	0	300	300	300	0.00775		1.219	0.762	9,321	0.0322	5.07	1.469
8	0	300	300	300	0.00775		0.023	0	9,321	0.0322	0.1	0.007
9	0	300	300	300	0.00775			0	9,321	0.0322	1	0.077
10	1	300	300	300	0.02019	0.02096		0	1,755	0.0547	0.5	0.141
11	1	396	300	324.4	0.02019	0.02096	0.330	0	2,254	0.0336	14.55	4.109
12	1	324.4	324.4	324.4	0.02019	0.02096	0.038	0	2,797	0.0416	2.08	0.591
13	1	324.4	324.4	324.4	0.02396	0.03026	0.330	0	2,123	0.0452	2.37	0.006
14	1	324.4	324.4	324.4	0.02396	0.03026		0	2,123	0.0452	1	0.002
15	0	324.4	324.4	324.4	0.00775			0	14,857	0.0287	0.5	0.039
16	0	324.4	324.4	324.4	0.00775		1.829	–0.762	14,857	0.0287	6.77	–0.546
17	0	324.4	324.4	324.4	0.00775		0.023	0	14,857	0.0287	0.09	0.007
18	0	324.4	324.4	324.4	0.00775		1.549	0	14,857	0.0287	5.73	0.444
19	0	324.4	324.4	324.4	0.00775		0.054	0	14,857	0.0287	0.2	0.016
20	0	319.8	319.8	319.8	0.00775			0	60,243	0.0202	1	0.199
21	0	319.8	319.8	319.8	0.02118			0	60,243	0.0202	0.5	0.099
22	0	319.8	319.8	319.8	0.02118		1.829	0	60,243	0.0202	1.74	0.347
23	0	319.8	319.8	319.8	0.02118			0	60,243	0.0202	1	0.199
24	0	319.8	319.8	319.8	0.02118		0.064	0	60,243	0.0202	0.06	0.012
25	0	319.8	319.8	319.8	0.02118		10.592	0	60,243	0.0202	10.1	2.007
26	0	319.8	319.8	319.8	0.02118			0	60,243	0.0202	0.5	0.099
27	0	319.8	319.8	319.8	0.02118		1.219	0	60,243	0.0202	1.16	0.231
28	0	319.8	319.8	319.8	0.02118		0.064	0	60,243	0.0202	0.06	0.012
29	0	319.8	319.8	319.8	0.02118			0	60,243	0.0202	1	0.199
30	0	319.8	319.8	319.8	0.02118			0	60,243	0.0202	0.5	0.099
31	0	319.8	319.8	319.8	0.02118		1.219	0	60,243	0.0202	1.16	0.231
32	0	319.8	319.8	319.8	0.02118		4.237	0	60,243	0.0202	4.04	0.803
												10.937

$$Nu_L = \frac{h\,L}{k} = 0.68 + \frac{0.67\,Ra_L^{1/4}}{\left[1+(0.492/Pr)^{9/16}\right]^{4/9}} \;, \tag{11}$$

$$Ra_L = Gr_L Pr \;, \tag{12}$$

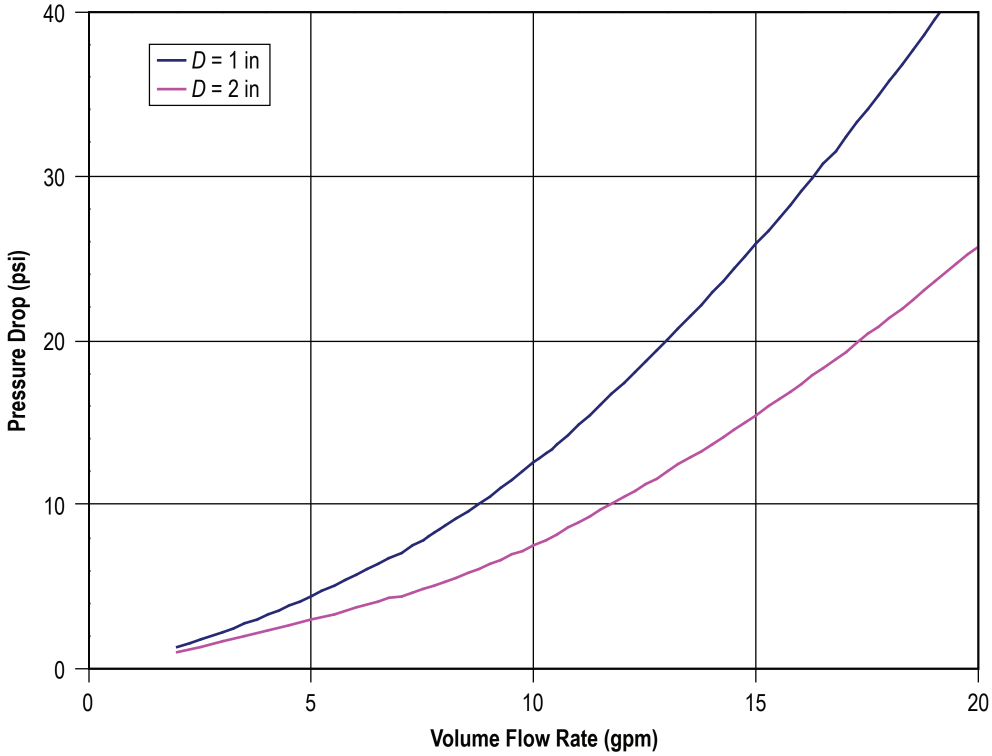

Figure 5. Computed system pressure-flow curves for water-cooling system.

and

$$Gr_L = \frac{g\beta\left(T_s - T_\infty\right)L^3}{v^2} \; , \tag{13}$$

where

L = 0.4572 m
g = 9.807 m/s^2
k = 0.165 W/m-K
v = 0.000149 m^2/s
Pr = 0.68
β = 0.003252 K^{-1}
T_s = 335 K
T_∞ = 300 K.

The resulting Grashof number is $Gr_L = 4.65\times10^6$, the Rayleigh number is $Ra_L = 3.16\times10^6$, and the Nusselt number is $Nu_L = 22$, resulting in a convection coefficient of $h = 8$ W/m^{2}K. The heat loss due to natural convection is ≈3.85 W; the resulting total heat loss—given by the sum of radiation and convection—is 5.6 W. When this heat loss is compared to the total extracted power of 1,000 W for test case F(-3), it represents <0.6% of the power with a corresponding temperature drop in the flowing water of 0.2 K. These effects are negligible and can be further reduced by the addition of multifoil insulation covering the return tubing inside and outside the test chamber. In addition, thermocouples will be mounted on the surface of the calorimeter return tubing ≈2 cm from the calorimeter exit. The internal and external temperature data can be compared to determine overall accuracy of the measurement technique in addition to serving as a backup.

3.4 General Fill and Test Procedures

A set of general procedures pertaining to the initial fill and conditioning for the heat pipe calorimeter water-cooling subsystem is outlined. Before loading, all system plumbing should be cleaned thoroughly and flushed to remove all particulates. A trickle purge using dry nitrogen can be placed on the system prior to filling to sweep any remaining volatile materials and to maintain the system at an acceptable condition if not in use for extended periods of time. The purge should be shut down and isolated prior to loading the system with water coolant. This outline will serve as a general approach and will be adjusted to match specific operational parameters required by the selected turnkey water coolant recirculation unit.

3.4.1 Flushing Primary Flow Circuit

The following procedure is used for flushing the primary flow circuit:

(1) Prior to flushing the primary flow circuit, all individual flow circuit tubing and pipe components should have been flushed (during assembly) to remove the bulk of potential debris.

(2) Close all heat pipe calorimeter inlet and outlet isolation valves.

(3) Open all primary water flow system isolation valves.

(4) Open expansion tank pressure relief valve and fill the system with water—of appropriate purity—through the expansion tank.

(5) Turn on pump and cycle water through the complete circuit using the inlet to outlet manifolds bypass line. This will purge trapped air and moves remaining debris to the system filter.

(6) Examine all fittings, welds, and instrumentation for water leaks. Tighten or replace as necessary.

(7) Check water level in expansion tank and add water if necessary.

(8) Shut down pump after operating for 8 hr.

(9) Drain system through inlet/outlet manifold and expansion reservoir drains.

(10) Remove and inspect expansion tank strainer and inline filters. Clean and/or replace if necessary.

(11) If significant debris is found, repeat this procedure until all inline filters and strainers are clean.

3.4.2 Flushing Complete Flow Circuit

The following procedure is used for flushing the complete flow circuit:

(1) Prior to flushing the complete flow circuit, all primary flow circuit tubing and pipe should have been flushed and verified to be clean per inspection of inline filters and strainers.

(2) Open all heat pipe calorimeter inlet and outlet isolation valves.

(3) Open all primary water flow system isolation valves.

(4) Close inlet to outlet manifold bypass isolation valve.

(5) Open expansion tank pressure relief valve and fill the system with water—of appropriate purity—through the expansion tank.

(6) Turn on pump and cycle water through the entire flow circuit, including the heat pipe calorimeters. This will purge trapped air and moves remaining debris to the system filter.

(7) Adjust pump bypass valve to achieve flow in calorimeters greater than that required for testing.

(8) Examine all fittings, welds, and instrumentation for water leaks. Tighten or replace as necessary.

(9) Check water level in expansion tank and add water if necessary.

(10) Monitor flow rate through each of the calorimeters and verify that full coolant flow is maintained. Flow drop will indicate onset of potential plugging.

(11) Shut down pump after operating for 4 hr.

(12) Drain system through inlet/outlet manifold and expansion reservoir drains.

(13) Remove and inspect expansion tank strainer and inline filters. Clean and/or replace if necessary.

(14) If debris is found, repeat this procedure until filters and strainers are clean.

3.4.3 Fill Water-Cooling Circuit

The following procedure is used to fill the water-cooling circuit:

(1) Open all system isolation, bypass, and flow control valves.

(2) Open expansion tank pressure relief valve and fill system with water—of appropriate purity—through the expansion tank.

(3) Turn on pump and circulate water to purge all trapped air.

(4) Monitor flow through the primary loop and all calorimeters to verify that it meets or exceeds the nominal design flow requirements. Adjust pump bypass valve if needed to achieve desired conditions.

(5) Examine all fittings, welds, and instrumentation for water leaks. Tighten or replace as necessary to repair.

(6) Operate pump system for 2 to 4 hr.

(7) As trapped air is purged, audible indications of air bubbles moving through the system will cease. Close the inlet to outlet manifold bypass isolation valve.

(8) Check water level in expansion tank and add water if necessary.

(9) Shut down pump after operating for 4 hr.

(10) Close expansion tank fill cap and relief valve.

(11) Close purge valve and pressurize the tank to 65 psia with Ar.

(12) Turn on pump and operate for 2 to 4 hr.

(13) Examine all fittings, welds, and instrumentation for water leaks. Tighten or replace as necessary.

(14) Shut pump down after operating for 4 hr. Close pump and expansion tank isolation valves.

3.4.4 Deaerate the Cooling Water Circuit

The following procedure is used for dearating the cooling water circuit:

(1) Prior to this operation, the water circuit should be filled and all trapped air purged. The expansion tank should be equipped with a heater, either an external blanket or internal element, and insulation.

(2) Open pump and expansion tank isolation valves. Open bypass valves. Verify that all other circuit flow valves are open.

(3) Turn on pump and monitor water flow rate and pressure in both the primary and calorimeter sections.

(4) Turn on expansion tank heater and bring water to a target temperature of approximately 350 to 400 K, i.e., below the boiling temperature of 414.8 K at 55 psi.

(5) Open vacuum isolation to provide a reduced pressure in the 10 to 14 psia range on the expansion tank ullage. This removes any dissolved gases that are released during heating. Ullage pressure and heating may need to be adjusted to prevent pump cavitation.

(6) Continue heating and circulation for up to 2 hr.

(7) Isolate the vacuum system and turn off expansion tank heater; allow system to cool.

(8) Maintain a blanket circuit pressure by adding Ar as necessary—up to a level of 65 psia.

(9) Check water level in expansion tank and refill as necessary by depressurizing tank and filling through the tank fill cap. Minimize exposure to the atmosphere and maintain a slight positive Ar purge pressure inside the expansion tank, if possible, during the operation. Repressurize tank to 60 psi with Ar.

(10) If the required fill amount is >20% of the expansion tank volume, repeat the deaerating process.

3.4.5 Normal Water Circuit Operation

The following procedure is used for the normal water circuit operation:

(1) Verify that water circuit pressure is at 65 psia.

(2) Open expansion tank and pump isolation valves.

(3) Verify that flow circuit valves on the calorimeter section are open.

(4) Turn on water pump and check for leaks.

(5) Monitor all circuit flow rates, pressures, and temperatures.

(6) Adjust pump flow control valve—and bypass valve, if necessary—to achieve a flow that is between 100% and 120% of the calorimeter full-flow requirement.

(7) Adjust each calorimeter flow control valve—located at the calorimeter exit—in order from the highest to lowest flow split. Iterate until flow in each of the calorimeters is within 10% of the target conditions specified in the test matrix.

(8) Monitor total system flow and increase—by closing the pump bypass valve—should the total flow be insufficient to maintain full flow conditions on all calorimeters.

(9) Continually monitor all water circuit instrumentation.

(10) Periodically verify water level in expansion tank.

(11) Water system may require periodic adjustment once RF supplies are engaged and power is extracted by the calorimetry system.

(12) Verify that the control system is engaged to shut down RF supplies should there be a loss of coolant flow or an over-temperature condition on any of the calorimeter branches or primary flow circuit.

3.5 General Procurement Specifications

Primary components for the calorimeter water-cooling subsystem have been identified. (Instrumentation is included in sec. 6.) The procurement of these items will be issued by MSFC using full and open competition. The final evaluation of vendor quotes will be based on the lowest cost technically acceptable approach. Appendix E provides a partial listing of components as identified at the current time. Categories include the following:

(1) A closed-loop recirculation system with sufficient cooling capacity (≈60 kW) to service all heat pipe calorimeters. This unit will be a turnkey commercial off-the-shelf item such as the Sentry Equipment Compact Cooling Water Isolation Skid CWIS-35 with a reservoir and flow sensors designed for continuous operation. Typical vendor cost is $12K to $15K, available within 6 to 8 wk.

(2) Inline water treatment components, including a UV element, DI cartridge, filters, and strainers. These are commercial off-the-shelf items, typically available within 4 to 6 wk with an estimated cost range of $2K to $4K, depending on the final number of components and desired operational life.

(3) Valves, including hand and remote operated, for isolation and control of water circuit components. These will be a combination of ball-and-plug-type valves making use of either compression or pipe fittings. In addition, pressure relief valves are required. Valve material will be stainless steel with soft goods compatible with water service. Typical vendor delivery is 2 to 4 wk with an estimated cost range of $15K to $20K.

(4) A number of plumbing components, such as tubing, fittings, vacuum valves, dial pressure gauges, and structural materials, are required. All of these are commercial off-the-shelf items, available from a variety of vendors and typically available within 4 wk or less. The sum of these components is expected to range from $7K to $10K.

(5) Part fabrication and assembly at machine shops as required to complete system. On-demand basis with estimated cost in the $5K to $8K range.

4. RADIO FREQUENCY HEATING SYSTEM

Radio frequency heating has been selected as the most favorable technique for powering the life test heat pipes. Several key benefits associated with using RF heating include the following:

- Provides a noncontact method of imposing evaporator power.

- Provides uniform power input over a small, well-defined surface area.

- Provides sufficient standoff between the RF inductor coils and the heat pipe to allow for easy heat pipe installation/removal.

- Provides superior durability suitable for long-duration operation.

The complete RF heater configuration selected for this project includes a number of component subsystems: the RF inductive coil assemblies, the interconnecting busswork between the coil elements and the power supplies, the RF power supplies, coolant flow to power supplies/inductive coil assemblies, and instrumentation. The following sections detail the approach, conceptual design, and hardware layout necessary for implementation.

4.1 General Heat Pipe Test Arrangement

The current baseline test matrix (table 8) identifies performance conditions for 16 heat pipes. To make better use of test hardware and to facilitate integration and test operations, these heat pipes can

Table 8. Proposed heat pipe life test matrix.

Test Identifier	Power Level (W)	Heat Pipe Temperature (K)	Gas Gap Mixture	Gas Gap Width (in)	Coolant Flow (gpm)	Coolant Delta Temperature (K)	Number of Units
G-Series	3,000	1,273	He-32%Ar	0.025	0.61	18.8	7
F(-4)	5,000	1,273	He-6%Ar	0.025	0.77	24.6	1
F(-3)	1,000	1,273	He-32%Ar	0.103	0.11	35.2	1
F(-2)	3,000	1,373	He-32%Ar	0.031	0.56	21.1	1
F(-1)	3,000	1,173	He-32%Ar	0.021	0.65	17.6	1
F(0)	3,000	1,273	He-32%Ar	0.025	0.61	18.8	1
F(1)	2,000	1,223	He-32%Ar	0.037	0.54	13.9	1
F(2)	4,000	1,223	He-32%Ar	0.017	0.67	22.8	1
F(3)	2,000	1,323	He-32%Ar	0.046	0.50	15.2	1
F(4)	4,000	1,323	He-32%Ar	0.020	0.63	24.0	1

be arranged into groupings with similar or scalable power and environmental requirements. Initial investigations indicate that one possible configuration involves dividing the 16 heat pipes across four separate test clusters; each of these clusters is fed by its own RF power supply. Three of these clusters make use of a configuration composed of five inductive coils laid out in a pentagonal arrangement (coil centerlines set at 72-deg intervals). Figure 6 illustrates this configuration with coil positions set to maximize the distance between each unit—limiting inductive coupling—while providing sufficient workspace to configure the hardware within the test chamber. The coils are supported by a structural element attached to the test chamber. The RF busswork passes through an insulated test chamber penetration/feedthrough.

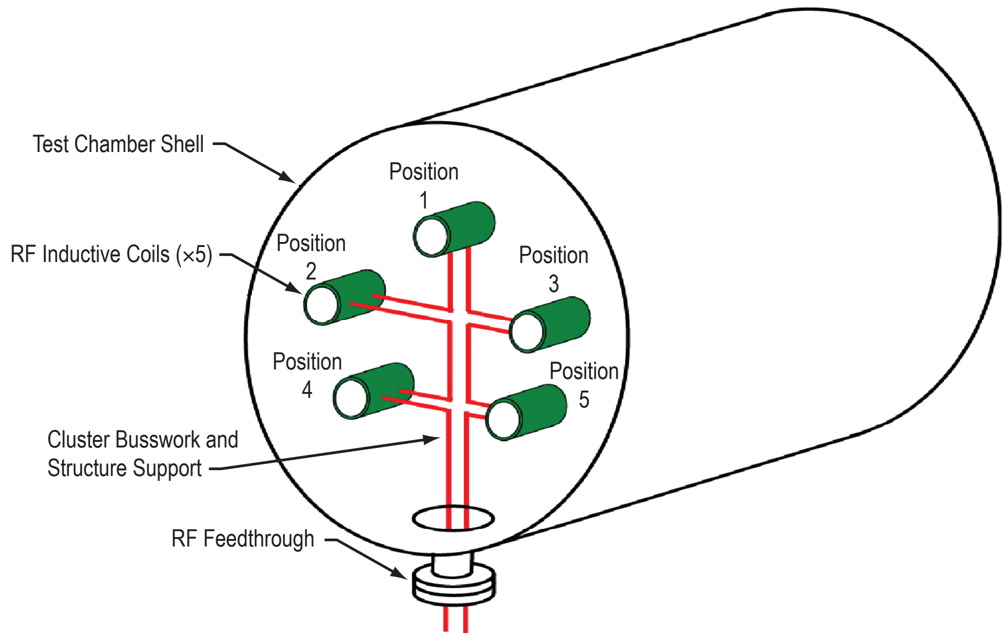

Figure 6. General test chamber layout showing the typical five-position RF coil cluster.

The coils within each cluster will be connected in series, with the coil geometry adjusted such that two conditions are possible—uniform power across all coil elements and fixed power variation between various coils within the cluster. Two of these clusters—representing 10 heat pipes—are to be sized for a uniform power condition set to an average power of 3 kW per heat pipe (neglecting environmental losses). This covers the complete G-series (seven units) and F-series heat pipes F(-2), F(-1), and F(0). The third cluster, composed of the remaining F-series heat pipes with the exception of the F(-4) heat pipe, provides a variation in power with inductive coil geometry adjusted to provide a scaling of 1, 2, and 4 kW in heat pipe power.

The F(-4) case will be contained in a separate test chamber to accommodate the higher 5-kW power level and to allow operation with a different atmospheric composition (higher He concentration). This chamber will also be equipped with its own inductive coil feed from a separate power supply. Table 9 provides a listing of each heat pipe's position within the four test chamber RF clusters.

Table 9. Position of heat pipes within test chamber clusters.

Test Chamber Cluster	Position 1	Position 2	Position 3	Position 4	Position 5
1	G(1)	G(2)	G(3)	G(4)	G(5)
2	G(6)	G(7)	F(0)	F(-1)	F(-2)
3	F(-3)	F(1)	F(3)	F(2)	F(4)
4	F(-4)	–	–	–	–

The RF inductive coil assemblies will be designed to maintain an approximate constant power distribution across all positions, even if positions are left open; i.e., no heat pipes are placed within the coils. This is a necessary operating condition since G-series heat pipes will be extracted at regular intervals for destructive evaluation, resulting in fewer units in test chamber clusters 1 and 2 over time. It may be advantageous to rearrange the clusters to consolidate heat pipes, rebalancing the electrical load and reducing the amount of necessary support hardware.

4.2 General Inductive Coil Geometry

The general layout of a possible RF inductive coil configuration is illustrated in figure 7. The unit consists of a three-turn inductor covered with a flux concentrator to minimize coupling with the water calorimeter and adjacent RF coils in the cluster while providing a more uniform and symmetrically heated area on the heat pipe surface. The assembly is composed of three cylindrical copper elements with a continuous RF power feed tube brazed to their surfaces. Each cylindrical element has a longitudinal split and is positioned with a gap to its neighboring element to prevent shorting. The flux concentrator is also constructed of three sections—one for each element—and surrounds the coil arrangement. A nonconductive potting material—vacuum compatible—will be used to assemble the complete RF inductive coil assembly.

When arranged in a pentagonal cluster, as illustrated in figure 8, each coil will be set on a 9-cm, center-to-center spacing with respect to its adjacent coils. These coils will be connected in series with coolant water circulated through the RF feeds. Water coolant flow—supplied at the RF power supply—should be adjusted to maintain the coil assembly temperature at <350 K to minimize the potential for damage. The three-turn inductive coils illustrated in figures 7 and 8 are sufficient to satisfy the uniform power requirements for test chamber clusters 1 and 2. The third test chamber cluster will require inductors with varied turns to satisfy power requirements. The initial baseline setup will require a two-turn inductor for the 1-kW position, a three-turn inductor for the 2-kW positions, and a four-turn inductor for the 4-kW positions.

The power to each cluster can be provided by a standard off-the-shelf insulated RF feedthrough such as that marketed by Insulator Seal Incorporated (part No. 9512010). The design of the structural support for the RF coil cluster arrangement will be performed in conjunction with the overall RF inductor system design and fabrication, to be issued as an open procurement to industry. However, at a minimum, the support must possess adequate rigidity to maintain positional tolerance, keeping the heat pipes centered in the coils, while providing sufficient strain relief on the feedthrough to prevent a possible failure (cracked insulator).

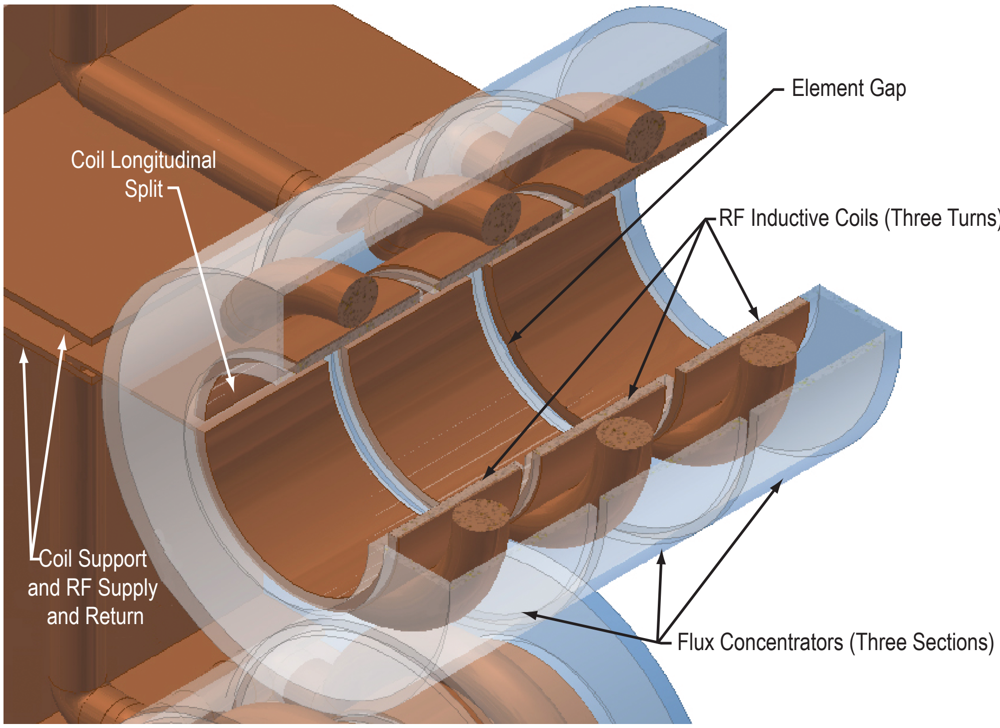

Figure 7. Sample RF inductive coil layout.

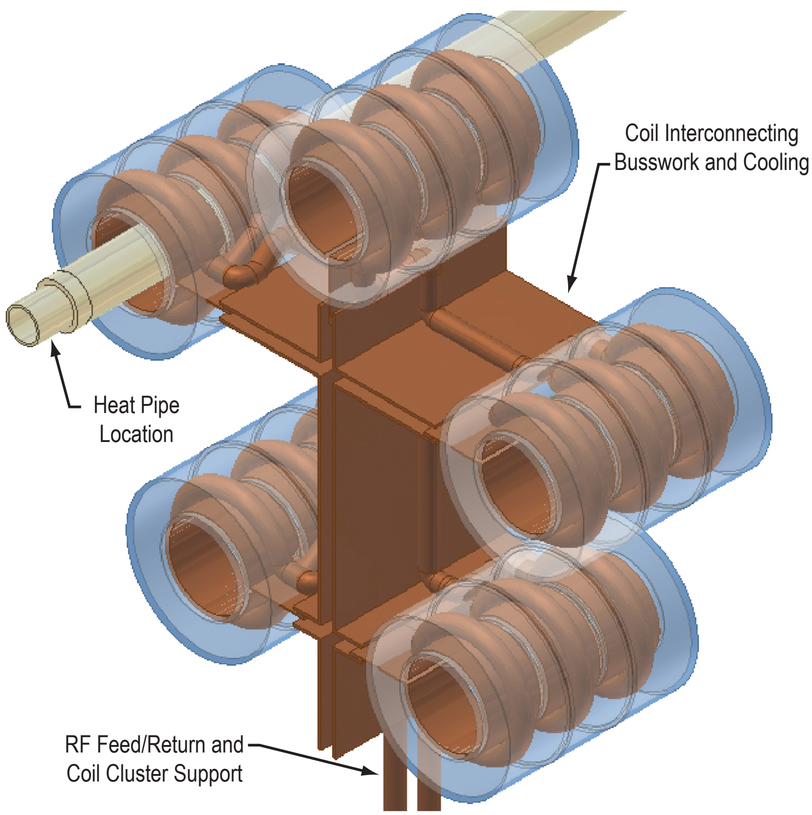

Figure 8. General test chamber section/RF inductive coil configuration.

4.3 Inductive Coil Sizing and Performance Parameters

A set of first-order assessments was made of the inductive coil layout to examine critical issues such as frequency and coil voltage requirements to achieve efficient power transfer to the heat pipe evaporator sections. These coil parameters are driven by geometric considerations, such as the heat pipe wall thickness, RF coil to heat pipe gap, and the number of inductor coil turns. Other parameters that must be considered include the potential for voltage breakdown, since testing will be performed in a low-pressure environment, and thermal losses to the inductive coil, which increases input power demands. The following sections detail the initial assessments performed to rough out the operational envelope for the RF power system.

4.3.1 Voltage Breakdown Considerations

A significant problem in low-pressure systems with imposed high voltage is a condition referred to as voltage breakdown. This condition can lead to a glow discharge with the potential for damaging the part under test, either by sputter or direct arc impingement. To minimize the potential for voltage breakdown, it is desirable to keep the voltage drop to ground across the series inductor string as low as possible. Direct current (DC) voltage breakdown potentials, referred to as Paschen curves, have been determined for various gases and are documented in the literature. Figure 9, generated from data collected by Weston, illustrates the variation of breakdown voltage for He, Ar, and He-Ar mixtures as a function of the product of pressure and gap distance.[15] Weston reported the lowest measured DC breakdown potentials for the He-Ar gas mixtures of interest, improving the conservative nature of estimates made in this work.

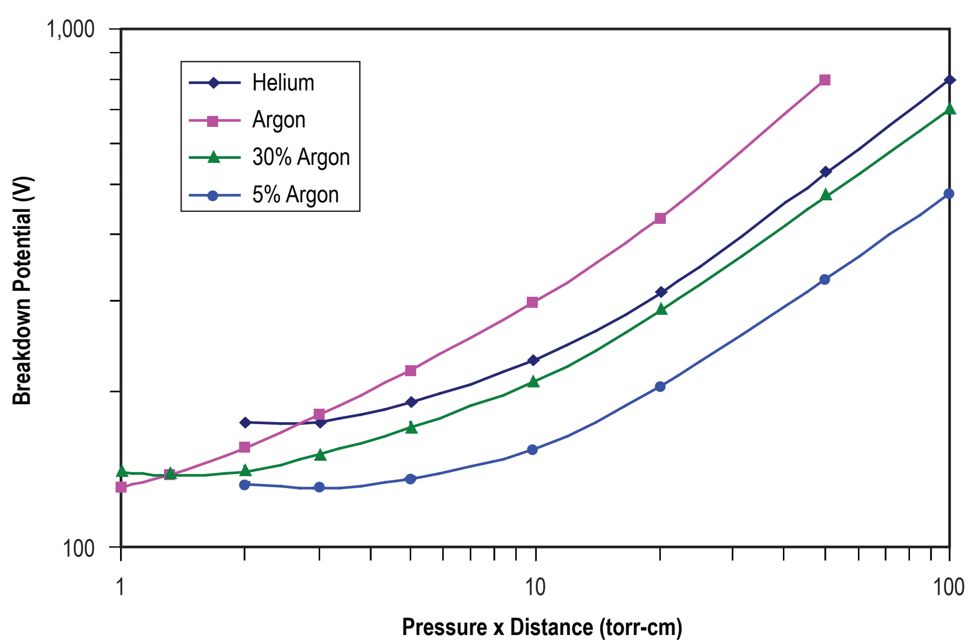

Figure 9. Direct current breakdown voltages in pure He, Ar, and He-Ar mixtures (Paschen curves).

For the conditions outlined in baseline testing (He-32%Ar and He-6%Ar), the typical total test chamber pressure will be maintained at ≈76 torr. Breakdown voltages are estimated using the curves shown in figure 10 for various gap distances. For example, with a heat pipe to inductive coil gap width set to 0.64 cm (0.25 in), the resulting breakdown potential is ≈300 V for a 5%Ar mixture and ≈450 V for a 30%Ar mixture. To maintain a safe margin against the potential onset of voltage breakdown, a factor of 2 reduction in applied voltage will be imposed on the RF system. This results in a maximum inductive coil voltage drop of 225 V for the five-position clusters and 150 V on the single-coil setup to be used for test case F(-4). An additional consideration is the effect of the RF frequency on the breakdown voltage. Radio frequency power is typically used to accelerate the onset of glow discharge, lowering the breakdown potential. However, the frequency range to achieve an appreciable decrease in breakdown voltage for gases such as He and Ar is in the 5^+ MHz range.[16,17] The He/Ar mixture is expected to follow the same trends.

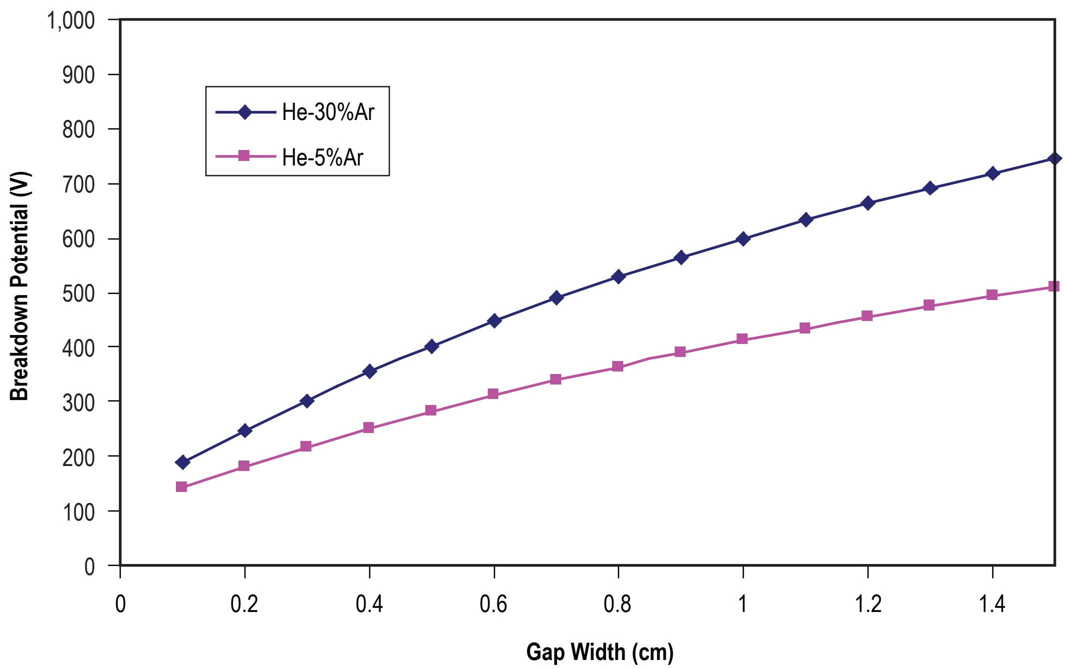

Figure 10. Breakdown voltage range with a total operating pressure of 76 torr.

For operating frequencies in the 10- to 50-kHz range, such as the proposed RF system, there should be little reduction in the breakdown potentials. However, checkout tests will be performed on a characteristic geometry using an inductive coil assembly for verification. If it is found that the planned test pressure is close to a breakdown threshold, the chamber pressure will be increased. (A 50-torr increase provides a 100-V improvement for the 32%Ar condition.) The high test chamber pressure (above 10 torr) was selected to place operation to the right of the Paschen minimum (fig. 9). In the event of a chamber leak, an increase in pressure will always result in an increasing breakdown voltage requirement, eliminating the potential for arcing.

4.3.2 Thermal Loss Considerations (Heat Pipe to Inductive Coil)

Although the RF inductive coil is a noncontact system, thermal losses from the heat pipe to the coil by both radiation and gas conduction are still present. It is important to characterize this heat transfer to the coil arrangement so that adequate cooling can be provided. To minimize this thermal loss it is advantageous to place the coil as far from the heat pipe as possible. This also carries the added benefit of further reducing the potential for voltage breakdown, increasing the product of pressure and distance. However, as the separation gap between the heat pipe surface and the inductive coil are increased, the induced coupling is adversely affected, requiring higher voltages to achieve power transfer. (This is further described in sec. 4.3.3.) The total heat flux between the heat pipe surface and the surface of the inductor ($\dot{Q}_{total}$) is given by:

$$\dot{Q}_{total} = \dot{Q}_{rad} + \dot{Q}_{cond} \quad , \tag{14}$$

where $\dot{Q}_{rad}$ is the radiation component and $\dot{Q}_{cond}$ is the conductive heat transfer load. The radiative component of the heat flux can be calculated using the Stefan-Boltzmann relationship with the surface emissivitiy (ε), temperature (T), and area (A) of each of the relevant surfaces:

$$\dot{Q}_{rad} = \frac{\sigma A_i (T_{hp}^4 - T_{ind}^4)}{1/\varepsilon_i + (A_i/A_o)(1/\varepsilon_o - 1)} \quad , \tag{15}$$

where σ is the Boltzmann constant. For this analysis, the emissivity of Mo-44.5%Re is assumed to be 0.15 and that of copper is 0.75; a high value is assumed for conservative calculations. Figure 11 illustrates the physical geometry used in this assessment. In addition, the static gas conduction heat flux component can be evaluated by the Fourier conduction heat transfer relationship for concentric cylinders,

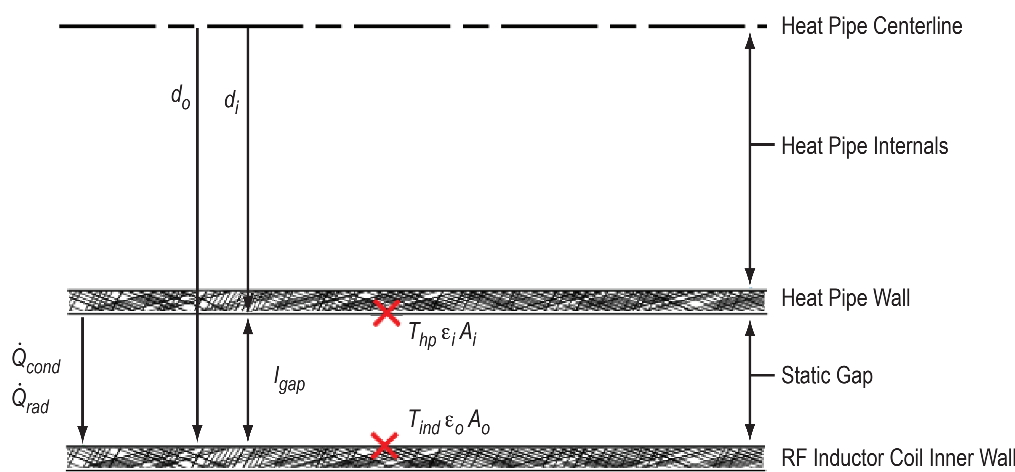

Figure 11. Radio frequency inductor to heat pipe geometry.

$$\dot{Q}_{cond} = \frac{2\pi L_c k(T_{hp} - T_{ind})}{\ln(d_o/d_i)} \ , \tag{16}$$

where L_c is the heat pipe length under the RF coil and d_o and d_i are the outer and inner diameters, respectively.

Based on this approach, a spreadsheet model was developed to estimate the thermal losses to the inductive coil as a function of the gap width (I_{gap}) for a maximum operating heat pipe temperature (1,373 K). The flow of water coolant through the inductive coil assembly is assumed to be sufficient to maintain an average coil temperature of 325 K. The complete spreadsheet is provided in appendix F with the results plotted in figure 12 (also includes estimated voltage breakdown values). As expected, small gap widths produce considerable heating rates on the inductive coil assembly (approaching that required by the actual heat pipe test). However, the heating rate drops off rapidly and becomes manageable at a gap width of 0.64 cm (0.25 in) with a value of ≈360 W.

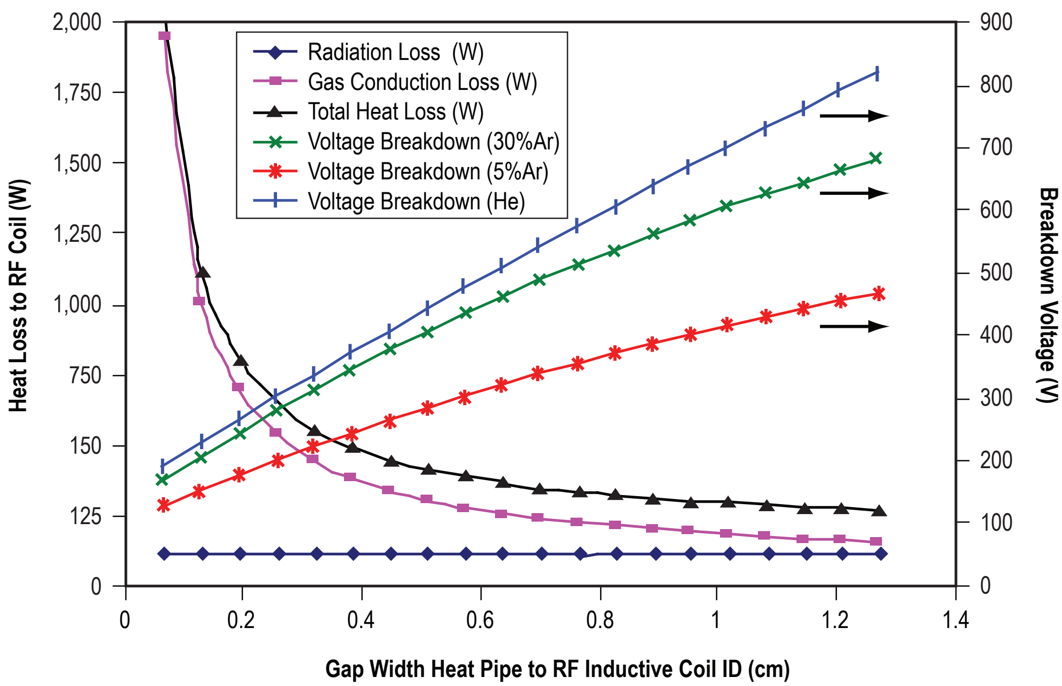

Figure 12. Heat pipe to RF inductive coil heat loss versus standoff distance (pressure = 76 torr).

An additional assessment is made to determine if the water coolant flow to the RF cluster (five inductive heater coils) is reasonable for the imposed heating rate. Total heating rate is the sum of thermal transport (heat pipe to RF coil) and the internal coil losses (RF efficiency). The internal RF coil losses are addressed in greater detail in the following section, but the appropriate expression is included here as a function of gap width (heat pipe to inductive coil):

$$\text{Coil internal loss} = 723\ (\text{gap width})^2 + 3{,}897\ (\text{gap width})^2 + 3{,}725\ , \tag{17}$$

where the resulting loss is in watts and the gap width is in centimeters. The total lost power (or coil heating) is shown in figure 13 as a function of the heat pipe to coil gap width. The curve has a bucket shape with a wide, flat bottom centered at ≈0.4 cm. The selected gap width of 0.64 cm is very near this minimum, representing a conservative selection, since any increase in inductor losses (actual application influences) will tend to shift the bucket minimum to the right. These heating rates are converted to water flow requirements, assuming that an acceptable rise in water temperature ($T_{out} - T_{in}$) across the coil cluster is 50 K, producing an average temperature of 325 K:

$$\dot{m}_{coolant} = \frac{\dot{Q}_{losses}}{c_p \, (T_{out} - T_{in})} \ , \tag{18}$$

where $\dot{m}_{coolant}$ is the water flow rate, c_p is the specific heat of water, and $\dot{Q}_{losses}$ is the total heat loss from the five inductive coil units (internal RF loss and thermal transport components).

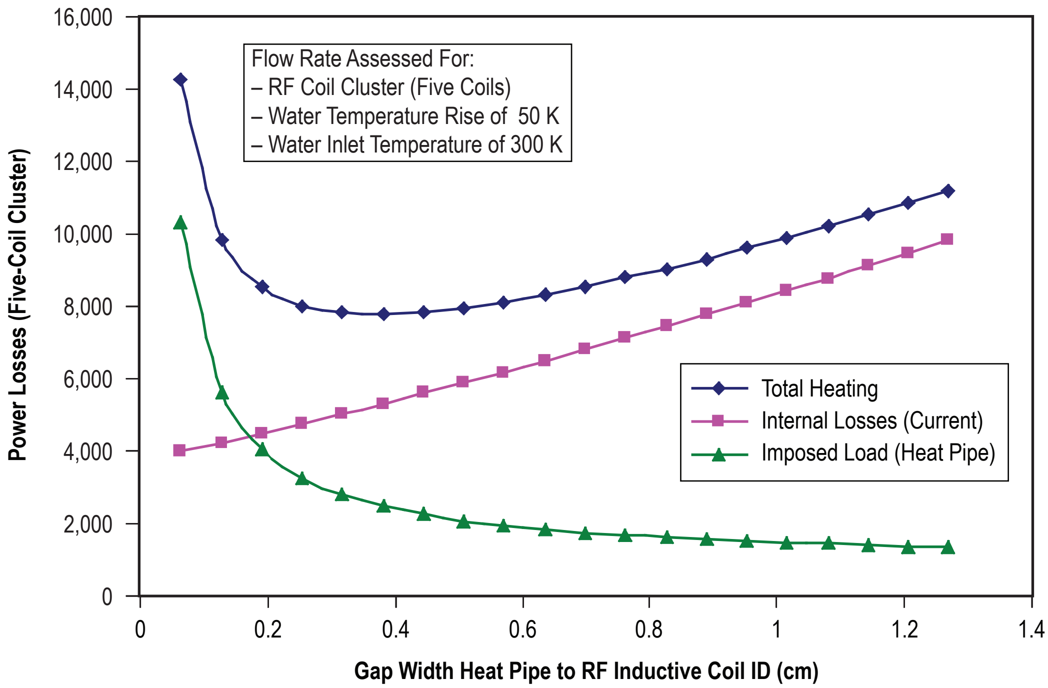

Figure 13. Radio frequency inductive coil cluster (five coils) power loss due to internal RF losses and thermal transport from heat pipe.

Figure 14 illustrates the variation in flow rate as a function of heat pipe to RF coil gap width distance. The individual flow components are also indicated. At a coil gap width of 0.64 cm (0.25 in), a reasonable flow rate per cluster of ≈3.2 gal/min is required. This flow rate will be selected at the current design baseline.

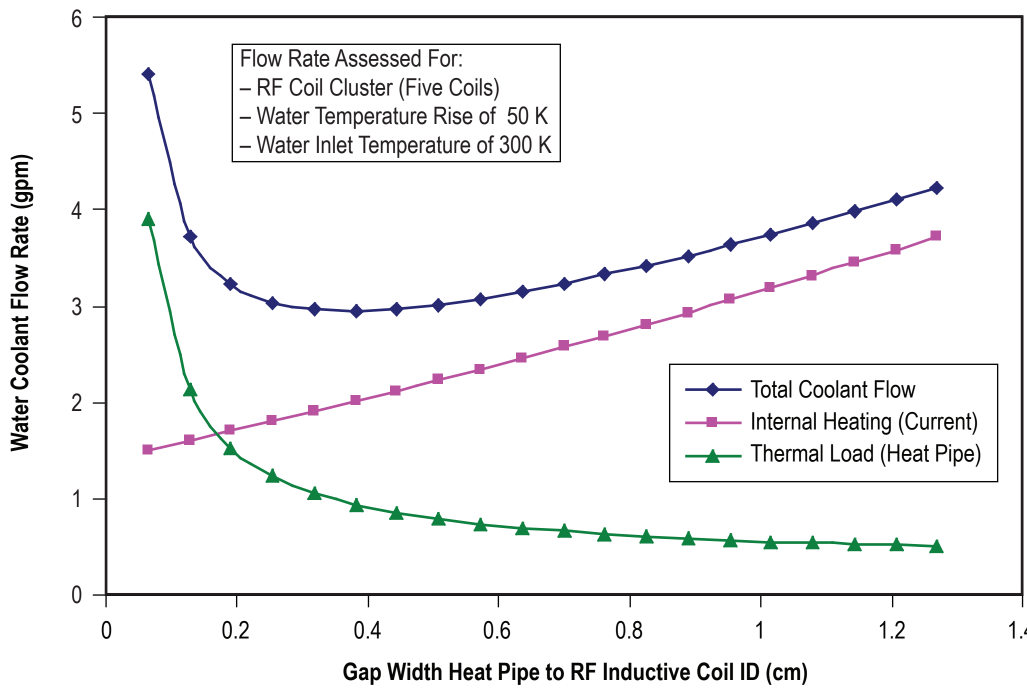

Figure 14. Radio frequency inductive coil cluster (five coils) required coolant water flow rate.

4.3.3 Radio Frequency Inductor Coil Modeling

To estimate the RF system heating capability and to establish voltage, current, and frequency requirements, a quick assessment was performed using both one- and two-dimensional modeling by Goldstein.[18] As identified in previous sections, it is important from a voltage breakdown and thermal loss standpoint to keep the inductive coil as far from the heat pipe evaporator section (or other grounded components) as possible. It is also critical to examine the effects of mutual inductance coupling on neighboring RF inductive coils (within the pentagonal array) and structural shunting components, such as the calorimeter assembly (positioned in close proximity). The modeling effort requires material resistivity data for the components of interest, including the Mo-Re heat pipe envelope and a thin layer of Na working fluid that is held along the interior surface of the heat pipe wall by the wick structure. These data are provided in appendix G. The only data readily available for Mo-Re was for a Mo-50%Re alloy. However, from an electrical standpoint, it should be nearly equivalent to the 44.5%-Re content material used in the heat pipe design. For all simulations, total RF power was estimated—coil losses and induced part power—using the 3-kW conditions. This assessment did not account for losses in interconnecting busswork, i.e., between the coils and to the power supplies.

An initial one-dimensional simulation was performed using the ELTA software package (Electro-Thermal Analysis marketed by BNV Corp.) to map out the general relationship between controlling parameters with a minimum of effort. This analysis assumes a 6.5-cm-long, single-turn inductive coil covering the evaporator which is at a temperature of 1,373 K. The goal of the initial effort was to determine the influence of applied RF on power transfer, required voltage, and efficiency for three offset gap widths (3.2, 6.4, and 9.6 mm). Results of the one-dimensional simulation are shown in figures 15–17. Initial estimates indicate that acceptable efficiency is reached above 10 kHz with a maximum at 20 kHz. (This range results from the hollow tube, which does not require the RF energy to penetrate deeply.) There is an ≈15% spread in efficiency between the 0.32 cm (0.125 in) and 0.96 cm (0.375 in) gap widths, with the smaller gap having higher efficiency. Required RF supply power is very high at low frequencies—expected due to low efficiency. The required supply power becomes approximately constant above a frequency of 10 kHz with minimal variation due to gap width. Coil voltage is notably sensitive to both gap width—gap becomes comparable with coil diameter—and supply frequency, producing higher voltage drops at large gaps and high frequency. A single coil is assumed for this analysis. In the actual application, a two- to three-turn coil would be employed. This design will result in a higher voltage for an equivalent power (voltage scales with inductor turns).

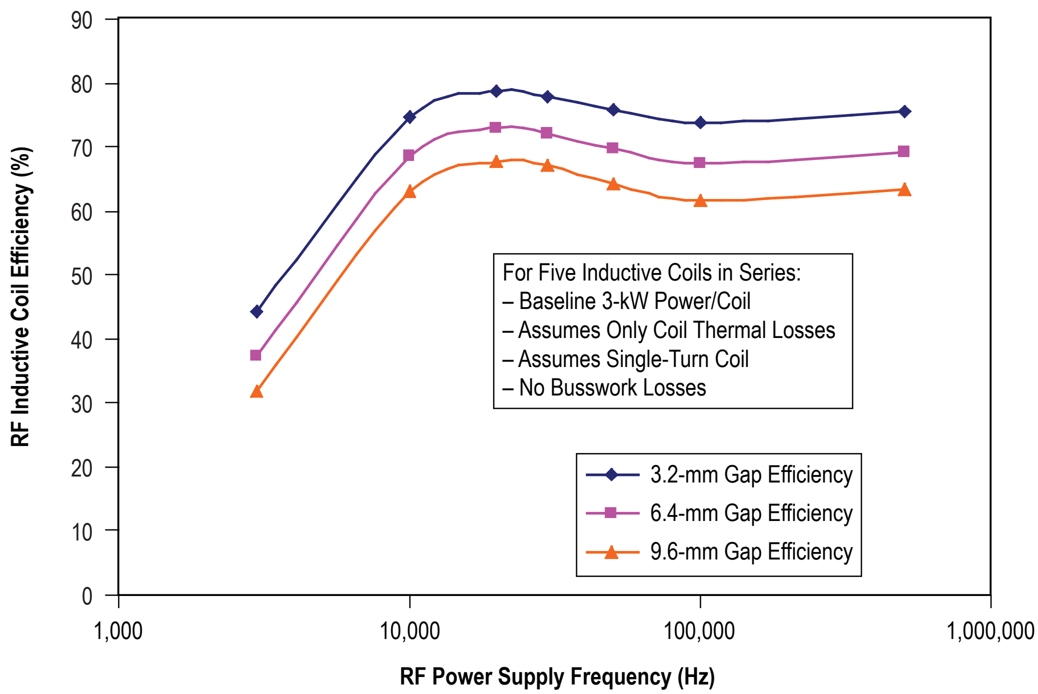

Figure 15. One-dimensional simulation results for inductive coil efficiency.

Overall, required power increases with increasing gap widths above 0.32 cm because the reduction in electrical efficiency is stronger than the higher thermal efficiency (material resistivity). However, the difference between 0.32- and 0.64-cm gaps is very small. In the actual test design, it is expected that the maximum efficiency will be shifted to slightly higher frequency due to electromagnetic effects. Required power supply output should be in the range of 20 to 25 kW at a properly tuned frequency (in the 25- to 40-kHz range) with a reasonable gap width set to 0.64 cm. The internal coil power loss as a function of gap width (eq. (17)) was established by curve fitting the difference in RF supply output power and the power induced in the heat pipe at 30 kHz for the gaps identified in figure 16. To accomplish this, the power supplies should be capable of providing an output frequency up to 50 kHz at 50 kW with an output voltage of 400 to 500 V. The design point is approximately one-half of the full output power so that overall thermal losses can easily be overcome. In addition, the supplies must be

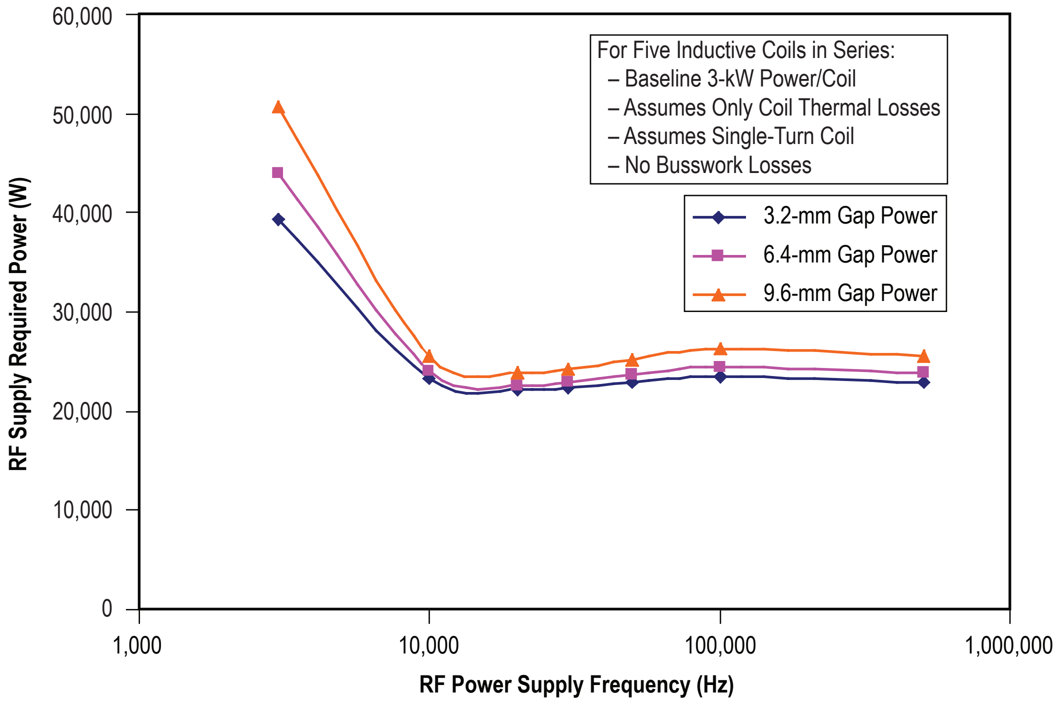

Figure 16. One-dimensional simulation results RF power supply output requirement (five coils).

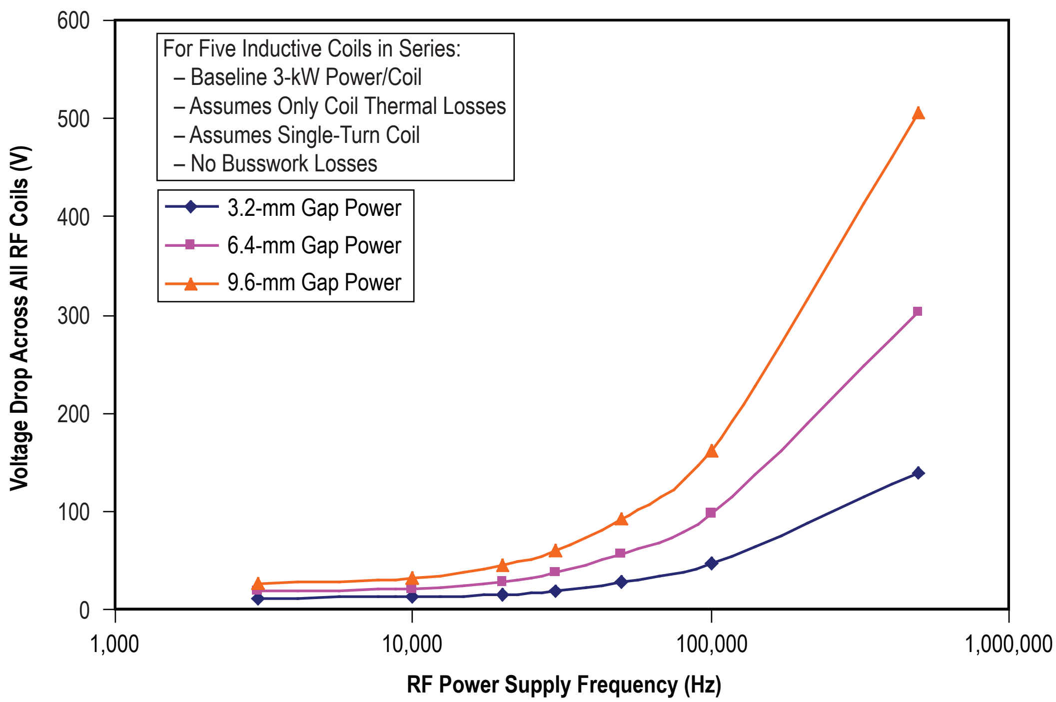

Figure 17. One-dimensional simulation results—coil assembly required voltage (five coils).

equipped with variable output transformers with turn ratios of 2:1, 3:1, and 4:1 to adjust the required output voltage to the test chamber clusters. For the final setup of the 3-kW case (used in test chamber clusters 1 and 2), it is expected that the clusters will make use of three-turn inductive coils. To provide for the various RF power levels within test chamber cluster 3, it is expected that a two-turn inductor will be used for the single 1,000-W coil, a three-turn inductor for the two 2,000-W coils, and a four-turn inductor for the two 4,000-W coils. Appendix H provides a spreadsheet summarizing the results of the one-dimensional simulations.

After establishing the general operating parameters using the one-dimensional model, a two-dimensional model was generated (using Flux2D® software marketed by CEDRAT Technologies) to examine the performance of a three-turn inductor for the 3-kW RF coil case. This model also examined shunting between the inductive coil and the heat pipe calorimeter, which is in close proximity, and the mutual inductance shared with neighboring coils. A total of four cases were modeled:

(1) Inductor with no neighboring coils; flux concentrator applied for shielding.

(2) Inductor with no neighboring coils; no concentrator.

(3) Inductor with a 3.5-in distance from centerline to centerline; flux concentrator applied for shielding.

(4) Inductor with a 3.5-in distance from centerline to centerline; no flux concentrator.

Results for each of these simulation cases are shown in figures 18–21, with tabulated data provided in appendix I. The benefit of using a flux concentrator is immediately evident. Magnetic field lines are contained primarily to the concentrator and heat pipe (figs. 18 and 20), providing more uniform heating across the heat pipe evaporator and lower overall power consumption. Without a concentrator, the power density at the heat pipe evaporator will be shifted to the back of the inductor due to shunting from the calorimeter (fig. 19). This leads to nonuniform loading along the heat pipe evaporator. With the concentrator, the power density distribution is nearly uniform and symmetric. In addition, coupling to the calorimeter is significantly reduced, dropping from 70 W without a concentrator to 6 W with a concentrator. (See tabulated data in app. I.) The concentrator also limits mutual induction or “cross talk” between the coils in the areas where the inductors are close (figs. 20 and 21).

In summary, flux concentrators provide sufficient shielding to render azimuthal variation of power in the evaporator and losses due to the calorimeter negligible. Without concentrators, the induction coil would need to be moved farther from the calorimeter and the inductors spread farther apart. Another advantage of applying the magnetic flux controller is that the coil current demand will be reduced (≈14%). This means that the losses in the busswork and other supplying circuitry will be significantly reduced (by ≈30%, proportional to I^2 heating), allowing more power to be available to overcome uncertainty in overall thermal losses. A heat pipe to inductor coil gap width on the order of 0.64 cm (0.25 in) is suitable from a thermal, voltage breakdown and RF power perspective and will be established as the current baseline.

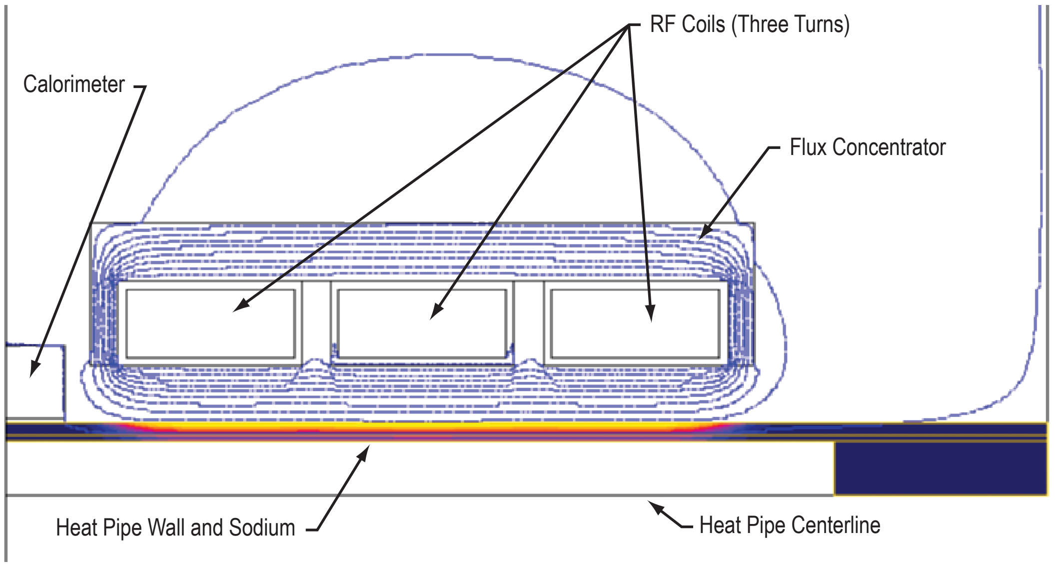

Figure 18. Radio frequency coil with flux concentrator in open space.

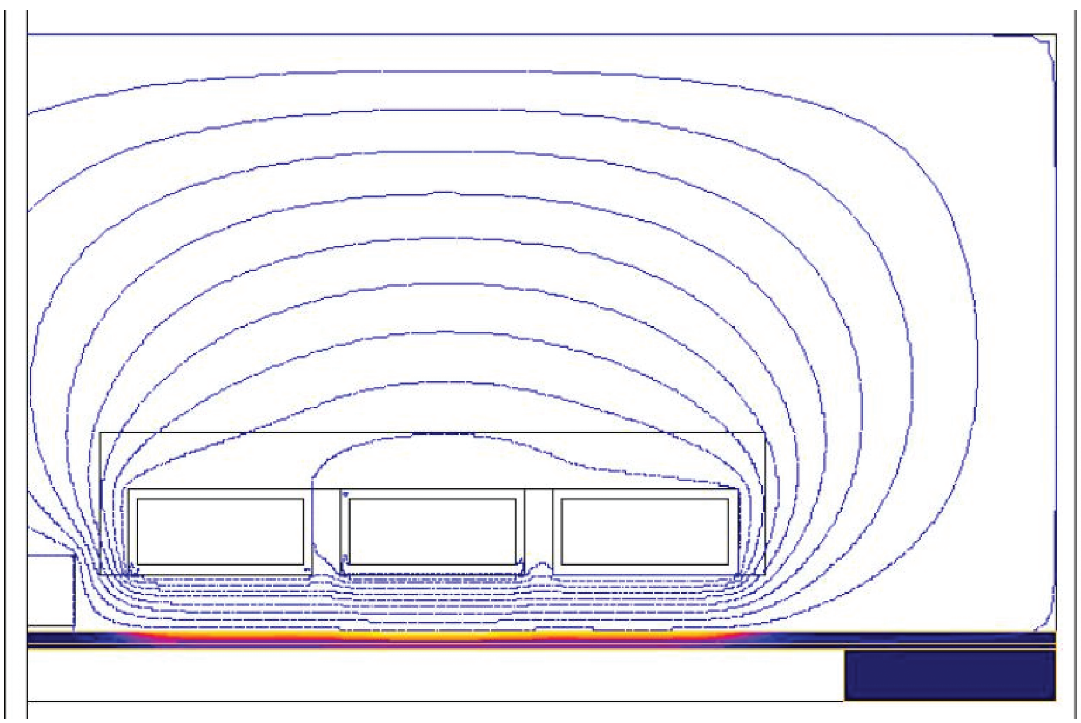

Figure 19. Radio frequency coil without flux concentrator in open space.

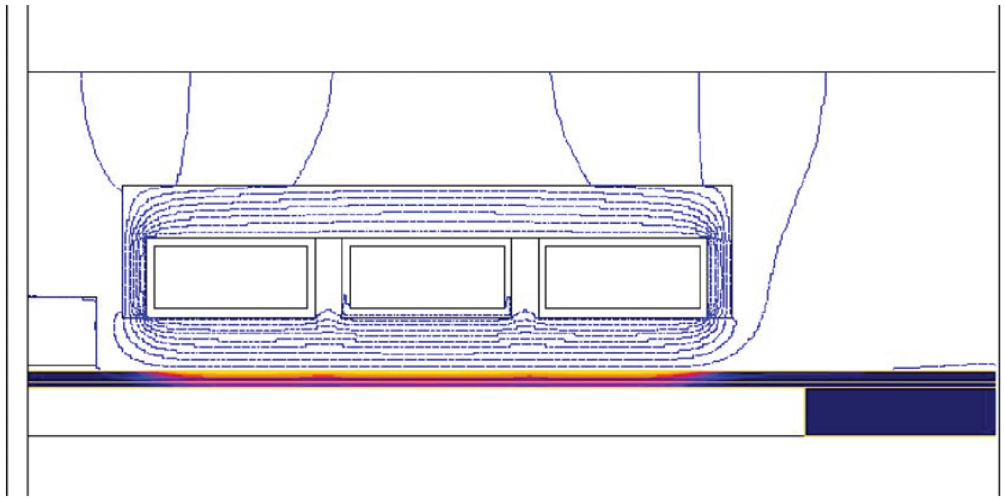

Figure 20. Radio frequency coil with flux concentrator; close to neighboring inductor.

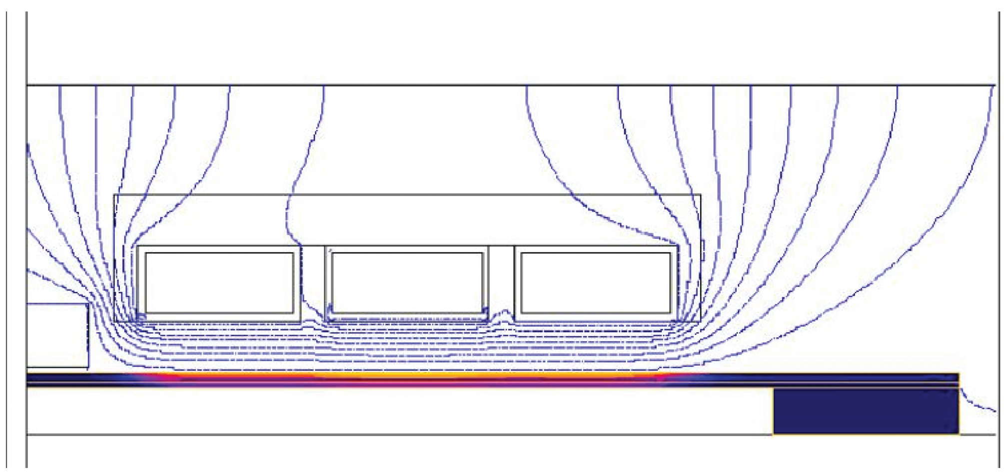

Figure 21. Radio frequency coil without flux concentrator; close to neighbor inductor.

4.4 Overall Radio Frequency Power System Layout

The general RF power subsystem hardware configuration is illustrated in figure 22. This layout is composed of several primary subsystems, including the following:

• Radio frequency inductive coil assemblies (clusters) with vacuum-compatible feedthroughs.

• Radio frequency power distribution busswork connecting the power supplies to the chamber.

• Radio frequency power supplies.

• Water cooling for both the power supplies and the RF inductive coil assemblies.

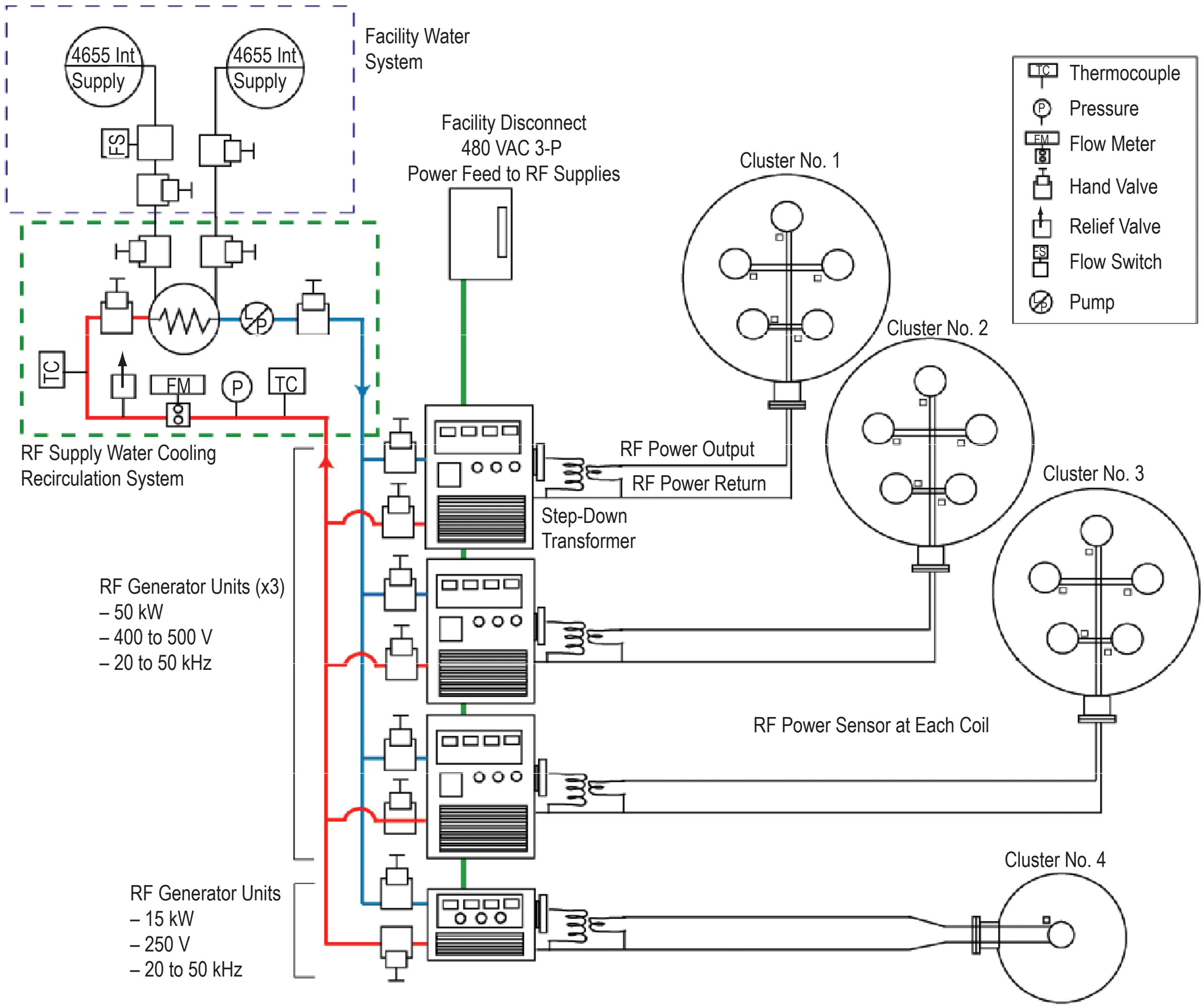

Figure 22. General RF power subsystem hardware layout.

There is a total of four RF coil assemblies, three of which are clusters (composed of five series connected coils) and one as a single element. All RF assemblies are positioned within the environmental test chamber and supported structurally by the RF power feed configuration. Total power flow through the inductor assemblies will be measured at the power supply; however, an attempt will be made to incorporate a power sensor at each RF inductive coil—the type and geometry are to be determined. The final design and fabrication of these complete RF coil assemblies with connecting busswork will be pursued through an open solicitation with a procurement specification discussed in the following section.

The RF coil assemblies are connected to the power supplies using a buss network and variable transformers to step down the power supply natural output voltage (typically 400 to 500 V) to a level sufficiently low to prevent a voltage breakdown condition. Each of the RF clusters is connected to a separate solid state RF power supply; three of these units are rated at 50 kW (powering clusters 1, 2, and 3) and one unit is rated at 15 kW (powering cluster 4). All power supplies and RF inductive coil assemblies require cooling that is provided by a closed-loop water circulation system that exchanges heat energy with the facility water system. This closed-loop water system provides a well-controlled interface to the facility, necessary for long-term reliable operation of the test equipment. This eliminates the possibility of transporting debris, etc. into the RF cooling system. It also provides for a more graceful shutdown should the facility system lose power. (There is excess cooling capacity in the circulation loop that can absorb heat as the RF supplies are shut down.) The typical temperature of the facility water system varies, depending on time of year. The primary storage tank is placed outside the building and will require a small water-cooling tower cell for the extended operations expected with this project.

Instrumentation will be provided to monitor the temperature and flow of the facility and recirculation cooling loops. The power supplies are equipped with internal detection systems to monitor the coolant flow to the RF inductive coil assemblies. Temperature measurements will make use of type K thermocouple probes. Flow rates will be measured using either turbine or mass flow meters (cost dependent). Flow switches will be used in lines that only require a flow indication, e.g., where the actual magnitude of the flow rate is unimportant. For instance, a flow switch may be incorporated in the facility feed lines. The RF power supplies are outfitted with control boards that provide for zero to 10-V input and output signals to control/monitor voltage, current, frequency, and power. This allows for remote computer-based control and monitoring.

4.5 General Procurement Specifications

Procurement specifications have been generated to cover several of the primary components necessary to complete the assembly and operation of the proposed heat pipe test system. These procurements will be issued by MSFC using full and open competition. The final evaluation of vendor quotes will be based on the lowest cost technically acceptable approach. The primary requirement areas include the following:

(1) Design and fabrication of RF inductive coil assemblies and power feed systems. This will include all four RF clusters—each test chamber section—with busswork to connect each RF coil cluster to a power supply. This requirement also includes instrumentation to monitor overall performance, such as sensors strategically positioned to monitor individual coil power. Appendix J contains the detailed RF inductive coil assembly procurement specification. Typical vendor delivery time is 12 to 18 wk.

(2) Closed-loop recirculation system to provide coolant to all RF power supplies and their inductive coil assemblies. The system will be a commercial off-the-shelf item, such as the Compact WRS (marketed by Inductoheat) which includes a pallet-mounted heat exchanger, pump, storage tank, stainless steel lines/tank, and cooling control relays. It is designed for long-term continuous operation. Typical vendor delivery time is 6 to 8 wk.

(3) Small RF power supply with 15 kW at zero to 60 kHz output to enable testing of the high-power heat pipe (cluster 4). The unit is a commercial off-the-shelf item such as the solid state Flexitune 15+ (marketed by Inductoheat) capable of 24/7 operation at 100% duty cycle with an internal control board providing zero to 10-V input and output signals allowing for remote monitoring and control. Typical vendor delivery time is 8 to 10 wk.

(4) A small cooling tower cell will be required to maintain cooling of the primary water supply. A unit on the order of 75 to 90 kW is sufficient to maintain a constant coolant temperature. Commercial

off-the-shelf items such as the TC-30-230, a 30-ton sheet steel unit, or a TC-45-F-230, a 45-ton fiberglass unit, both marketed by Advantage Engineering Inc. are suitable for this application. Both provide up to 90 gpm with a processed water temperature of 300 to 310 K. Typical vendor delivery time is 2 to 4 wk.

(5) Plumbing components such as valves, including hand and remote operated, fittings, gauges, and structural material for setup and operation of the RF cooling circuit components. These will be ball-type valves making use of either compression or pipe fittings. In addition, pressure-relief valves are required. Valve material will be stainless steel with soft goods compatible with water service and includes appropriated flow and temperature sensors. Typical vendor delivery is 2 to 4 wk.

(6) Part fabrication and assembly at machine shops, as required to complete system.

(7) Radio frequency power sensors/meters includes instrumentation to monitor overall performance, such as sensors strategically positioned to monitor individual coil power, structural supports, etc. to route busswork, and additional feedthroughs for instrumentation—temperature, power sensors, and optical. These are typically off the shelf with delivery ranging from 4 to 8 wk.

5. PURIFIED INERT GAS CONDITIONING SYSTEM

The ambient oxygen concentration is critical to the lifetime of refractory metals operated at increased temperature for a relatively long time. For the proposed testing, the refractory metal components will be operated in a low-pressure, ultra-high-purity (UHP) noble gas environment (Ar and He mixed to a predetermined partial pressure of each gas) so that the thermal coupling between the heat pipe and calorimeter can be controlled. To achieve the desired gas purity, successive dilutions and pumpdown of the system are required. The pumpdown procedure will also include an initial bake-out of the system at ≈525 K to drive off water vapor (and other volatiles) from the gas lines, vacuum chamber, and test components. A generally accepted vacuum level for testing Mo-Re alloys is in the 10^{-6} torr range. Given a direct pumpdown from air to 10^{-6} torr, the oxygen concentration is 0.28 ppb in the vacuum test environment. Hence, the target maximum oxygen concentration in the test chambers will be 0.28 ppb at the desired operating pressure of ≈76 torr (the set pressure used in calculating gas conditioning requirements).

5.1 Sizing and Performance

As discussed in report *NASA/TP—2010–216435*,[1] a series of calculations was performed to assess the oxygen concentration in the heat pipe test chambers over successive dilutions with UHP fill gas, assuming an initial oxygen concentration of 209,500 ppm in the air filling the test chambers (20.95% oxygen by volume). Calculations were performed assuming three cylindrical test chambers having approximate dimensions of a 24-in diameter (23.625 in ID) by 36-in length (total volume 48,000 in^3 (0.78 m^3) for all three chambers). These test chambers will be used for the 1-, 2-, 3-, and 4-kW heat pipe tests. An additional smaller chamber will be constructed for the 5-kW heat pipe test. All heat pipe life testing will be performed with a low-pressure fill of mixed He and Ar in the test chambers. The UHP He and Ar, purchased from Sexton Supply, Huntsville, AL, have a guaranteed minimum purity of 99.999%. The UHP He has a maximum oxygen content of 3 ppmv; UHP Ar has a maximum oxygen content of 1 ppmv.

To obtain the oxygen concentrations shown in figure 23, the test chambers are first pumped from atmospheric pressure to 10^{-3} torr, e.g., operating only the roughing pump connected to the test chambers. Note that the plots correspond to a 76-torr chamber pressure, the approximate pressure at which the heat pipe life tests will be performed. Initially, pumping the chamber to a pressure below the desired operating pressure results in a drastic reduction in the oxygen concentration from 209,500 ppm to 0.3 ppm at 10^{-3} torr. Direct pumpdown to only 76 torr reduced the oxygen concentration to approximately 2×10^4 ppm, as shown in figure 23 prior to fill with UHP gas at 76 torr. After this initial pumpdown, the chambers were backfilled to 76 torr of UHP He or Ar and again pumped down to 10^{-3} torr to further reduce the oxygen concentration in the test chambers. After just two dilutions with UHP gas (He or Ar), the test chambers reach the minimum purity level achievable, given the purity of the supply gas. While these calculations ignore any additional contamination from impurities in the lines and test chamber, they do provide an ultimate baseline for the minimum achievable oxygen concentration for a given fill gas and operating pressure without additional gas purification. The test procedure will also include an initial bake-out of the system (under vacuum), which will assist in driving out

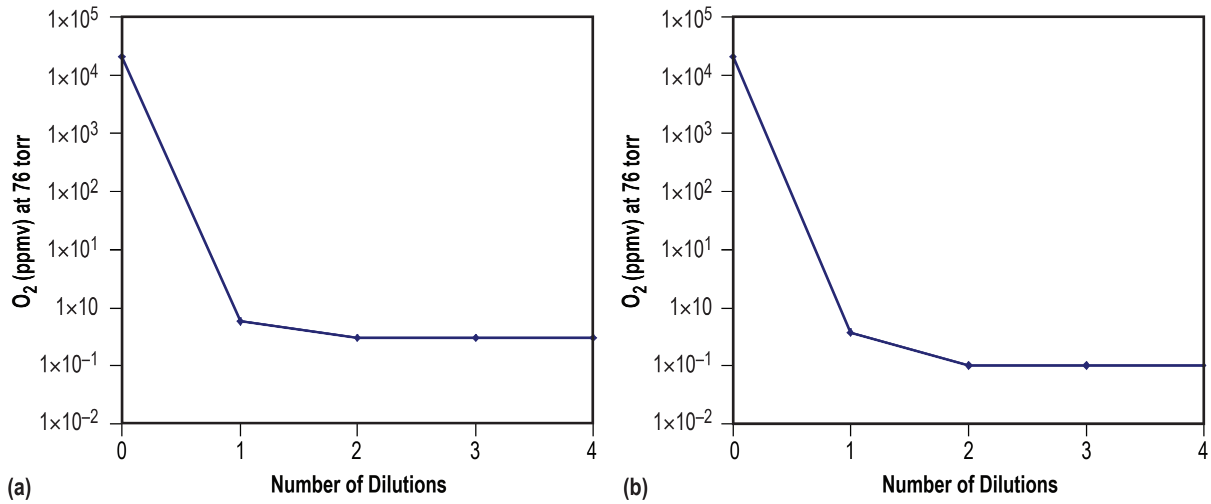

Figure 23. Oxygen concentration (ppmv) in the heat pipe test chambers following successive dilutions with (a) UHP He or (b) UHP Ar fill gas.

volatile impurities, primarily water if the system is thoroughly cleaned and degreased, from the test components and fill lines to reduce additional impurities in the system. For additional discussion on system bake-out and the suggested test procedure, refer to sections 5.1.2 and 5.1.4.

The 5-kW heat pipe life test will be performed in a smaller test chamber having an approximate diameter of 12 in and a length of ≈36 in, yielding a total volume of 1,296 in^3 (0.021 m^3). Because the same supply gases will be used in this chamber, the ultimate minimum purity level of the fill gas will be limited to the same levels shown in figure 23 (0.3 ppm O_2 for He, 0.1 ppm O_2 for Ar) without additional gas purification.

As discussed in *NASA/TP—2010–216435* (Design of a Refractory Metal Life Test Heat Pipe and Calorimeter, sec. 4.2.1), the gas mixture will be selected to achieve the desired gas conductivity across the gap between the heat pipe condenser and the calorimeter.[1] The gas mixture selected for the lower power (1–4 kW) heat pipe tests was He-32%Ar (molar fraction). The increased heat flux for the 5-kW test and the minimum gap width established for fabrication purposes (0.020 in) requires that the Ar content in the gas mixture be reduced to 6% (molar fraction) for this test. The partial pressure of each gas in the mixture is given by the molar fraction multiplied by the total gas pressure. For instance, for a total pressure of 100 psig and a 32% Ar mix, the partial pressure of Ar will be 32 psig and the partial pressure of He will be 68 psig. Partial pressures will be used to establish the proper gas ratios in the He/Ar mixing procedure.

5.1.1 Gas Purification

Additional purification of the UHP gases will be required to meet the required oxygen concentration of <0.28 ppb (comparable to 10^{-6} torr) for testing Mo-Re alloys. To accomplish this purification, an SAES ambient temperature microtorr gas purifier will be used to clean the incoming gases and an SAES monotorr point-of-use purifier will be incorporated in the test chamber recirculation system. Figure 24 illustrates a conceptual layout of the test chamber gas purification system.

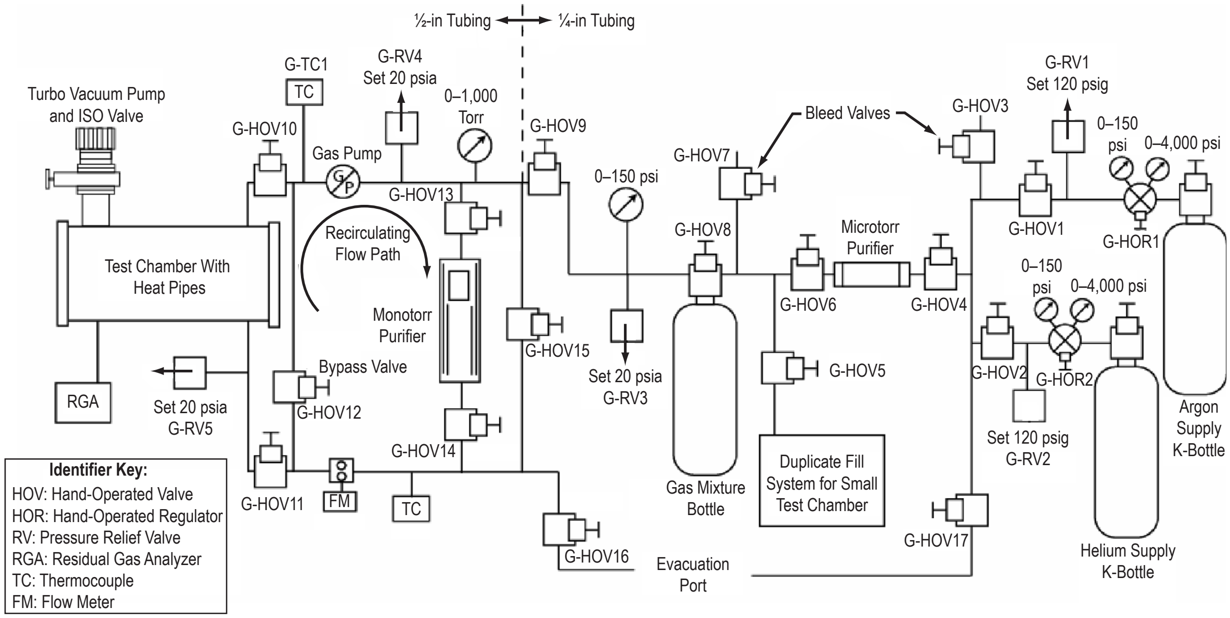

Figure 24. Test chamber gas mixture and purification system.

The design of the gas mixture and purification system is such that the recirculating gas system can be fully isolated from the gas mixing/fill system using the hand valve G-HOV9, allowing the gas mixture bottle to be charged with an appropriate He/Ar mixture prior to test chamber fill. The small test chamber fill system will be connected to the main fill system just after the microtorr purifier (G-HOV5 opens the fill line to this chamber), such that the same He and Ar supply bottles and initial purification system may be used for both systems. The premixed fill gas can be mixed to the desired partial pressures of He and Ar to meet both test requirements using separate gas mixture bottles and recirculating gas systems.

The microtorr purifier, which has an advertised performance for purifying both He and Ar to a final oxygen concentration of 1 ppb, will be employed on the inlet flow line. Over multiple gas dilution cycles, this new value of oxygen concentration in both He and Ar produces the trends shown in figure 25. After only two dilution cycles, starting from atmospheric pressure, the final oxygen impurity concentration is just 0.1 ppb at a 76-torr test chamber pressure. This condition meets the acceptable oxygen concentration (≈0.28 ppb) for testing Mo-Re alloys.

The valves selected for the inlet low-temperature, high-pressure side of the gas purification system will be stainless steel Swagelock SS-4H bellows valves having a ¼-in tube fitting on both the inlet and outlet ports. These valves have a maximum temperature rating of 315 ºC (590 K) and a maximum pressure rating of 1,000 psig. The low-pressure recirculation system will use ½-in stainless steel tubing and all valves will be Swagelock SS-8BW-V47. These valves use VCR fittings and are less prone to leakage, making them appropriate for long-term use on the recirculation system. Details of all system components are provided in appendix K.

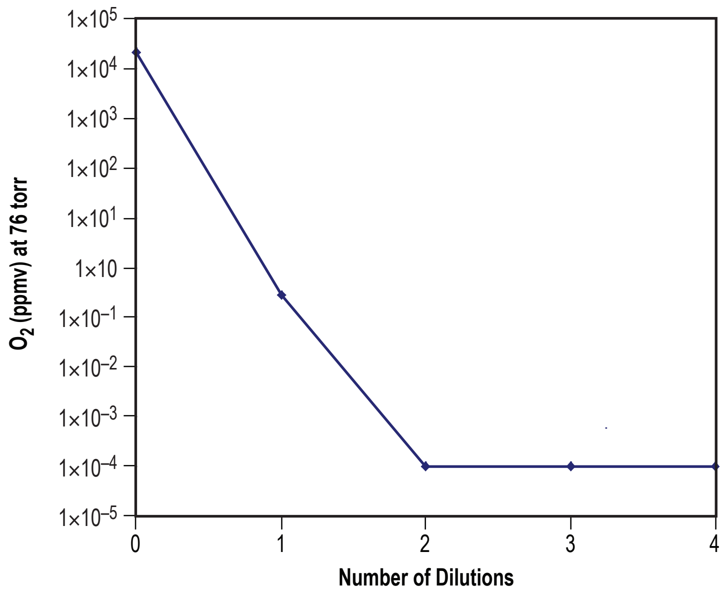

Figure 25. Final oxygen concentration in the heat pipe test chambers with UHP gas, purified using an inline SAES microtorr ambient gas purifier to 1 ppb O_2 prior to chamber inlet.

The "gas mixture bottle" will be limited to a maximum pressure of 100 psi (0.69 MPa) to prevent overpressurizing any system components. The microtorr purifier located just upstream of the gas mixture bottle has a pressure limit of 150 psi and pressure relief valves on the fill lines (G-RV1 and G-RV2) will be set to 120 psi. The mixed gas will be used to fill the three larger test chambers at a pressure of ≈76 torr (0.10 MPa). The volume of a single test chamber (ID = 23.625 in, L = 36 in) is given by:

$$V=\pi * (23.625\ \text{in})^2 * 36\ \text{in}/4=15{,}781\ \text{in}^3=0.259\ \text{m}^3\ . \tag{19}$$

Hence, the total volume of the three test chambers that are to be filled by the gas mixture is 0.78 m^3. Ignoring any volume of gas trapped in the flow lines and applying the ideal gas law, $pV=nRT$, the desired volume of the gas mixture bottle can be obtained:

$$p_{chamber}V_{chamber}=p_{bottle}V_{bottle}$$

$$(10{,}000\ \text{Pa})\ (0.78\ \text{m}^3)=(690{,}000\ \text{Pa})\ V_2$$

$$\rightarrow V_2=0.011\ \text{m}^3\ . \tag{20}$$

To allow for multiple dilutions of the fill gas in the test chambers, the gas mixture bottle should have sufficient capacity for at least three complete fills of the test chambers at 76 torr (0.10 MPa). Hence, the total volume of the gas mixture bottle for the three large test chambers should have a minimum volume of 0.033 m^3, which corresponds to an approximate 34-L water capacity. A steel H-bottle (DOT specification 3AA), rated to a maximum pressure of 2,015 psi, has an approximate volume of 43.4 L of water, meeting the minimum requirements for the mixed gas cylinder. Specifications on this cylinder are included in appendix K.

To maintain the purity level of the test chamber environment during test operations, an SAES monotorr point-of-use purifier with a recirculation pump will be incorporated in the recirculating gas loop. During chamber fill, the monotorr will be isolated from the flow path. After sufficient dilutions have been performed for the test chamber gas and the desired pressure achieved, valve G-HOV9, which separates the gas fill and recirculating systems, should be closed. An additional series of valves is provided to allow recirculation of the gas in the test chambers with or without incorporation of the monotorr purifier (by closing G-HOV13 and G-HOV14 and opening G-HOV15). The test chambers may be bypassed by closing G-HOV10 and G-HOV11 and opening G-HOV12.

Within the monotorr purifier, getter materials are used to irreversibly trap gaseous impurity molecules. These impurities are captured on the surface of the materials and, upon heating, diffuse into the bulk of the getter. Note that if the filters inside the monotorr are inadvertently exposed to air, the filters will be immediately filled, and the unit will require extensive overhaul before it can be applied again in the purification loop. The internal heater within the monotorr device has an operating temperature of 400 °C; as a result, gas exiting the monotorr will have an elevated temperature up to as much as 400 °C, which may require that the lines be cooled by water circulation downstream of the monotorr. For this reason, the gas pump is located upstream of the monotorr purifier to prevent overheating of the pump internals. When used with Ar or He, the monotorr purifier can remove molecules of H_2O, O_2, H_2, CO, CO_2, N_2, and hydrocarbons. The performance of the purifier is dependent on the pumping speed at which it is operated. Table 10 provides a summary of the performance guarantee for the SAES monotorr phase II 3000 for rare gases.

Table 10. SAES monotorr phase II 3000 performance guarantee for rare gases.

	Pumping Rate	
Impurity	0–20 slpm	20–50 slpm
O_2	<1 ppb	<1 ppb
H_2O	<1 ppb	<1 ppb
CO	<1 ppb	<1 ppb
CO_2	<1 ppb	<1 ppb
N_2	<1 ppb	<10 ppb
H_2	<1 ppb	<10 ppb
CH_4	<1 ppb	<10 ppb

The gas pump on the recirculating gas purification system will be specified to provide a volumetric flow rate of up to 20 slpm at a system pressure of ≈0.1 MPa. At this operating pressure, a gas temperature of ≈300 K, this corresponds to ≈207 alpm (actual liters per minute). To convert this volumetric flow rate into a mass flow rate for the He/Ar mixture, the density of the mixture must be determined at the specified test conditions. Assuming no particle interactions in the gas mixture, the mixture density is given by

$$\rho_{\mathrm{mix}} = \frac{\rho_{\mathrm{Ar}} V_{\mathrm{Ar}} + \rho_{\mathrm{He}} V_{\mathrm{He}}}{V_{\mathrm{Ar}} + V_{\mathrm{He}}} \quad . \tag{21}$$

The density of pure He at 300 K and 0.1 MPa is 0.016 kg/m^3; that of pure Ar is 0.16 kg/m^3. For the He-32%Ar mixture, the calculated mixture density is 0.062 kg/m^3. Given this density, the maximum mass flow rate, corresponding to a volumetric flow rate of 20 slpm, of the gas mixture is 0.2 g/s. To put this rate into perspective, the total mass of gas in the three test chambers at 0.1 MPa is (0.78 m^3)*(0.062 kg/m^3) = ≈50 g. At the maximum mass flow rate of 0.2 g/s, it would require 250 s to fully cycle the gas in the test chambers. The calculated density of the He-6%Ar mixture is 0.025 kg/ m^3. This lower density results in a lower mass flow rate of 0.086 g/s at the same volumetric flow rate of 20 slpm.

Pressure relief valves have been incorporated throughout the gas purification loop for safety purposes. On the high-pressure side of the fill system, all relief valves (G-RV1, 2, 3) are set to 120 psig to prevent overpressure of the microtorr purifier (max 150 psig). All valves that will be used in this purification system are rated to a maximum pressure of 1,000 psig. The monotorr purifier is limited to a maximum of 100 psig, but the limiting pressure requirement will be that which can be placed on the test chamber. Because the chamber is designed to operate at subatmospheric pressure (14.7 psi), the relief valves on the recirculating lines (G-RV4, 5, 6) will be set to 20 psia. An additional relief valve is included within the recirculation loop to prevent overpressurizing the test chambers.

A rough calculation of the pressure drop around the recirculating gas loop was performed to ensure that it would not affect system operation. For this purpose, it is assumed that the length of tubing from the test chamber to the monotorr inlet was ≈4 ft (≈1.2 m) and from the monotorr exit back to the test chambers was ≈4 ft (≈1.2 m). The simplified flow loop for the pressure calculation is shown in figure 26.

The stated maximum pressure drop across the monotorr is <10 psi at the maximum flow rate of 50 slpm and the maximum rated pressure of 100 psig. Assuming that the pressure drop scales linearly with flow rate, as in a straight section of pipe, the pressure drop reduces to <4 psi, also at the maximum rated pressure of 100 psig. Recall that the recirculating loop will be operated at a pressure of ≈1.5 psig (≈76 torr). Again, assuming that the pressure drop will scale linearly with the system pressure, this reduces the pressure drop across the monotorr to ≈0.06 psig (414 Pa). Loss coefficients for additional system components are summarized in table 11.

The loop pressure drop is given by

$$\Delta p = \rho f \, {}^{L}\!/_{D} \, {}^{\bar{v}^2}\!/_{2} \ , \tag{22}$$

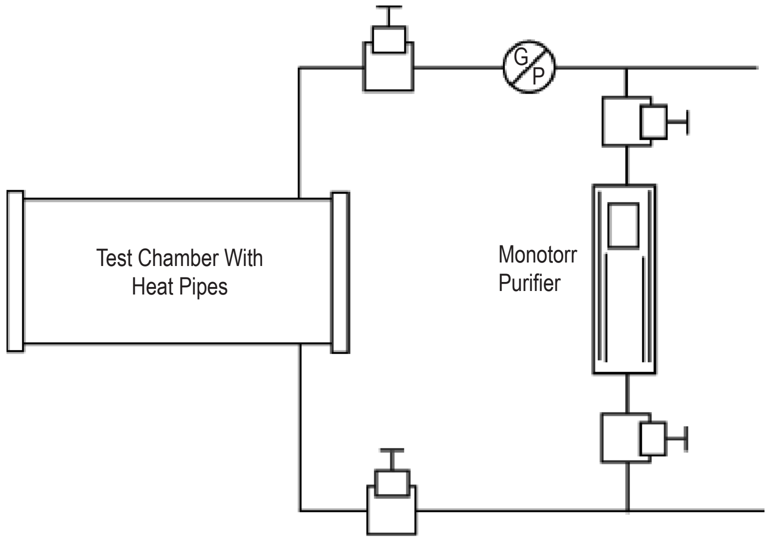

Figure 26. Simplified test loop for pressure drop calculation.

Table 11. Loss coefficients for system pressure drop calculation.

Component	Loss Coefficient or Equivalent Length
Chamber exit/pipe entrance	$K_{ent} = 0.5$
Elbow, 90°	$L_e / D = 30$
Tee, flowthrough branch	$L_e / D = 60$
Valves, bellows (approximated as globe valves)	$L_e / D = 350$
Chamber entrance/pipe exit	$K_{exit} = 1$

*Note: Loss coefficients provided in Fox and McDonald.[19]

where the friction factor for laminar flow (Reynolds number (Re) <2,300) is

$$f = {}^{64}\!/_{Re} \ , \tag{23}$$

and

$$Re = \frac{\rho \bar{v} D}{\mu} \ . \tag{24}$$

To include the major and minor head losses in the pressure drop, the relationship

$$h_l = K \ {}^{\bar{v}^2}\!/_{2} \quad \text{or} \quad h_l = f \ {}^{L_e}\!/_{D} \ {}^{\bar{v}^2}\!/_{2} \ , \tag{25}$$

and

$$h_l = \Delta p / \rho \, , \tag{26}$$

where L_e / D corresponds to the equivalent length of straight pipe, should be used. For the He-32%Ar mixture, having density 0.062 kg/m^3, viscosity 2.35×10^{-5} kg/m-s, and a maximum flow velocity of 27.1 m/s (at 20 slpm, 0.1 MPa, 300 K), the pressure drop becomes ≈25 torr (3,400 Pa) for ½-in tubing. This result neglects any possible pressure drop across the gas pump, as it has not yet been selected for this application. The pressure drop along the same path for the He-6%Ar mixture will be reduced due to ≈23 torr (3,100 Pa) due to the reduced gas density.

5.1.2 System Bake-Out

The test procedure will include an initial bake-out of the system (under vacuum), which will assist in driving out volatile impurities, primarily water if the system is clean and degreased, from the test components and fill lines to reduce additional impurities in the system. An endothermic process, desorption (or outgassing) is accelerated by increased temperature. The rate at which gas appears to emanate from a surface is referred to as the outgassing constant. This value is usually given in torr-L/s-cm^2. It is advisable to begin a degassing program by first pumping down the system at room temperature to remove physically adsorbed water before commencing the baking cycle. If heat is applied at atmospheric pressure, it could result in activated chemisorption of physically adsorbed gas, which would require a prolonged heating cycle to remove.

In *Vacuum Technology*, Roth summarized several works that have determined the outgassing rate for stainless steel under various conditions.[20] Edwards reports that the upper bound for the outgassing rate of low surface area metals, such as stainless steel, is 1.7×10^{-5} torr-L/s-cm^2.[21] As the baking/air-exposure cycle is repeated, Odaka et al. report that a constant minimum outgassing rate for stainless steel 316L is achieved in just a few cycles.[22] The minimum rate measured by Odaka et al. was 1×10^{-13} torr-L/s-cm^2. The outgassing rate for stainless steel can also vary based on the surface treatment in addition to the temperature cycling history. Data compiled by Roth indicate the approximate ranges of outgassing rates for stainless steel that are summarized in table 12.[20] Note that untreated, degreased, and polished samples were outgassed over 4 to 8 hr of pumping. The baked condition experienced the baking cycle summarized in table 12.

Table 12. Approximate outgassing rates of stainless steel as reported in Roth.[20]

Material Treatment	Outgassing Rate (q_D) (torr-L/s-cm^2)
Untreated	$\approx10^{-7}$–10^{-8}
Degreased	≈1–7×10^{-9}
Polished	$\approx10^{-9}$–5×10^{-11}
Baked High range q_D: 24 hr @ 300 °C Mid range q_D: 100 hr @ 400 °C Low range q_D: 3 hr @ 1,000 °C (bake-out cycles applied sequentially)	$\approx5\times10^{-11}$–10^{-14}

The three large test chambers alone have an approximate surface area given by:

$$\begin{aligned} SA &= 3[\pi DH + 2\,\pi D^2/4] \\ &= 3\,\pi[24\text{ in} \times 36\text{ in} + (24\text{ in})^2/2] \\ &= 10{,}800\text{ in}^2 = 7\times10^4\text{ cm}^2\ . \end{aligned} \tag{27}$$

At a chamber pressure of 76 torr, the maximum volume that will emanate from the untreated chamber surfaces would be approximately

$$(10^{-7}\text{ torr-L/s-cm}^2)\times(7\times10^4)/76\text{ torr} = 9.2\times10^{-5}\text{ L/s}\ . \tag{28}$$

If bake-out is performed at a pressure of 10^{-6} torr, the volumetric outgassing rate becomes 7×10^3 L/s, but with significantly lower vapor density. Increasing the chamber wall temperature decreases the outgassing rate to $\approx10^{-11}$ to 10^{-14} torr-L/s-cm^2, depending on the temperature and elapsed time for the bake-out. At 10^{-6} torr, this corresponds to approximately 0.7 to 7×10^{-4} L/s. To interpret these outgassing rates, the density of the water vapor at the pressure and temperature for each condition must be taken into account to determine the mass of water vapor emanating from the chamber surface per unit time. These results are summarized in table 13.

Table 13. Approximate volume and mass of water vapor emanating from the three large test chamber surfaces per unit time.

Test Condition	Density of Water Vapor (g/m^3)	Volumetric Outgassing Rate (L/s)	Mass of Water Vapor Leaving Chamber Surfaces per Time (g/s)
300 K, 76 torr	72	9×10^{-5}	6.5×10^{-6}
300 K, 10^{-6} torr	9.4×10^{-7}	7×10^3	6.6×10^{-6}
570 K, 10^{-6} torr	4.9×10^{-7}	7×10^{-1} (low range) 7×10^{-4} (high range)	3.4×10^{-10} 3.4×10^{-13}

Note: Density assumes that water vapor can be represented as an ideal gas.

Table 13 illustrates the significant reduction in the mass of water vapor leaving the surfaces of the test chamber after extended baking at elevated temperature. Therefore, test procedures will include a bake-out of the test chamber and all flow lines at 250–300 ºC for up to 24 hr prior to chamber fill with UHP gas.

5.1.3 Gas Sampling: Residual Gas Analyzer Mass Spectrometer

Residual gases in a vacuum chamber derive from the original gas content of the chamber, gas emission from the chamber walls or from hardware in the chamber, or leaks from the outside of the chamber. To determine the actual gas content in the heat pipe test chambers and to assess the effectiveness of the bake-out and gas purification processes, a residual gas analyzer (RGA) will be employed to verify the partial pressure of various gaseous components in the test chambers throughout test.

A Dycor Dymaxion Mass Spectrometer made by Ametek Process Instruments (model DM100M) will be employed in the heat pipe life test system. All mass spectrometers measure a current that is either directly due to or is derived from ions produced in a source and selected by some mass to charge selection device. The Dycor Dymaxion Mass Spectrometer utilizes a quadrupole mass analyzer. A hot filament in the RGA is used to create electrons of a suitable energy. These electrons then generate a stream of ions, where the rate depends on the pressure, temperature, and species of the individual molecules. The stream of ions is then electrostatically focused toward the mass filter. A quadropole mass filter consists of four metal rods having a time-varying electrical voltage applied, selected to only ions of a particular mass to enter along the axis and to pass through to the opposite end. After passing through the mass filter, ions are focused toward a Faraday cup and the current is measured using a highly sensitive ammeter. The resulting signal is proportional to the partial pressure of the ion species that was passed by the mass filter. Because the current produced by residual gases is very small, a sensitive signal amplifier is also required in the system to detect very small partial pressures of the various gases that may be present. The Dycor DM100M can be used to detect masses up to 100 amu at a minimum detectable partial pressure of 5×10^{-12} torr.

A sampling system serves as a bridge between the sample environment and the vacuum environment of the mass spectrometer (10^{-4} to 10^{-9} torr). If the sample environment is at or below 10^{-4} torr, the sample can be analyzed directly. Higher pressure sample environments will require a pressure reduction sampling system. In these instances, a high-conductance inlet (HCI) can be fitted to the sample chamber. The HCI consists of a length of tubing that is installed between the sample chamber and the mass spectrometer inlet. When the sample chamber is between 10^{-4} torr and atmospheric pressure, an aperture inlet (AI) is employed. The AI consists of a small aperture within a valve that connects the sampling system to the vacuum environment. The high-conductance valve is first closed tightly before slowly opening the AI to evacuate the bypass arm. The aperture size and chamber pressure are directly related through eq. (29):

$$\text{Aperture size } (\mu) = 50/(\text{sample chamber pressure (torr)}) \quad . \tag{29}$$

Hence, for a maximum sample chamber pressure of 100 torr, the recommended aperture size is 5 μ. The Dycor User’s Manual also indicates that, for “atmospheric sampling” ($10-10^3$ torr), the RGA will require a capillary tube inlet (CTI) of varying length to accommodate the pressure of the application.

The Dycor DM100M is additionally equipped with RS-232 and RS-485 communications ports such that the RGA can communicate with the experimental system over a network. This feature allows for the RGA to be used for both the large test chambers and the smaller test chamber, as shown in figure 27. Solenoid-operated valves, which can be operated remotely, are included to allow automatically switching between the test chambers to sample the fill gas with the RGA. With both G-SOV1 and G-SOV2 closed, the RGA can be initialized and pumped down. To sample the gas content of the large test chamber, G-SOV1 would be opened and the RGA allowed to run for a predetermined sampling time. To switch over to the small test chamber, G-SOV1 would first be closed, the RGA allowed to operate for a period of time to clear the lines, and then G-SOV2 would be opened. To minimize both the cycle time and amount of removed chamber gas, the solenoid valves shall be located as close to the RGA as physically possible. The control system will include times at which the RGA should switch between

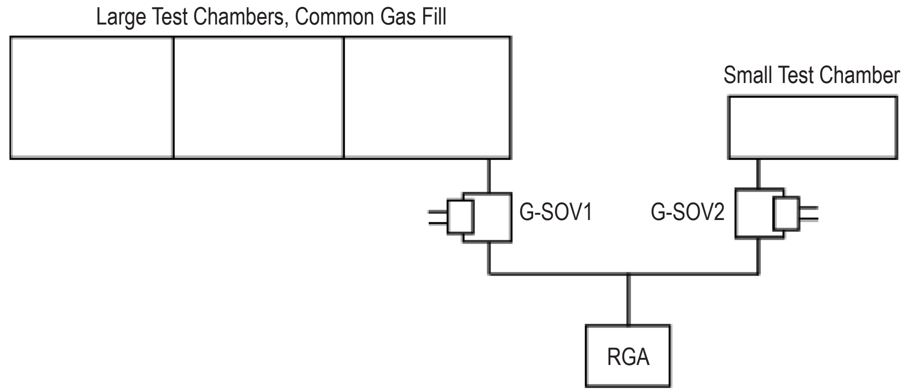

Figure 27. Residual gas analyzer sampling system.

test chambers, and will include engineering controls should the gas in the test chambers be out of the required bounds, e.g., high oxygen concentration.

5.1.4 Gas Fill and Test Procedure

A general procedure for initial pump-down, bake-out, and gas fill of the heat pipe life test chambers is provided below. Before performing bake-out operations, the test chambers and gas system components should be connected to a low-flow, high-purity inert Ar or N purge for 24 hr. This purge will assist the bake-out process by both sweeping out residual atmosphere and drying the internal surfaces of the test hardware. The purge should be shut down prior to initiating any of the following procedures. These general procedures are written for operation of a single heat pipe test chamber system. For additional test chambers, the procedures would be identical, with the exception of component identifier tags. All test chamber systems would share a common inert gas supply and microtorr purifier.

5.1.4.1 Gas System Bake-Out. The procedure for gas system bake-out includes the following:

(1) Check that all hand valves are closed prior to bake-out or initializing the gas purification system. Cycle G-SOV1 and G-SOV2 (to the RGA) to ensure that they are closed.

(2) Wrap all components downstream of G-HOR1 and G-HOR2 with heater tape to allow bake-out of the gas fill lines, valves, and mixture bottle. Strategically place thermocouples on the lines and components to monitor temperature. (Use the handheld thermocouple (TC) meter to read thermocouples.) Place at least one layer of aluminum foil over the heater tape to minimize thermal losses to the environment. (Note: The gas supply bottles and regulators are not included in this bake-out procedure as they are upstream of the purification system and the regulators cannot withstand the temperatures required for bake-out.)

(3) Evacuate the gas feed system using the evacuation port by opening G-HOV16 and G-HOV17. Then open valves G-HOV12, G-HOV15, G-HOV9, G-HOV8, G-HOV1, and G-HOV2 to rough down the complete feed system. (Note: Valves G-HOV13, G-HOV14, G-HOV4, and G-HOV6 should remain closed to protect the microtorr and monotorr units. These valves should only open when system is under vacuum or charged with inert gas.)

(4) Maintain pumping and achieve a vacuum condition of 10^{-3} torr or lower.

(5) Open the monotorr and microtorr isolation valves G-HOV4, G-HOV6, G-HOV13, and G-HOV14 to remove any residual inert gas contained in the purifiers.

(6) Maintain pumping and monitor the pressure (pressure should be 10^{-3} torr or lower); hold this condition for several hours.

(7) During the hold period, use a He leak detector to test all fittings and valves for leaks. Set the detectors range to read a minimum of 1×10^{-9} std cc/s He.

(8) Once leak check is completed and pressure has reached a stable low value, apply power to the heater tapes to increase the temperature of the gas feed system and all components to ≈250 ºC. Hold this temperature for a minimum of 12 hr. System bake-out of 24 hr is desirable.

(9) Monitor test chamber vacuum level; there should be an initial increase in pressure followed by a slow decay as the outgassing rate decreases.

(10) Turn off heater tapes and let system cool to room temperature; continue evacuating the system during cooling.

(11) Close the monotorr and microtorr isolation valves G-HOV4, G-HOV6, G-HOV13, and G-HOV14 to protect the purifiers.

(12) Close evacuation port isolation valves G-HOV16 and G-HOV17.

(13) The gas feed system is now ready to be charged with required gases.

5.1.4.2 Test Chamber Bake-Out. The following are procedures for test chamber bake-out:

(1) Verify that chamber isolation valves G-HOV10 and G-HOV11 are closed.

(2) Wrap the test chamber with heater tapes. Strategically place thermocouples on test chamber to monitor temperature. (Use the handheld TC meter to read thermocouples.) Place at least one layer of aluminum foil over the heater tape to minimize thermal losses to the environment. Also place heater tape on the RGA sensing lines up to the RGA internal isolation valve. (Note: Allowable bake-out temperature at the RGA interface is lower than that used on the rest of the system.)

(3) Evacuate test chamber using roughing/turbopump combination to a pressure of 10^{-6} torr or lower; monitor pressure.

(4) Open RGA isolation valves G-SOV1 and G-SOV2 such that the sensing line is evacuated up to the RGA internal isolation valve.

(5) Maintain pumping with a vacuum condition of 10^{-6} torr or lower and hold for several hours.

(6) During the hold period, use a He leak detector to test all fittings and valves for leaks. Set the detectors range to read a minimum of 1×10^{-9} std cc/s He.

(7) Once leak check is completed and pressure has reached a stable low value, apply power to the heater tapes to increase the temperature of the test chamber and RGA sensing lines to ≈250 ºC. Hold this temperature for a minimum of 12 hr. System bake-out of 24 hr is desirable.

(8) Monitor test chamber vacuum level. There should be an initial increase in pressure followed by a slow decay as the outgassing rate decreases.

(9) Turn off heater tapes and let system cool to room temperature; continue evacuating the system during cooling.

(10) Close the RGA isolation valves G-SOV1 and G-SOV2 to protect the RGA.

(11) Close turbopump isolation valve and roughing valve locking up a vacuum inside the turbopump.

(12) The test chamber is now ready to be loaded with gases using multiple dilution cycles.

5.1.4.3 Charging the Gas Mixture Bottle. The procedure for charging the gas mixture bottle follows:

(1) Ensure that the gas fill lines are isolated from the recirculating gas purification system by closing the test chamber gas system isolation loading valve G-HOV9.

(2) Open gas mixture bottle isolation valve G-HOV8.

(3) Open microtorr purifier isolation valves G-HOV4 and G-HOV6 to fill the test chamber.

(4) Open Ar isolation valve G-HOV1. Slowly open Ar regulator G-HOR1 to fill the gas mixture bottle to the required partial pressure for the desired gas mixture:

- He-32%Ar: 32 psig Ar
- He-6%Ar: 6 psig Ar.

(5) Close Ar supply regulator and isolation valve G-HOR1 and G-HOV1.

(6) Open He isolation valve G-HOV2. Slowly open He regulator G-HOR2 to fill the gas mixture bottle to a total pressure of 100 psig, achieving He partial pressure of 68 psig and 94 psig for the 32% and 6% Ar mixtures, respectively.

(7) Close He supply regulator and isolation valve G-HOR2 and G-HOV2, respectively.

(8) Close microtorr purifier isolation valves G-HOV4 and G-HOV6.

(9) The gas mixture bottle is now charged with an appropriate mixture ready for loading into the vacuum chamber.

5.1.4.4 Gas Loading the Test Chamber. The following procedure is for gas loading the test chamber:

(1) Open the test chamber isolation valve G-HOV10.

(2) Open test chamber gas system isolation loading valve G-HOV9.

(3) Slowly open gas mixture bottle isolation valve G-HOV8 and fill the test chamber to a pressure of ≈76 torr; close G-HOV8 once the pressure is reached.

(4) Close test chamber gas system isolation loading valve G-HOV9.

(5) Open RGA isolation solenoid valve G-SOV1 so that the test chamber gas mixture can be sampled.

(6) Evacuate test chamber to a pressure of 10^{-3} torr or lower and hold for 30 min.

(7) Repeat steps (2)–(6) until the RGA shows a maximum oxygen concentration on the order of 0.3 ppb. This should be achieved in two fill cycles.

(8) Close test chamber isolation valves G-HOV10.

(9) Test chamber system is ready for operation.

5.1.4.5 Initialize the Recirculating Gas Loop. Initializing the recirculating gas loop procedure follows:

(1) Verify that test chamber isolation valves G-HOV10 and G-HOV11 are closed.

(2) Verify that monotorr isolation valves G-HOV13 and G-HOV14 are closed.

(3) Open RGA isolation solenoid valve G-SOV1 so that the test chamber gas mixture can be sampled.

(4) Open gas system bypass valves G-HOV12 and G-HOV15.

(5) Start the gas pump. (Both the test chamber and the monotorr have been isolated from the system.)

(6) Open monotorr isolation valves G-HOV13 and G-HOV14 to initiate flow through the monotorr with the test chamber still isolated from the system. Turn on power to the monotorr unit.

(7) Close gas system bypass valve G-HOV15.

(8) Open test chamber isolation valves G-HOV10 and G-HOV11 such that gas will be cycled both through the test chamber and the monotorr purifier. Maintain this state of operation throughout testing as needed.

(9) Close gas system bypass valve G-HOV12.

(10) Periodically monitor test chamber atmosphere with RGA.

(11) Test chamber is ready to support test operations.

5.2 General Procurement Specifications

Primary hardware procurements necessary to complete the assembly and operation of the proposed gas handling system have been identified. Solicitations will be issued by MSFC using full and open competition. The final evaluation of vendor quotes will be based on the lowest cost technically acceptable approach. The current baseline requires two test chambers, each of which will make use of purified gas—the large chamber with three test sections containing 15 heat pipes and the smaller chamber containing a single heat pipe. These systems will share a common inert gas supply system and primary inlet purifier. However, two complete gas conditioning systems (ratios of He-32%Ar and He-6%Ar) and two complete purifying circulation systems attached to each test chamber will be required. The primary components within test systems include the following:

(1) Microtorr purifier units (marketed by SAES Inc.) to provide single-pass control to the common gas supply hardware. These are commercial off-the-shelf items with a delivery of 4 to 6 wk.

(2) Monotorr purifier units to provide the primary conditioning over the life of the test evaluation. These units are commercial off-the-shelf items with a delivery of 4 to 6 wk.

(3) Recirculation pump (sealed bellows-type unit or equivalent with low permeability and particulate generation) to circulate the inert gas mixture through the monotorr purifier. These units will in all probability be a modified version of commercial off-the-shelf items. Delivery is estimated to range from 8 to 16 wk. To conserve funds, the lowest cost technically acceptable unit will be pursued.

(4) Vacuum pump system to condition and recycle the test chamber and gas handling system. Two turbopump units will be used, a 300-L/s pump for the large chamber and a 70-L/s pump for the smaller chamber. A single roughing unit should be sufficient with a 600-L/min rating. These units are off-the-shelf items with a delivery of 4 to 8 wk.

(5) A variety of gas system plumbing components such as isolation valves, relief valves, tubing, flow meters, fittings, instrumentation, and structural materials are required. All of these items are commercial off-the-shelf available from a variety of vendors with typical deliver of 4 wk or less.

(6) Part fabrication and assembly at machine shops, as required to complete system.

To assist in setting up the gas system, there are a number of items that can be borrowed from in-house inventory and other projects while these systems are being built and tested. Appendix K provides a more detailed listing of primary components selected for use in the gas purification system.

6. INSTRUMENTATION

The planned operations for the accelerated life test heat pipe experiment will require round-the-clock testing for intervals of up to 6 mo with the full duration expected to reach 3 yr. To maintain the test system throughout this period, a robust data and control system must be in place. This system will consist of a combination of computers and distributed real-time controllers (RTCs) connected via a local area network. The computer(s) will record the test data and provide the user with an interface for monitoring and controlling operations. The distributed RTCs will provide independent monitoring of all key instrumentation and contain uploaded programming for normal operations, redline conditions, and shutdown protocols. The RTC provides the first line of defense in maintaining the overall health of the system. In the event of a computer error/crash or localized power outage, the RTCs will also safely shut down and/or place components in a safe mode, using stand-alone internal programming. The selection of instrumentation type and quantity is critical. The most durable types of instruments must be selected to prevent inadvertent test cuts due to an instrument malfunction. This necessitates components that are noncontact type and have few moving parts. Having the minimum amount of instrumentation needed to achieve the test objectives is also important. Unnecessary instrumentation results in larger, unwieldy data files and increases the risk of a false cut should one of the "extra" instruments fail. Additional instrumentation should only be added for monitoring purposes and should not be used to generate control interrupts. Finally, all instrumentation must be readily accessible, except for items located inside the test chambers, such that they are easy to repair or replace in the event of a malfunction.

6.1 Data Acquisition and Control Methodology

The test setup is divided into a number of subsystems, each with its own control requirements and instrumentation for monitoring and control purposes. To achieve test objectives, the integrated test system must operate continuously without regular operator observation. This implies automated routines with criteria, such as limits and operating bands, governing the establishment of warning, shutdown, and cut conditions. The method in which test warnings and cuts are implemented is extremely important, especially with regard to startup transients. They must be implemented such that artificial cut conditions, which prevent the hardware from reaching its steady-state requirements, are not introduced. A series of checkout tests will be necessary to determine the best methods for implementing both warning and cut protocol. At present, a total of four primary subsystems have been identified:

(1) Radio frequency power supplies and power distribution network—This subsystem provides both monitoring and control functions, including RF power system current, voltage, power, frequency, and coolant operating temperature. Each RF power supply is factory equipped with internal systems to protect against over-temperature or current conditions that will shut the unit down immediately; however, these internal controls should not be relied upon for the controlled termination of a test. Several primary redline cuts based on supply output power and inductive coil water-coolant temperature and flow are envisioned. The typical warning band for RF system power would be ±6% with a cut condition set to ±10%. Typical coolant flow and temperature warning bands would both be set to ±10% with a cut at ±15%. If a flow

switch rather than a flow meter is used on the water-cooling circuit, a loss of flow indication will be used as the cut condition. (The use of flow switches must be examined in more detail as past experience with these instruments has not been favorable.) In the event of a cut condition, the programmable logic controller (PLC)/computer will shut down the RF power supplies. The water coolant systems could be shut down a short time later if necessary, allowing sufficient time to cool hot components.

(2) Test chamber environment gas conditioning circuit—This subsystem only provides monitoring functions of line temperatures, flow rate, and test chamber pressure. The primary redline cut currently envisioned is based on deviation in test chamber pressure (high/low), which would signal a potential leak—atmospheric, coolant, or heat pipe. The typical warning band would be set to ±8% with a redline cut set to ±12% of the nominal test set condition. In addition, this system also includes monitoring and control of the RGA, including cycling of its solenoid isolation valves, and providing data to the data acquisition system regarding test chamber gas species partial pressures. In the event of a cut condition, the RTC/computer system would command the RF power supplies to shut down immediately. Termination of coolant flow could also be commanded shortly after RF power shutdown once sufficient heat has been removed from components to prevent hardware damage.

(3) Heat pipe calorimeter water circulation circuit—This subsystem only provides monitoring functions, including calorimeter temperatures, flows, and overall system pressure. Three primary redline cuts are envisioned. The first two cuts are based on variations from the nominal operating flow and exit temperature for each heat pipe. The typical warning band would be set to ±10% while that for a cut would be set at ±15% of the nominal test set conditions. The third cut is based on bulk facility coolant flow and is indicated by a flow switch (or flow meter). Detecting the loss of facility coolant flow allows for an orderly shutdown of all RF power supplies since there will be sufficient thermal capacity within the calorimeter circulation coolant loop to remove any excess heat, thus avoiding potential damage to test hardware or ancillary systems.

(4) Heat pipe temperature sensing—This subsystem provides monitoring only of the heat pipe evaporator temperature in the small gap between the RF inductive coil and the calorimeter. There is one proposed primary redline cut based on a high/low temperature indication from the heat pipe surface. The typical temperature warning band would be set to ±6% and the redline cut to ±10% of the nominal test conditions. During initial test evaluation, periodic observation of the temperature measurement trends will be required to determine the level of temperature shifting due to potential (slow) changes in material surface emittance, impacting the radiation component of overall heat transfer. In the event of a cut condition, the PLC/computer will command the RF supplies to shut down. Water cooling will continue as necessary to remove residual heat from the test hardware and support equipment.

As evidenced by this summary, there are a large number of individual responses that can be used to indicate both warning and shutdown conditions. In many cases, it may be important to implement a voting structure or combination of these responses to better determine the overall magnitude of a warning. A properly constructed interpretation routine could possibly differentiate between instrumentation malfunctions and actual heat pipe or support subsystem failure, which will aid in troubleshooting. For example, if while monitoring the combined heat pipe temperature, calorimeter coolant flow, and calorimeter outlet temperature, one of the instruments fails while the other two continue to track per the nominal test conditions, then instead of performing a cut, a warning mode could be entered until the malfunctioning instrument can be replaced.

Instrumentation within each of these subsystems is tied into an RTC that provides data to the host computer via a local network. In addition, a visual alarm indicator will be set up to continuously status the current machine condition. This alarm will consist of a green, amber, and red light arrangement visible throughout the test laboratory. The normal status indicator is green and remains lit when all subsystems are operating within allowable limits. The amber indicator signals a warning that one or more of the monitoring parameters are nearing a cut status or that a subsystem has suffered a recoverable fault. (It is recommended that the user examine the cause of the warning.) A shutdown condition is indicated by a red light, signaling that the test has been terminated due to a redline violation or an irrecoverable subsystem fault. Each of the data system components will be powered using an uninterruptible power supply that will provide at least 10 to 15 min of operation in the event of a full-facility power loss. This will allow sufficient time to monitor the ambient cooling of all components and provide final commands to be issued by all RTCs and test components so that if power returns, the system will be placed in a safe shutdown mode. The general layout of the subsystems is illustrated in figure 28.

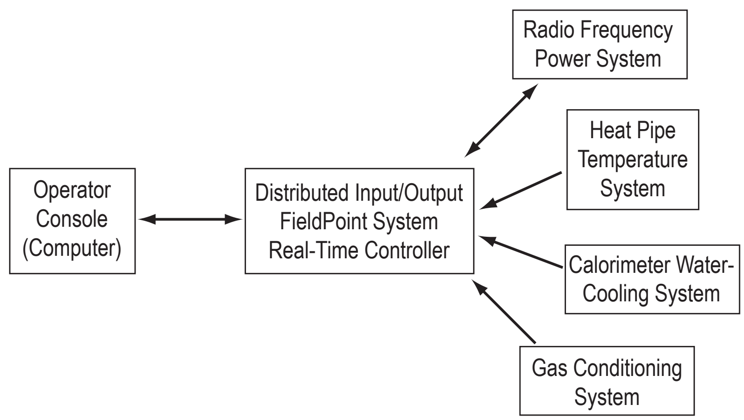

Figure 28. General data acquisition and control system subsystems.

The hardware that will be employed for both data acquisition and control includes a National Instruments (NI), FieldPoint (FP) modular distributed I/O system (serves as the RTC), and an operator console running Windows XP professional. The FP units, which are real-time (RT) controllers, acquire data from instrumentation distributed within the subsystems and provide the capability to impose RT decisions and actions (related to limit criteria) on hardware components. The operator console will host NI LabVIEW© applications that store acquired data and provide a graphical user interface for operating and monitoring the system. After acquiring data, the FP units will distribute the data in real time to the operator console via a local area network. The RT controller will monitor the data. In the event of an out-of-limit condition, the RTC will execute preprogrammed instructions to shut down the RF power system and safe the system. The outlined control system will also be used to ensure that the heat pipe and support hardware are brought up to operating temperature in a controlled manner and maintained at their steady-state conditions. Continuous monitoring will be provided to verify overall system health.

6.2 Instrumentation Components and Procurement Specifications

6.2.1 Water-Cooling Subsystem

The RT application will monitor the water-cooling subsystem flow rates and temperatures for out-of-limit conditions. In the event of coolant circulation failure or an over-temperature condition, the RF power to all or to the appropriate heat pipes will be interrupted. The specific flow rate and calorimeter temperature value limits shall be determined based on final pretest calculations and checkout test data for the assembled system. Depending on the final test chamber configuration, if an out-of-limit condition occurs in a limited portion of the system, it should be possible to selectively shut down the RF heating to the appropriate subset of heat pipes. In the event of a loss of coolant flow to the primary calorimeter recirculation system, a loss of flow in the facility supply, or a coolant over-temperature condition, all RF power supplies will be shut down. Appendix L provides a partial listing of the primary instrumentation components. This equipment is typically off-the-shelf with a 2- to 4-wk delivery.

As a baseline, each of the 16 calorimeter outlets will be equipped with a turbine flow meter (like the model FTB9511 from Omega Engineering or the MF150-CB-PH precision turbine from Sponsler) with a range of 0.1 to 2 gpm and a type K thermocouple in close proximity (to assess fluid properties for mass flow calculations). Alternatives to the turbine-type unit are a paddlewheel-type meter, such as the model 04004SN2 by Proteus Industries, and a thermal mass flow meter that has no moving parts, like the Weber model 4411.3 meter. The paddlewheel meter has the added benefit of also providing temperature and pressure measurements without the need for additional signal conditioning. All meter types shall be compared with a final decision based on a combination of cost, accuracy, and long-duration dependability/stability. Typical vendor availability is 4 to 8 wk.

To obtain the most accurate measure of the heat removed by the calorimeter, as determined from the temperature rise across the calorimeter, a thermocouple will be located inside the test chamber as close to the calorimeter output as feasible. This thermocouple will be attached to the surface of the copper calorimeter feed tube. As a backup, an additional thermocouple probe will be inserted, using a compression fitting, into the calorimeter output line after it exits the chamber, minimizing the potential for water leakage in the test chamber. Thermistors will be considered as replacement to thermocouples on the calorimeter to improve accuracy.

The calorimeter recirculation flow circuit—upstream of the test chamber calorimeter inlet manifolds—will be equipped with a larger turbine-type flow meter, such as the Omega model FTB-905 or Sponsler SP3/4-CB-PHL, having a linear range of 2.5 to 29 gpm and a local type K thermocouple. A thermal mass flow meter is not practical for this location due to the high flow rate. The facility water coolant inlet to the calorimeter recirculation subsystem heat exchanger will be equipped with a flow meter and both the inlet and outlet lines will be equipped with type K thermocouples. The cooling water inlet and outlet to the heat exchanger will also be equipped with type K thermocouples. The facility flow meter may be exchanged for a flow switch. However, inlet and outlet thermocouples will still be present to assess whether or not the facility system is providing both sufficient flow and cooling.

6.2.2 Gas Conditioning Subsystem

Purified inert gas is circulated throughout all test chambers during test processes and is periodically sampled by an RGA. The flow rate, temperature, and pressure of this gas will be monitored by the RT control system to confirm operation. In the event that the RT application monitors an out-of-limits flow condition, the RGA-measured partial pressures will be used to determine if the RF power subsystem should be interrupted or if the test be allowed to continue. It is anticipated that over long periods of operation, less scrubbing of the test chamber atmosphere will be required, such that a 100% duty cycle on the gas conditioning system may not be required.

The RGA unit will be monitored by the RT controller used to automatically control the remote operated solenoid valves to sample the test chamber gas mixture at a user-specified rate. (The sampling rate is expected to be set at ≈6-hr intervals.) In the event that the gas composition is found to be out of limits, manual sampling can be performed to verify partial pressures and the RF power supplies can be interrupted as necessary. The initial warning will be set to 1 ppb oxygen with a high cut estimate set to 3 ppb oxygen. (The value of 3 ppb corresponds to a vacuum chamber pressure of 10^{-5} torr when evacuated from atmospheric conditions.) The RGA is equipped with a digital control interface (RS-232 or RS-485) that allows for remote operation. Typically, the RT controller will evacuate the gas line connecting the RGA to the test chambers to clear it, then open one of the isolation valves (G-SOV1 or G-SOV2) to capture a gas sample that is analyzed for warning or cut limits. The isolation valve is then closed. This routine is repeated at the user-specified intervals for each test chamber. The isolation valves will be bellows-style valves with pneumatic actuators and solenoid controllers. These are off-the-shelf items. Also, there will be additional cost to set up the plumbing (hardware components), structural mounting, and electronic control interface between the RGA and RTC.

A flow meter is specified for the gas conditioning system since it provides an indication as to how well the system is circulating the gases; a flow switch would provide only binary output. This makes it easier to troubleshoot possible issues related to insufficient purification. The use of a flow switch is also questionable at the low system operating pressures. Measuring the mass flow in the gas circulation system will be difficult because of the low gas pressure (50–100 torr) and the potential for a variable mixture of He/Ar (adjusted to obtain the desired heat pipe heat flux). There are two types of flow meters that may be used—a thermal mass flow meter, such as the Fox Thermal Instruments Model 10A, or a laminar volumetric flow meter. The mass flow meter uses a thermal sensor to measure mass flow directly and, unlike the volumetric flow meter, is not affected by changes in pressure and temperature. With a volumetric flow meter, the pressure and temperature, along with the appropriate gas properties, must be used to compute the mass flow rate. Consequently, a thermal mass flow sensor can replace a volumetric flow meter and its associated pressure transducer. In addition, a thermal mass flow meter provides an accurate and repeatable measurement over its entire range of operation. Volumetric flow meters cannot provide this wide range of measurement and are especially inaccurate for low flow conditions. A thermal mass flow meter has no moving parts and is inherently more reliable than a volumetric flow meter. In addition, a turbine flow meter is not a good fit due to its low accuracy at low flow (zero to 150 slpm) conditions. Therefore, the thermal mass flow meter appears to be the best overall fit for the specific conditions within the gas system. A single mass flow meter, with appropriate calibration, has a delivery time of 4 to 8 wk. Specifics concerning the operation and possible calibration techniques for both the mass flow and laminar volumetric flow meters (issues with the He/Ar mixture) are included in appendix M.

6.2.3 Radio Frequency Heating System

The RF heating system will consist of four separate power supplies, one for each heat pipe cluster. Each of the power supplies will have three zero to 10-V analog inputs to control the frequency, current, and voltage, and four zero to 10-V analog outputs will be used to report the measured frequency, current, voltage, and power. The RT application will monitor the system for out-of-limit conditions. In the event of a limit violation, the RF power to the affected heat pipe cluster(s) will be interrupted. The RF supplies will be equipped with a commercial water-cooling station that will cool both the supplies and the RF inductive coils. This unit will be instrumented from the factory with flow indicators or meters and thermocouple probes that can be tied into the RT application and tested for both warning and cut conditions. To piece this system together, a variety of cabling, electronics, and support components will be required. These are typically off the shelf with 2- to 4-wk delivery.

6.2.4 Heat Pipe Temperature Measurement

A key parameter in assessing a heat pipe's performance is the temperature at the evaporator exit. Two types of instruments can be used to measure this temperature, and a trade-off assessment must be made to select the most suitable type. First, a traditional type C thermocouple could be attached to the heat pipe surface. Alternatively, a two-band optical pyrometer can provide the measurement using a noncontact technique. A number of the comparisons are summarized in table 14.

Table 14. Thermocouple to pyrometer comparison.

Two-Band Pyrometer	Type C Thermocouples
Expensive hardware	Inexpensive hardware
Mounted outside of the test chamber; no contact with heat pipe	Must be directly attached to the surface of the heat pipe by bonding or spot welding
No potential for debonding or contamination of heat pipe alloy	If bonded, frequent debonding occurs. For long-term testing, the nickel foil used in bonding will diffuse into the heat pipe alloy
No potential for pitting the heat pipe surface	If spot welded, pitting of heat pipe surface can occur and potentially embed or trap impurities
Eases operations involving loading and unloading of heat pipes	Over the duration of the program there will be many bonding/spot welding cycles covering nondestructive evaluation and thermocouple repair
No potential for localized cooling	Leads act as fins, locally cooling at the measurement location
Minimizes potential for degradation due to high temperature; two-band reduces affect of surface emissivity changes	Long-term degradation of thermocouple wires at high temperature introduces unknowns
Easy to repair; unit is positioned external to the test chamber	Difficult to access; located inside the test chamber, requiring backup thermocouples to be attached
Low maintenance cost with minimal down time and manpower usage for repair	High maintenance cost with large down time and manpower usage for repair

Based on the summary provided in table 14, it is readily evident that the use of two-band optical pyrometers for all heat pipe measurements will significantly reduce the overall setup and maintenance effort when compared to the use of thermocouples inside the test chamber system. This, coupled with overall reliability and the elimination of potential contamination or damage to the heat pipe, provides justification for the selection of the two-band pyrometer for use in the baseline system for the planned testing.

Two optical pyrometer units have been identified—the MI-SQ5 series from Mikron and the Modline 5R series from Ircon. Details for each these units are listed in appendix N. The two-band pyrometer makes high-temperature measurements by obtaining the ratio of radiation intensities at two adjacent wavelengths rather than using the absolute intensity, as with the single-band pyrometer. The vendor reports that this technique results in a temperature measurement that somewhat reduces the dependence on emissivity, is unaffected by dirty viewing windows and contaminants in the field of view, is independent of target size, as long as a minimum percentage of the target falls within the sighting reticule, and is unaffected by a moving target within the field of view. Both models support an RS-485 digital interface that will allow the RT controller to communicate with multiple sensors over a single RS-485 connection. The distance from the outside edge of the glass to the heat pipe surface is ≈12 in. However, this may decrease to 11 in or less if the RF inductive coils are spaced out to reduce inductive coupling. This distance is within factory-available focal lengths and will accommodate a spot diameter of <0.24 in. A standard temperature range of 1,000 to 1,500 K will easily cover all operations. To verify the operation and ease of use, checkout testing is planned using loaner units from the factory. Current vendor information indicates, depending on the options selected, 17 optical pyrometers will be required. Availability is typically 6 to 8 wk. Additional materials/fabrication of support brackets, adjustable mechanical positioners, and cabling to set up and connect all the pyrometers to the test chambers and data system will also be needed.

In addition to the pyrometers, a supplemental luminosity measurement is currently being investigated to monitor each cluster of heat pipes for potential hot spots on the heat pipe evaporator that might not be visible to the two-band pyrometer. The proposed technique will make use of a photodiode in a view port at the evaporator end of the heat pipe cluster. From this vantage point, the diode could pick up any significant increase in brightness—produced by a dryout—through the 0.25-in-gap width between the RF coil and heat pipe evaporator. When the system is at its normal operating conditions, the average sensed luminosity (brightness) will be recorded and set as the baseline. Any increase above this brightness level would result in a warning or cut condition with typical values of 5% and 10%, respectively. If any cut limit is exceeded, the RT controller will shut down the RF power supply.

Within the test chamber, a series of low-temperature surface measurements will be taken at nonrefractory metal locations using type K thermocouples spot welded to the surface. These locations will include heat pipe supports and the calorimeter flow outlet, totaling ≈32 thermocouples inside the test chambers.

6.2.5 Test Chamber Vacuum Gauging

To monitor test chamber pressure conditions during all operational phases, including bake-out, gas conditioning/loading, and normal test procedures, a vacuum pressure system will be required. This system must have sufficient instrumentation to measure a pressure range from 1 atm to $<10^{-6}$ torr. Three types of gauges are needed to cover this range—a capacitance manometer (1,000 to 1 torr), a convection Pirani gauge (1 to 10^{-3} torr), and a cold cathode gauge (10^{-3} to 10^{-8} torr). The preferred solution is a multigauge controller, like the KJLC multigauge (marketed by the Kurt J. Lesker Company). This instrument has five slots for sensor boards and one slot for an RS-232 or RS-485 serial interface board. Appendix O provides a listing of the component specifications. Vendor estimated availability is 2 to 4 wk.

6.2.6 FieldPoint-Distributed Inlet/Outlet System and Real-Time Controller

All data acquisition and control will be performed via an NI FP modular distributed I/O system. The system will include modules for reading and writing analog current and voltage signals, modules for reading thermocouples, and modules for reading and writing digital signals. The FP system will also include an RT controller, such as the FP-2010 marketed by NI, for performing automated control and for monitoring measurements used in comparison with out-of-limit conditions. The RT application will be developed with LabVIEW and will be downloaded to the controller. An RT controller was chosen to handle this functionality because it is more reliable and deterministic than a computer running a Windows OS. The RT controller's operating system is not burdened with the user interface, data recording, and overhead associated with a Windows desktop OS. Also, this controller is compatible with existing instrumentation and development tools already being used within the laboratory. The RTC will be used to acquire all measurements (flow rates, temperatures, and pressures), perform closed-loop control of the RF power supplies, and monitor measurements for limit (warning and cut) violations. Appendix P provides a listing of the outlined components and specifications. The current vendor estimated availability is 2 to 6 wk.

6.3 Data Quality

To maintain the highest quality test data, all sensor and data processing equipment must be calibrated at regular intervals. Data acquisition equipment and sensors will be received with standard factory calibration and, for an additional cost, can be delivered with a National Institute of Standards and Technology (NIST) traceable certification. All manufacturers recommend that their units be calibrated periodically, typically at yearly intervals. Some units, like thermocouples, cannot be recalibrated; they are simply replaced when they are out of calibration. There are NIST-certified devices available that can be used to field check their calibration. There are several options available to satisfy the requirement for periodic calibration, each carrying a different level of expense and impact to the hardware systems:

(1) The first option would require sending all units back to the factory or to a qualified standards lab. The turnaround time can range from 1 to 4 wk, depending on the company and work load. If testing is to resume during recalibration intervals, it will be necessary to purchase spare units and to send the units out only a few at a time. In this scenario, calibration would be a continuous process requiring a large number of components, rendering it a logistical nightmare. However, if all instrumentation is calibrated at the same time, as when the system is down for heat pipe nondestructive evaluation (NDE), this could streamline the process. Procurement for standards lab service will have to be initiated several months in advance to ensure that there will be no delays in calibration once the test hardware is opened for NDE.

(2) A second option is to have the instrumentation calibrated in the field. It may not be possible to calibrate some sensors, e.g., flow meters, in the field. However, it should be possible to field calibrate the bulk of the instrumentation. Most of the cost would be to cover the service company's technician travel and onsite time to perform calibrations. This approach may offer considerable cost savings relative to sending everything out for calibration, and will certainly reduce the down time. It will still be necessary to initiate the procurement for this service well in advance of its needed date.

Another option to reduce cost is to periodically check the calibration in-house and to send out instruments for recalibrating only when they are found to be out of calibration. This may not be possible for all types of sensors but should be possible for most types of data acquisition and signal conditioning equipment. The in-house calibration check could be performed using a portable calibrator, like the Model X88 from Ronan. This instrument is designed to calibrate and measure instruments, devices, and systems utilizing current, voltage, ohms, frequency, and thermocouple inputs or outputs. Ronan recommends that the Model X88 be verified at 3- to 6-mo intervals using precision standards traceable to NIST. Since most instrumentation typically remains within calibration longer than the factory recommendation, this option may be the most cost effective. The downside to this approach is that NIST-traceable certifications will not remain in effect for the entire test, and instruments found to be out of calibration at critical times could impact testing. This option is the most desirable choice for maintaining the calibration of the FP I/O modules. These modules can be swapped out with a spare and checked without impacting the test. Modules found to be out of calibration can be replaced entirely and, if cost effective, sent out for calibration.

7. SUMMARY

General descriptions of test subsystems to support the hardware evaluation of Mo-44.5%Re alloy/Na heat pipes have been identified. This includes both limited performance testing to determine heat pipe operational envelopes followed by round-the-clock testing of all 16 units. As identified, each of these subsystems is laid out to meet the requirement for a 3-yr period of continual operation. Initial outlines for hardware operating procedures have been identified where necessary and will be used during checkout testing of hardware during fabrication and assembly. Key subsystems include the following:

- Radio frequency heating of the 16 modules is very practical, making use of 30- to 50-kHz supplies with low voltage output (<200 V) to minimize the possibility of voltage breakdown. The inductive coils will be equipped with flux concentrators to minimize mutual inductance and stray heating, providing both a more uniformly heated area and less overall power consumption. Expected electrical to thermal efficiency is 50% to 70%.

- Coupling of the heat pipe condenser to a water calorimeter is based on the use of a static gas gap. The atmospheric concentration of oxygen at 0.3 ppb, comparable to that of a 10^{-6} torr vacuum, is required. Initial assessment shows that a gas recirculation circuit using a vacuum-type diaphragm pump and a hot getter purifier operating at a pressure of 76 torr can meet this goal.

- Separate water-cooling circulation subsystems will be procured to support operation of the RF power/inductive coils and the heat pipe calorimeter assemblies. This system will have to remove an estimated 85 kW during normal operation.

The requirement for round-the-clock testing places a heavy burden on both the data acquisition and control subsystems. The high power levels needed for the complete setup further complicates this burden. Continuous monitoring of the heat pipes and each subsystem is provided to maintain up-to-date indication of the overall system health. The selected approach is to use a distributed system of computers and RT controllers connected through a local network. This approach provides the best overall redundancy, allowing the RT controllers to rapidly respond to both warning and redline issues with or without computer involvement.

APPENDIX A—ENVIRONMENTAL TEST CHAMBER ENGINEERING DRAWINGS

Figure 29 shows preliminary engineering drawings outlining the large environmental test chamber assembly with support stands. A total of three units are required for the proposed testing. The shell and support structure are shown in detail in figures 30 and 31, respectively.

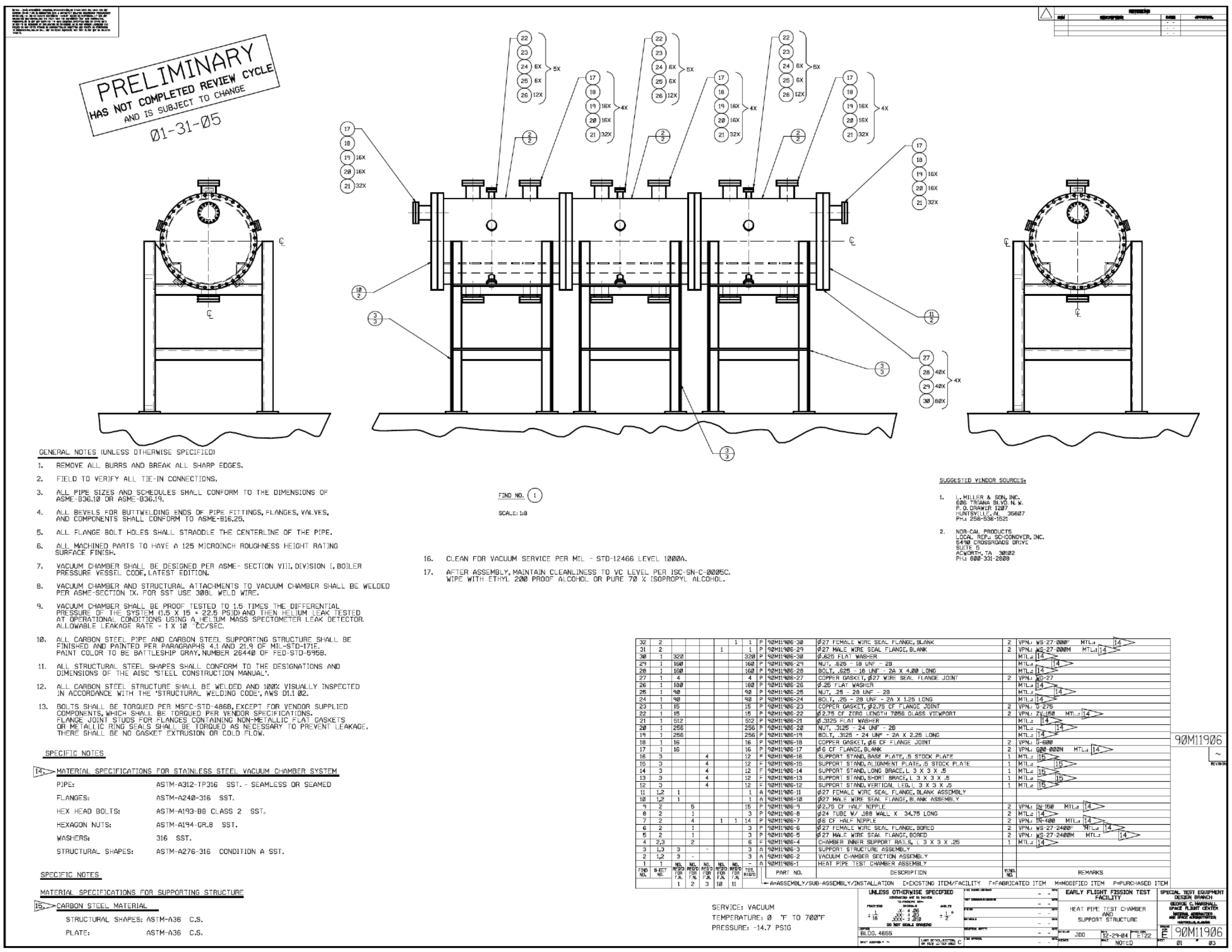

Figure 29. Test chamber assembly (three segments integrated) (Dwg. No. 90M11906).

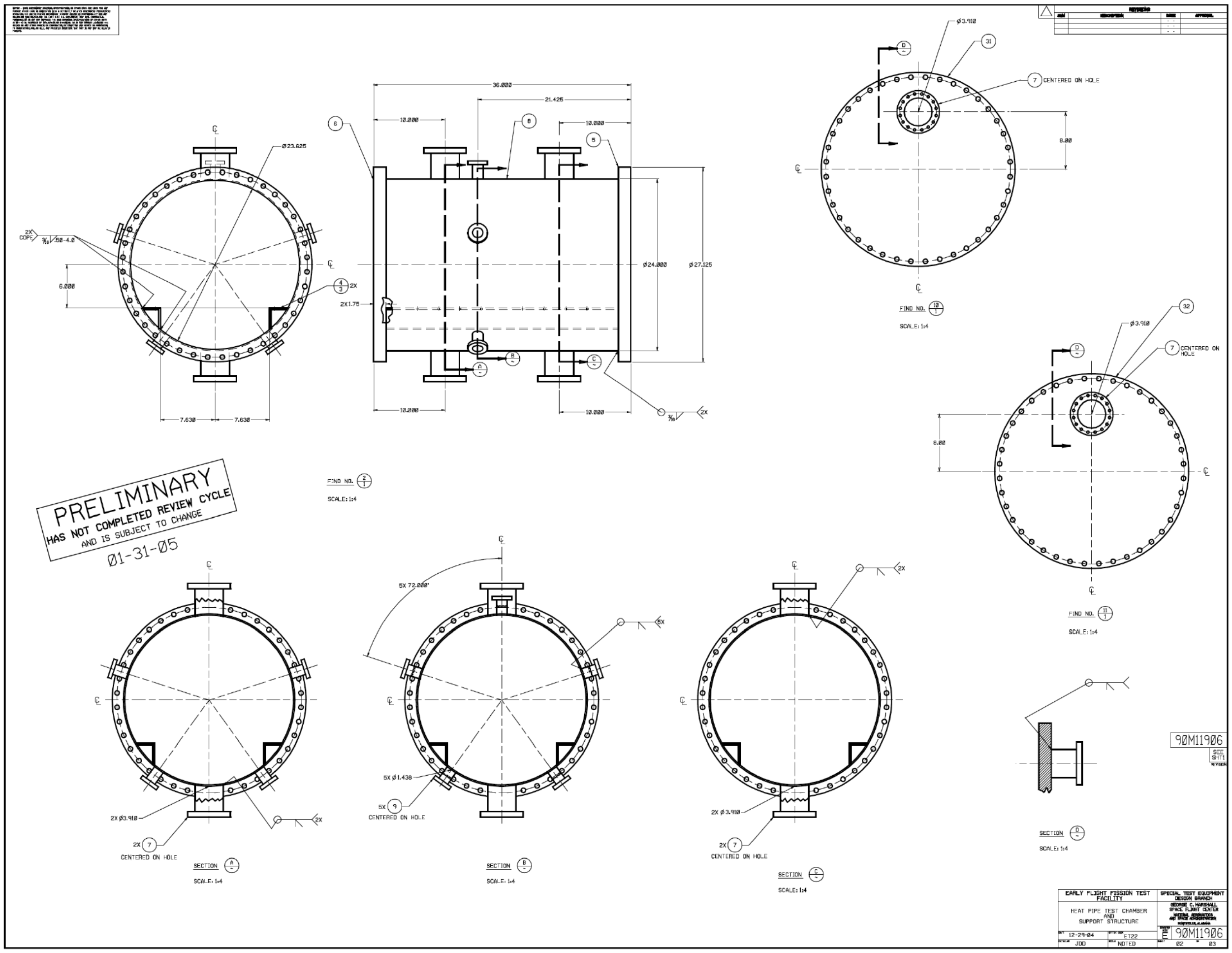

Figure 30. Detail test chamber shell (Dwg. No. 90M11906).

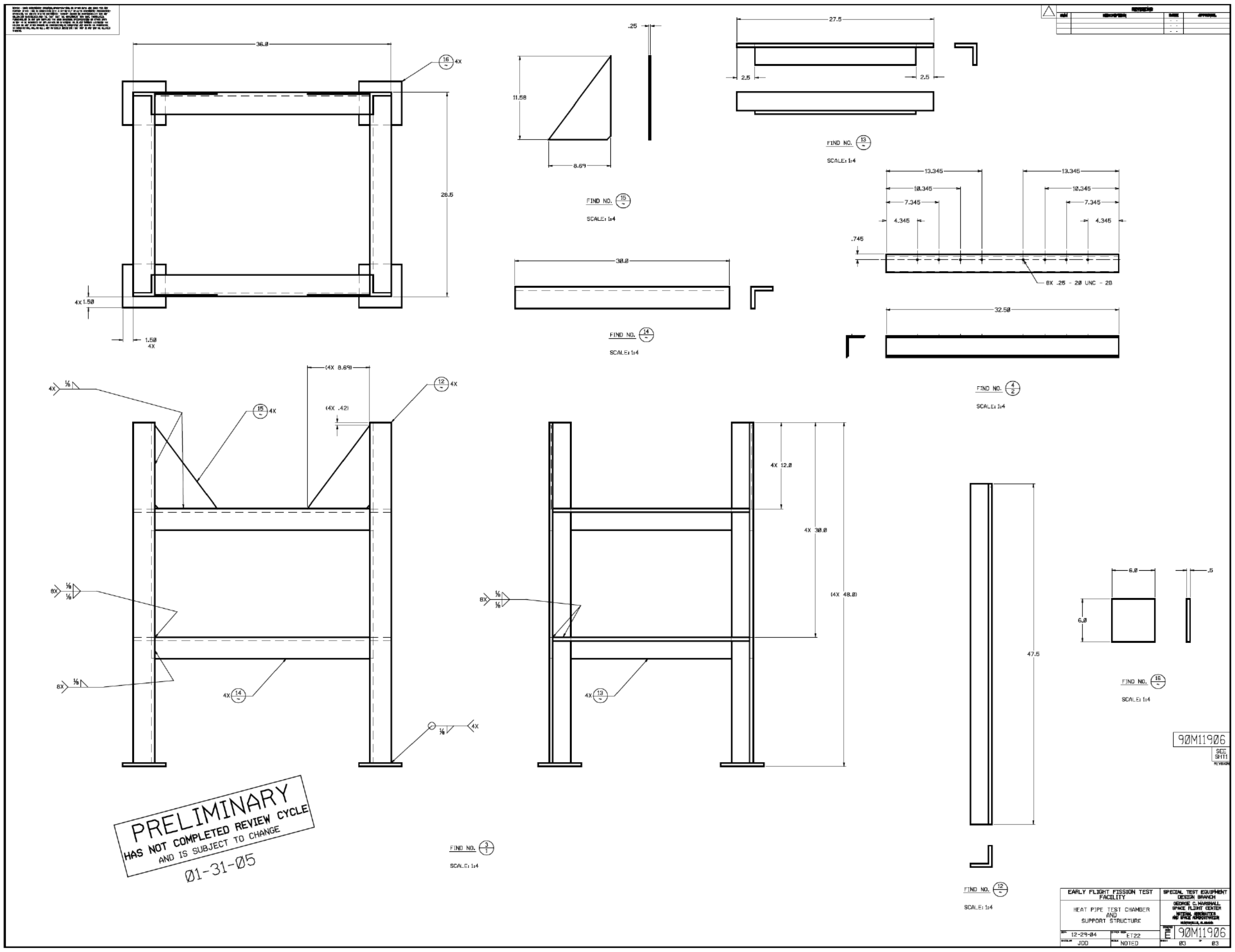

Figure 31. Detail test chamber support structure (Dwg. No. 90M11906).

APPENDIX B—HEAT PIPE CLUSTER SUPPORT ENGINEERING DRAWINGS

Preliminary engineering drawings outlining the heat pipe and calorimeter cluster attachment support structure and individual mounting bracket are shown in figure 32. A total of three support structures and 16 mounting brackets are required for the proposed testing. Detailed drawings of the attachment support structure are shown in figure 33 and the heat pipe and calorimeter mounting bracket in figure 34.

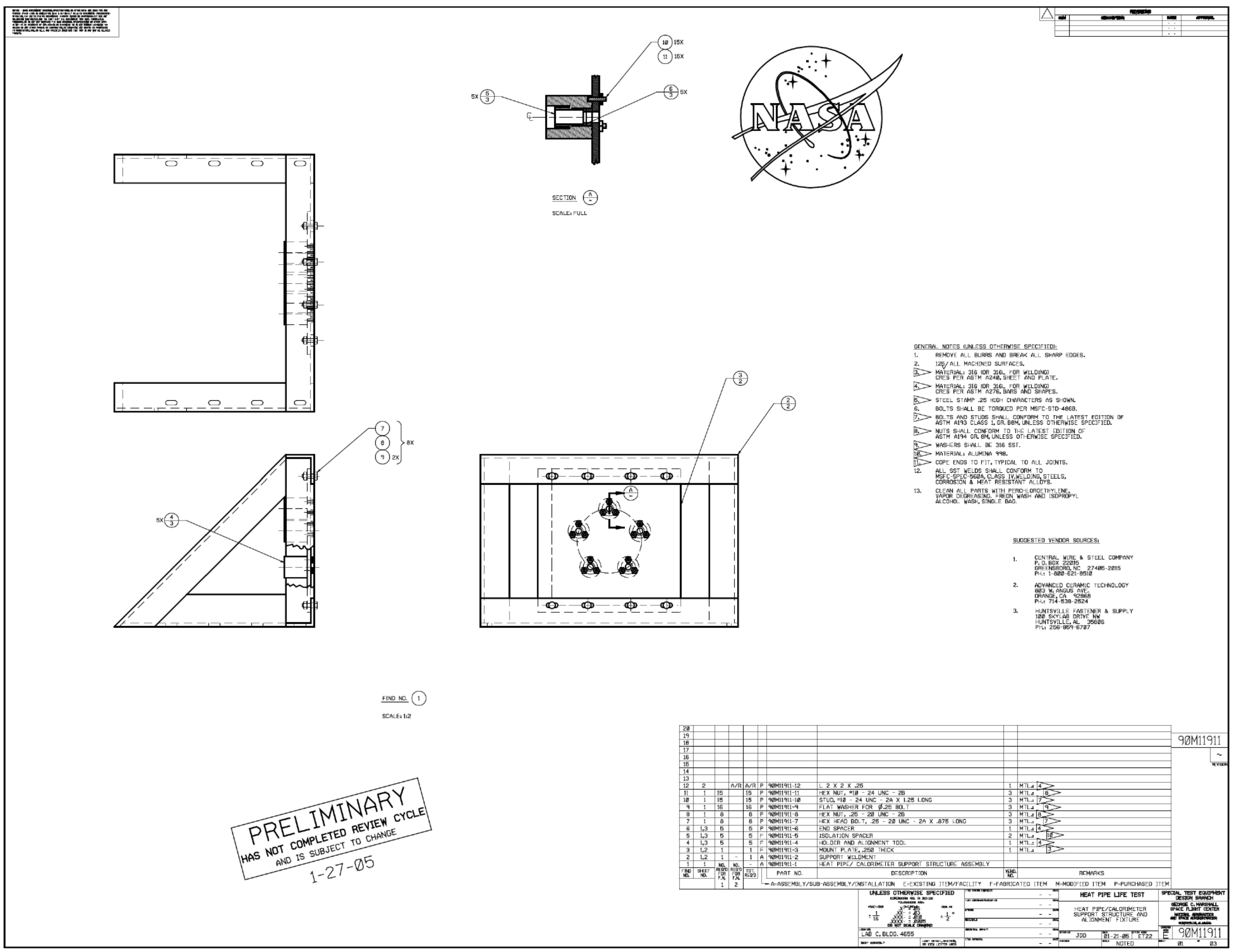

Figure 32. Heat pipe and calorimeter cluster attachment support and bracket assembly (Dwg. No. 90M11911).

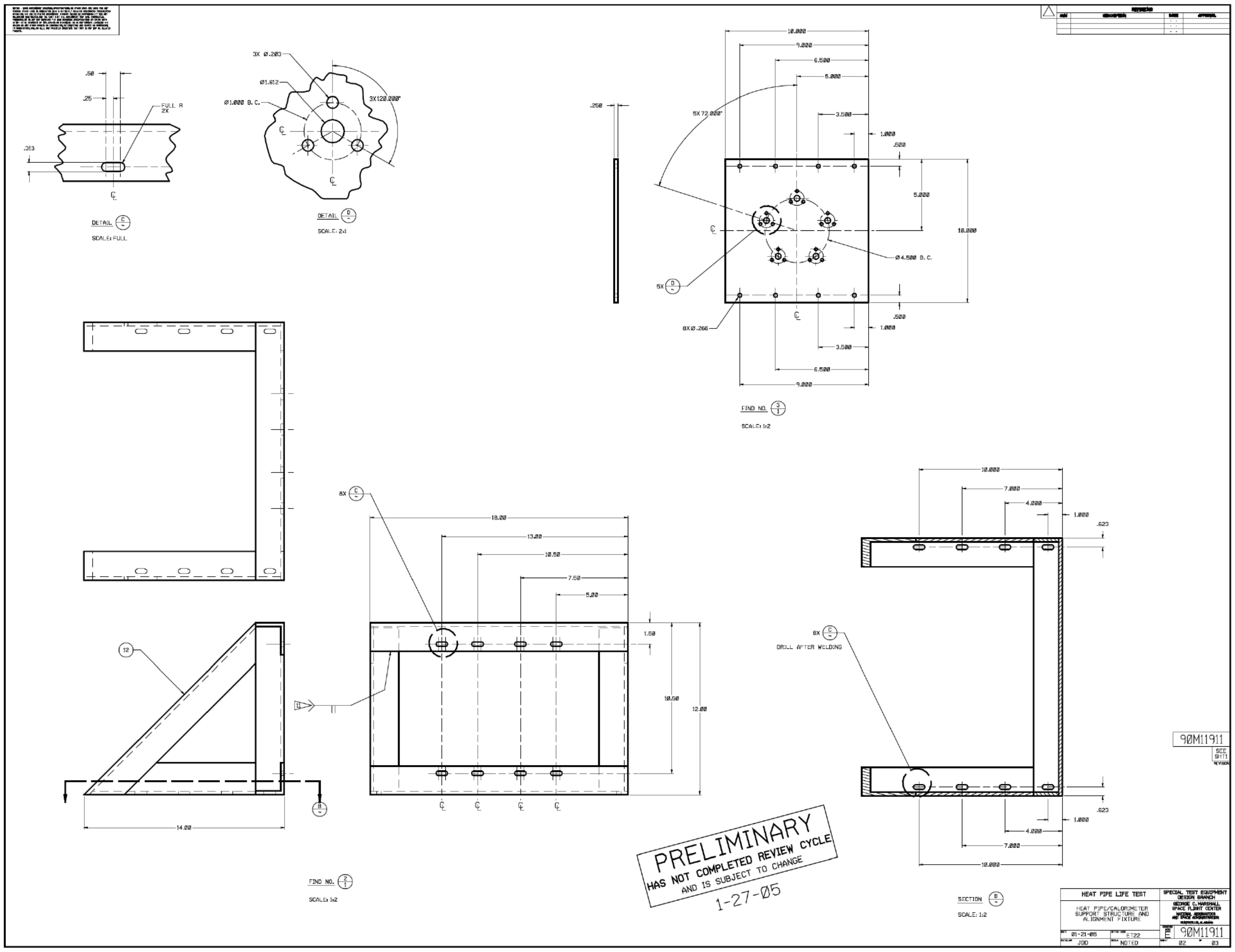

Figure 33. Attachment support structure details (Dwg. No. 90M11911).

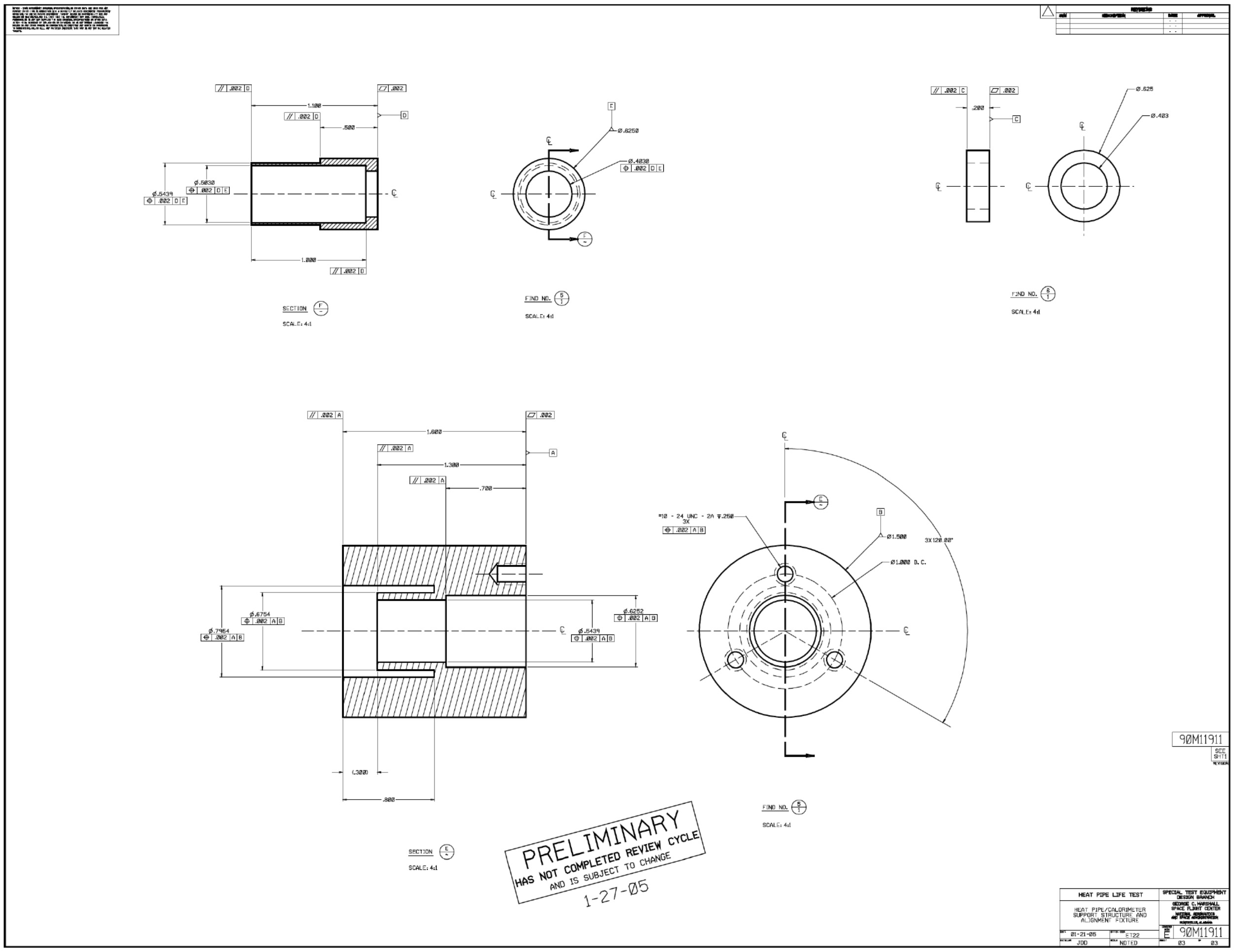

Figure 34. Heat pipe and calorimeter mounting bracket detail (Dwg. No. 90M11911).

APPENDIX C—CALORIMETER ENGINEERING DRAWINGS

Figures 35 and 36 show the preliminary engineering drawings detailing the layout of the copper (or stainless steel) heat pipe calorimeter element. A total of 16 calorimeters will be required to support the proposed testing.

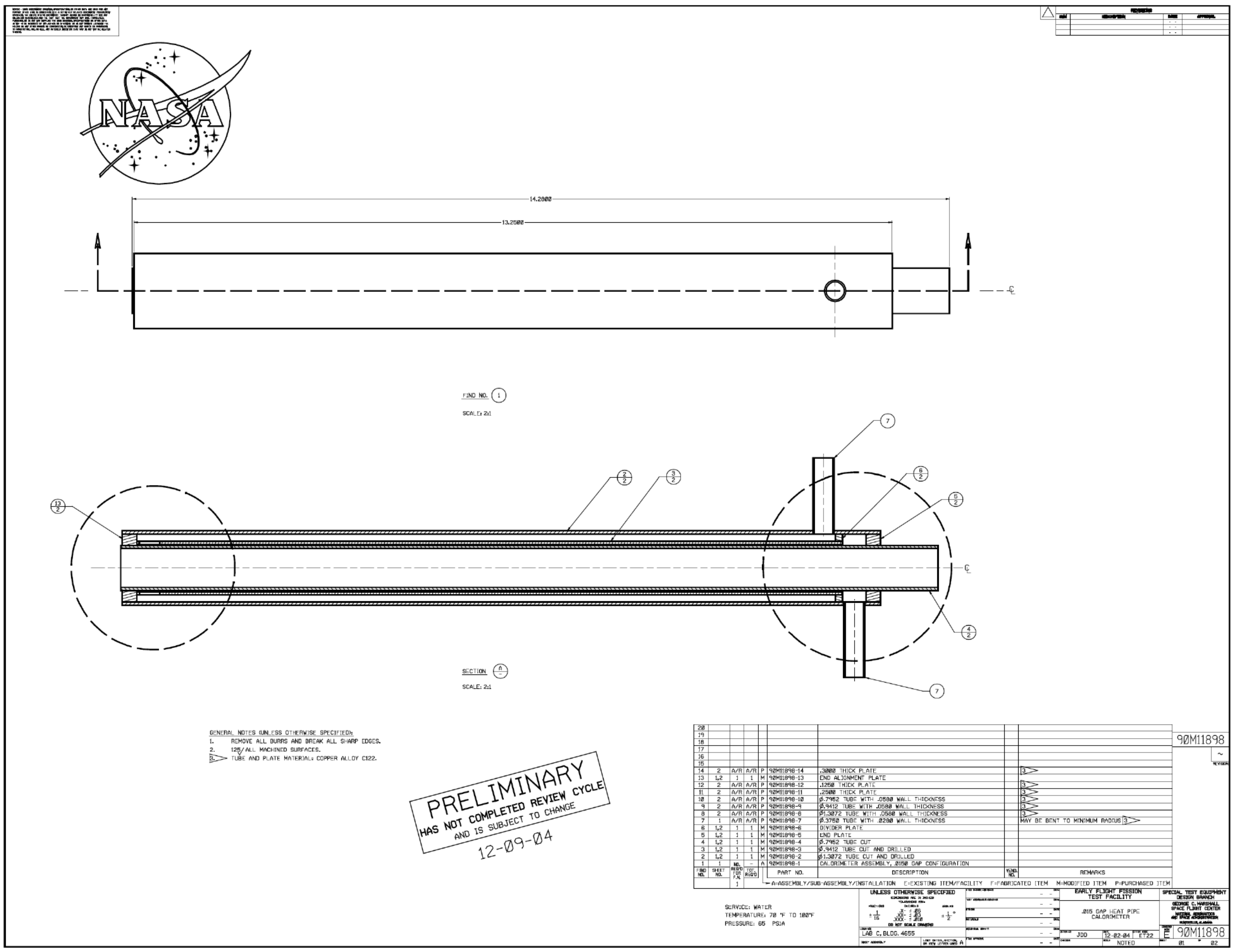

Figure 35. Heat pipe calorimeter assembly (Dwg. No. 90M11898).

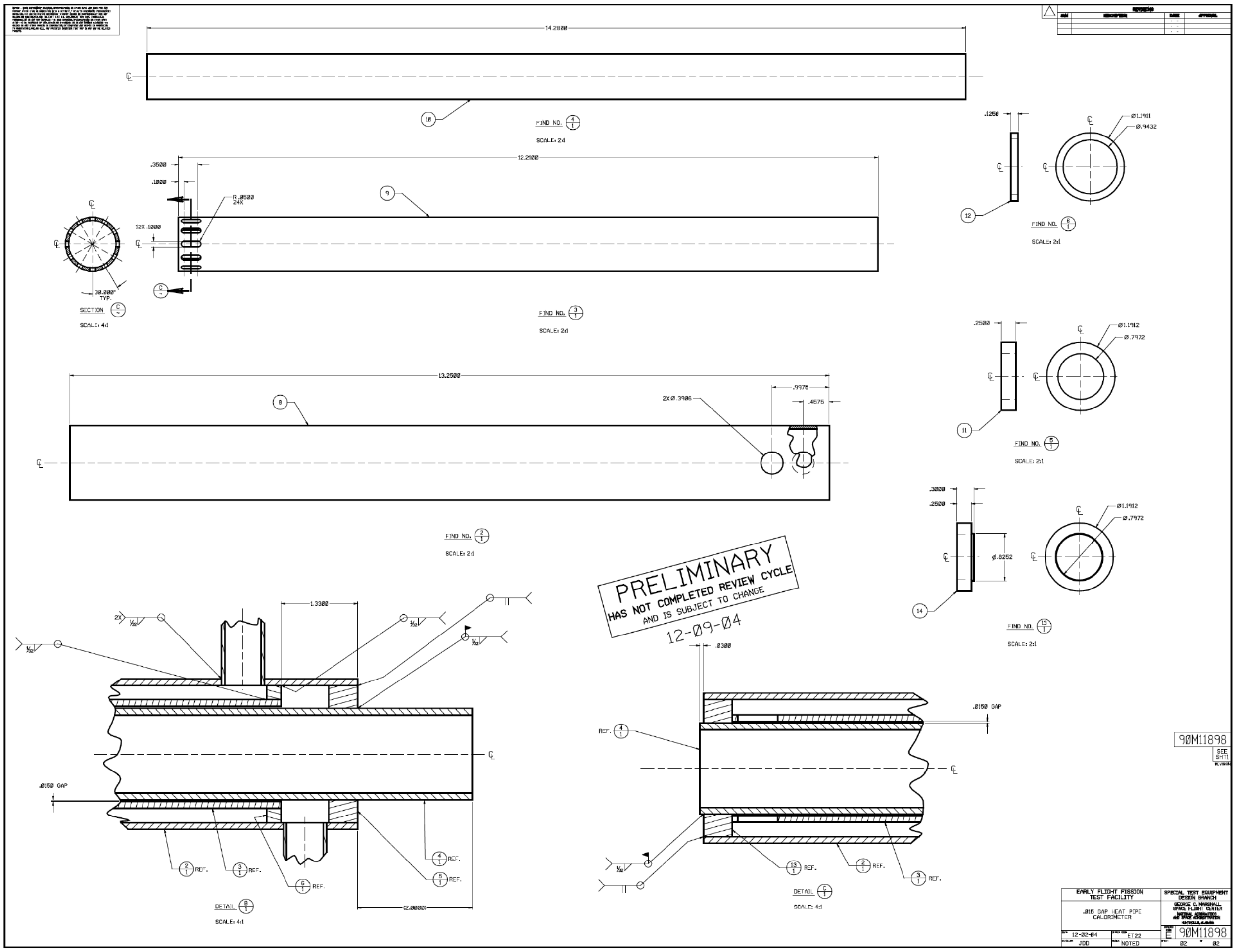

Figure 36. Calorimeter design detail (Dwg. No. 90M11898).

APPENDIX D—ENVIRONMENTAL TEST CHAMBER PROCUREMENTS

Table 15 provides a partial list of general hardware required for fabrication of the environmental test chambers, summarizing the primary components. All structural components, attachment hardware, and chamber envelope material are stainless steel.

Table 15. General hardware needed for fabrication of environmental test chambers.

Item	Model No./Description	Specifications	Quantity Needed
Large flange sets Nor-Cal Products Inc.	WS-27-2400M WS-27-2400F	27-in-diameter male wire seal flange, bored	3 each M 3 each F
Large flange sets Nor-Cal Products Inc.	WS-27-000M WS-27-000F	27-in-diameter male wire seal flange, blank	3 each M 3 each F
Large pipe section Nor-Cal Products Inc.	NA suitable for vacuum application	24-in diameter by 34-in length – surface electropolished	3 each
Small chamber flanged full nipple Kurt J. Lesker	2×WSFB14X000M 2×WSFB14X1200M Custom-length barrel must be quoted	12-in tube section with wire seal flange sets on ends	1 unit
Test chamber ports and flanges and connecting hardware—bolts Nor-Cal Products Inc.	Variety of half nipples with conflate-type flanges, bolts/washer sets, copper/wire seals, feedthroughs, etc.	All hardware items for 4- and 2-in half-nipple tube flanges to equip/connect all chambers and support hardware	Various
Optical view ports	TBD – based on pyrometer needs	TBD depending on final pyrometer selection and wavelength	16
Optical view ports	TBD – based on general access	TBD size for general viewing	7
Structural material	Variety parts to fabricate chamber supports and internal frames. Mechanical positioners. Calorimeters/heat pipes. Refractory materials to set up internal supports	Angle, plate and tube stock, stainless steel and refractory metal. Positioners for adjusting heat pipe locations	NA
Vacuum relief valves	Set point 15 psia, with large orifice	Prevent test chamber overpressure – vacuum compatible	4

APPENDIX E—CALORIMETER COOLING SUBSYSTEM PROCUREMENTS

A partial summary of the primary components required in the setup of the heat pipe calorimeter water circulation subsystem is shown in table 16.

Table 16. General hardware list for assembly of the heat pipe water-cooling subsystem.

Item	Model No.	Specifications	Quantity Needed
Might pure ultraviolet water purifier	MP36C	12 gpm per unit	2
DI cartridge	TBD	1 to 2 gpm	2
Calorimeter flow control valve Alabama Fluid Systems	SS-6BW	SS plug valve 3/8-in connections Max temp: 120 °C	20
Flow control valve Alabama Fluid Systems	SS-68TS32 SS-65TS16 With actuators	SS ball valve 1- to 2-in connections Max temp: 120 °C	4
Calorimeter Isolation valve Alabama Fluid Systems	SS-62TS6	SS ball valve 3/8-in connections Max temp: 120 °C	20
Isolation valve Alabama Fluid Systems	SS-68TS16	SS ball valve 1- and 2-in connections Max temp: 120 °C	6
Bypass and drain valves Alabama Fluid Systems	SS-63TS8	SS ball valve 1/2-in connections Max temp: 120 °C	7
Tubing, piping, flanges, and other components/hardware	NA	3/8-,1/2-, 1-, 2-, and 4-in with fittings, stainless steel and copper vacuum, heaters, etc.	NA
Pressure relief valves Alabama Fluid Systems	RL4S8	SS 1/2-in relief; set pressure 100 psig Max temp: 120 °C	5
Recirculation water system skid Sentry Equipment Inc.	CWIS-35	Complete system with pump, reservoir, flow control, and instrumentation	1

APPENDIX F—RADIO FREQUENCY INDUCTIVE COIL THERMAL LOAD WORKSHEET

General assessment of the RF inductive coil thermal load due to radiation and gas conduction between the heat pipe evaporator and inner surface of the RF coil and the estimated total coolant flow requirement due to thermal and internal coil heating (I^2) losses are shown in table 17.

Table 17. Heat transfer loss estimates between RF inductive coil and heat pipe surface.

NRPCT WI#2 2/16/09

Heat Transfer Loss Estimates for RF Inductive Coil to Heat Pipe Surface

user input field

$$Q_{rad} = \frac{\sigma A_i (T_{hp}^4 - T_{ind}^4)}{1/\varepsilon_i + (A_i/A_o)(1/\varepsilon_o - 1)}$$

$$Q_{cond} = \frac{2\pi L_c k (T_{hp} - T_{ind})}{\ln(d_o/d_i)}$$

Heat Pipe Temperature	1373	K		
Inductive Coil Avg Temperature	325	K		
Emissivity of copper coil	0.75			
Emissivty of Mo-Re heat pipe	0.15			
Boltzmann Constant	5.67E-08			
Length Section under inductor	3	inches	0.0762	m
Heat Pipe Outside Diameter (OD)	0.625	inches	0.015875	m
Heat Pipe Area Under Inductor	5.8875	inches^2	0.00379838	m^2
Helium Thermal Conductivity	0.3	W/m-K		

Voltage Breakdown Relationship
V = 0.0162(P*D)2 + 5.3143(P*D) + 403.24
where P= pressure in torr and D= distance in cm
and D is 1/2 the difference in the heat pipe OD and the Inductor coil ID

Test Chamber Gas Pressure
76 torr

Gap Heat Pipe to Coil Gap inches	Gap Heat Pipe to Coil Gap m	Area Ratio Heat Pipe to Inductor ID	Effective Emissivity	Radiation Heat Transfer W	Conduction Heat Transfer W	Total Heat Transfer W	He-30%Ar Break Down Voltage V	He-5%Ar Break Down Voltage V	He Break Down Voltage V	Gap Heat Pipe to Coil Gap cm
0.025	0.00064	0.926	0.143	109.38	1954.91	2064.29	168.69	127.21	191.69	0.064
0.050	0.00127	0.862	0.144	109.71	1013.69	1123.40	207.30	153.14	229.13	0.127
0.075	0.00191	0.806	0.144	110.01	699.41	809.42	244.39	177.93	266.14	0.191
0.100	0.00254	0.758	0.145	110.27	541.91	652.18	280.01	201.63	302.72	0.254
0.125	0.00318	0.714	0.145	110.50	447.14	557.64	314.20	224.29	338.86	0.318
0.150	0.00381	0.676	0.145	110.70	383.76	494.47	347.00	245.95	374.57	0.381
0.175	0.00445	0.641	0.145	110.89	338.33	449.22	378.46	266.67	409.85	0.445
0.200	0.00508	0.610	0.146	111.06	304.13	415.19	408.64	286.49	444.69	0.508
0.225	0.00572	0.581	0.146	111.21	277.42	388.63	437.58	305.45	479.10	0.572
0.250	0.00635	0.556	0.146	111.35	255.96	367.31	465.31	323.60	513.08	0.635
0.275	0.00699	0.532	0.146	111.48	238.33	349.81	491.90	340.99	546.63	0.699
0.300	0.00762	0.510	0.146	111.60	223.57	335.17	517.39	357.67	579.74	0.762
0.325	0.00826	0.490	0.146	111.71	211.03	322.73	541.82	373.68	612.41	0.826
0.350	0.00889	0.472	0.147	111.81	200.22	312.03	565.24	389.07	644.66	0.889
0.375	0.00953	0.455	0.147	111.90	190.82	302.72	587.71	403.89	676.47	0.953
0.400	0.01016	0.439	0.147	111.99	182.55	294.54	609.25	418.18	707.85	1.016
0.425	0.01080	0.424	0.147	112.07	175.22	287.29	629.93	431.98	738.79	1.080
0.450	0.01143	0.410	0.147	112.14	168.67	280.81	649.79	445.36	769.31	1.143
0.475	0.01207	0.397	0.147	112.22	162.78	275.00	668.87	458.35	799.39	1.207
0.500	0.01270	0.385	0.147	112.28	157.46	269.74	687.23	471.00	829.03	1.270

Coil Loss Heating as a function of Distance
Loss (W) = 722.66*gap^2 + 3896.9*gap + 3725

Water Coolant DT	50	K
Water Coolant Cp	4180	J/kg-K
Water Density	989	kg/m3

$$\dot{m} = \frac{Q_{heating}}{C_p (T_{out} - T_{in})}$$

5 Inductive Coil Assemblies (1 Cluster)

Gap Heat Pipe to Coil Gap inches	Gap Heat Pipe to Coil Gap cm	Inductive Coil Loss (internal) Heating W	Coil Heating From Heat Pipe W	Total Coil Heat Load W	Total Water Coolant Flow Rate kg/sec	Total Water Coolant Flow Rate gpm	Percentage Coolant Flow Coil Internal gpm	Percentage Coolant Flow Heat Transfer gpm
0.025	0.064	3975.4	10321.4	14296.8	0.34	5.4	1.5	3.9
0.050	0.127	4231.6	5617.0	9848.6	0.24	3.7	1.6	2.1
0.075	0.191	4493.6	4047.1	8540.7	0.20	3.2	1.7	1.5
0.100	0.254	4761.4	3260.9	8022.3	0.19	3.0	1.8	1.2
0.125	0.318	5035.1	2788.2	7823.3	0.19	3.0	1.9	1.1
0.150	0.381	5314.6	2472.3	7787.0	0.19	2.9	2.0	0.9
0.175	0.445	5600.0	2246.1	7846.1	0.19	3.0	2.1	0.9
0.200	0.508	5891.1	2075.9	7967.1	0.19	3.0	2.2	0.8
0.225	0.572	6188.1	1943.2	8131.3	0.19	3.1	2.3	0.7
0.250	0.635	6490.9	1836.6	8327.5	0.20	3.2	2.5	0.7
0.275	0.699	6799.6	1749.0	8548.6	0.20	3.2	2.6	0.7
0.300	0.762	7114.0	1675.8	8789.9	0.21	3.3	2.7	0.6
0.325	0.826	7434.3	1613.7	9048.0	0.22	3.4	2.8	0.6
0.350	0.889	7760.5	1560.2	9320.6	0.22	3.5	2.9	0.6
0.375	0.953	8092.4	1513.6	9606.0	0.23	3.6	3.1	0.6
0.400	1.016	8430.2	1472.7	9902.9	0.24	3.7	3.2	0.6
0.425	1.080	8773.8	1436.4	10210.3	0.24	3.9	3.3	0.5
0.450	1.143	9123.3	1404.1	10527.3	0.25	4.0	3.5	0.5
0.475	1.207	9478.5	1375.0	10853.5	0.26	4.1	3.6	0.5
0.500	1.270	9839.6	1348.7	11188.3	0.27	4.2	3.7	0.5

APPENDIX G—MOLYBDENUM-RHENIUM AND SODIUM RESISTIVITY PROPERTIES

Resistivity data were used in assessing coupling between the RF inductive coils and the heat pipe envelope/internal sodium (table 18).[23] The only data readily available for the Mo-Re alloy are for Mo-50%-Re, shown in table 19.[24] This variation is expected to introduce minimal uncertainty since the alloy's electrical performance should be nearly identical to that of the Mo-44.5%-Re, which is used in the actual heat pipes. Electrical resistivity curves for Na and Mo-50%Re are shown in figure 37.

Table 18. Sodium resistivity.

Temperature (K)	Resistivity ($\mu\Omega$-cm)
373	10
473	13
523	14.8
573	16.5
623	18
873	27
1,073	34
1,273	41
1,473	48

Table 19. Mo-50%Re resistivity.

Temperature (K)	Resistivity ($\mu\Omega$-cm)
273	5
773	30
1,023	40
1,273	48
1,773	60

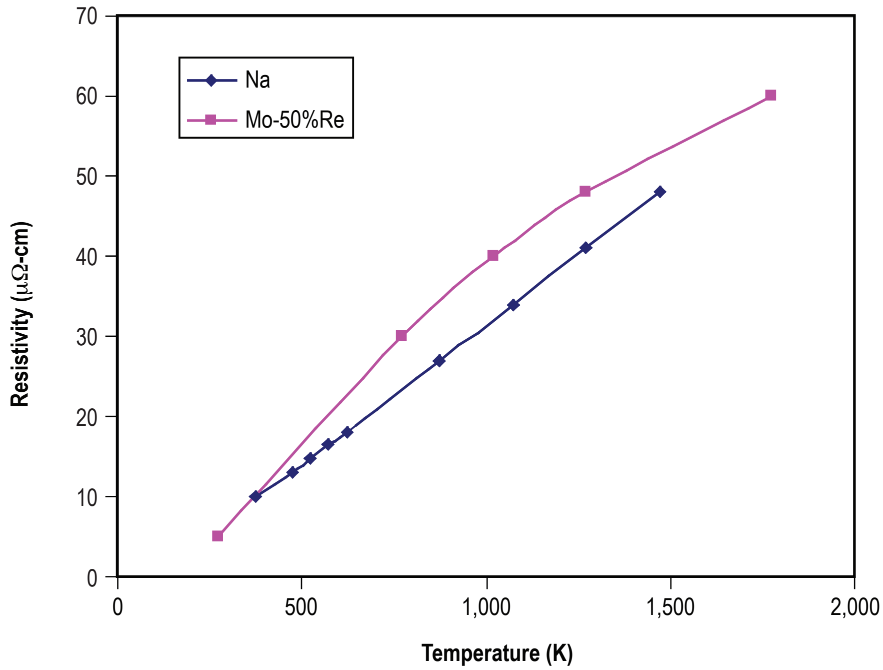

Figure 37. Electrical resistivity curves for Na and Mo-50%Re.

APPENDIX H—RADIO FREQUENCY INDUCTIVE COIL ONE-DIMENSIONAL SIMULATION RESULTS

Results generated using the ELTA software to produce one-dimensional results with the following input assumptions are shown in table 20:

Heat pipe temperature:	1,373 K
Heat pipe power condition:	3,000 W
RF coil/heat pipe heated length:	6.5 cm
Heat pipe outside diameter:	1.60 cm
Heat pipe inside diameter:	1.35 cm
Sodium layer thickness:	0.063 cm
RF inductive coil:	One turn over heat pipe evaporator.

These results assume no heat pipe thermal loss except for that to the RF coil (gap dependent) as given by:

For 3.2-mm gap:	560 W
For 6.4-mm gap:	370 W
For 9.6-mm gap:	300 W.

Table 20. Radio frequency inductive coil one-dimensional simulation results using one- and five-coil calculations.

			One-Coil Calculations (Does Not Include Busswork)				Five-Coil Calculations (Does Not Include Busswork)			
Frequency (Hz)	Gap (mm)	Electrical Efficiency (%)	Cal. Power (W)	Pipe Power (W)	Total Power (W)	Coil Voltage (V)	Cal. Power (W)	Pipe Power (W)	Total Power (W)	Coil Voltage (V)
3,000	3.2	44.3	3,000	3,557	8,029	2.3	15,000	17,785	40,147	12
10,000	3.2	74.7	3,000	3,557	4,762	2.5	15,000	17,785	23,809	13
20,000	3.2	78.7	3,000	3,557	4,520	3.1	15,000	17,785	22,598	16
30,000	3.2	77.9	3,000	3,557	4,566	3.9	15,000	17,785	22,831	20
50,000	3.2	75.9	3,000	3,557	4,686	5.6	15,000	17,785	23,432	28
100,000	3.2	73.9	3,000	3,557	4,813	9.5	15,000	17,785	24,066	48
500,000	3.2	75.6	3,000	3,557	4,705	27.8	15,000	17,785	23,525	139
3,000	6.4	37.4	3,000	3,367	9,003	3.6	15,000	16,835	45,013	18
10,000	6.4	68.7	3,000	3,367	4,901	4.2	15,000	16,835	24,505	21
20,000	6.4	73.0	3,000	3,367	4,612	5.7	15,000	16,835	23,062	29
30,000	6.4	72.1	3,000	3,367	4,670	7.5	15,000	16,835	23,350	38
50,000	6.4	69.8	3,000	3,367	4,824	11.3	15,000	16,835	24,119	57
100,000	6.4	67.5	3,000	3,367	4,988	19.5	15,000	16,835	24,941	98
500,000	6.4	69.3	3,000	3,367	4,859	60.5	15,000	16,835	24,293	303
3,000	9.6	31.9	3,000	3,302	10,351	5.3	15,000	16,510	51,755	27
10,000	9.6	63.2	3,000	3,302	5,225	6.3	15,000	16,510	26,123	32
20,000	9.6	67.8	3,000	3,302	4,870	8.9	15,000	16,510	24,351	45
30,000	9.6	67.0	3,000	3,302	4,928	12	15,000	16,510	24,642	60
50,000	9.6	64.1	3,000	3,302	5,151	18.4	15,000	16,510	25,757	92
100,000	9.6	61.5	3,000	3,302	5,369	32.3	15,000	16,510	26,846	162
500,000	9.6	63.5	3,000	3,302	5,200	101.2	15,000	16,510	26,000	506

APPENDIX I—RADIO FREQUENCY INDUCTIVE COIL TWO-DIMENSIONAL SIMULATION RESULTS

Results generated using the Flux 2D (marketed by CEDRAT Technologies) software to produce two-dimensional results with the following input assumptions are shown in table 21:

Heat pipe temperature:	1,373 K
Heat pipe power:	3,300 W
RF coil/tube length:	7.28 cm
Heat pipe outside diameter:	1.6 cm
Heat pipe inside diameter:	1.35 cm
Sodium layer thickness:	0.063 cm
RF inductive coil:	Three turn over heat pipe evaporator.

Table 21. Radio frequency inductive coil two-dimensional simulation results using one- and five-coil calculations.

One-Coil Calculations (Does Not Include Busswork)									
Frequency (Hz)	Gap (mm)	Boundary Type	Concentrator Type	Electrical Efficiency (%)	Calorimeter Losses (W)	Pipe Power (W)	Total Power (W)	Coil Current (A)	Coil Voltage (V)
50,000	6.4	Infinity	Fluxtrol 50	66.9	4.8	2,642	3,949	1,300	29.3
50,000	6.4	Infinity	None	65.5	41.9	2,044	3,122	1,300	25.2
50,000	6.4	Close	Fluxtrol 50	66.9	5	2,653	3,964	1,300	29.4
50,000	6.4	Close	None	65.7	45.2	2166	3,298	1,300	25.9
One-Coil Recalculated for 3,300-W Pipe Power (Does Not Include Busswork)									
Frequency (Hz)	Gap (mm)	Boundary Type	Concentrator Type	Electrical Efficiency (%)	Calorimeter Power (W)	Pipe Power (W)	Total Power (W)	Coil Current (A)	Coil Voltage (V)
50,000	6.4	Infinity	Fluxtrol 50	66.9	6.0	3,300	4,933	1,453	33
50,000	6.4	Infinity	None	65.5	67.6	3,300	5,040	1,652	32
50,000	6.4	Close	Fluxtrol 50	66.9	6.2	3,300	4,931	1,450	33
50,000	6.4	Close	None	65.7	68.9	3,300	5,025	1,605	32
Five-Coil Recalculated (Does Not Include Busswork)									
Frequency (Hz)	Gap (mm)	Boundary Type	Concentrator Type	Electrical Efficiency (%)	Calorimeter Power (W)	Pipe Power (W)	Total Power (W)	Coil Current (A)	Coil Voltage (V)
50,000	6.4	Infinity	Fluxtrol 50	66.9	30.0	16,500	24,663	1,453	164
50,000	6.4	Infinity	None	65.5	338.2	16,500	25,202	1,652	160
50,000	6.4	Close	Fluxtrol 50	66.9	31.1	16,500	24,654	1,450	164
50,000	6.4	Close	None	65.7	344.3	16,500	25,123	1,605	160

APPENDIX J—RADIO FREQUENCY INDUCTIVE COIL ASSEMBLY DESIGN AND FABRICATION WITH ASSOCIATED BUSSWORK SPECIFICATIONS

J.1 Integrated Financial Management Program Procurement

Description: Detailed design and precision manufacture of high-efficiency, long-life specialty RF inductive coil assemblies. These units should be ready for use and include feedthroughs and power feeds (busswork) to connect inductive coil assemblies to power supplies.

Material: Copper and other materials suitable for high-vacuum and low-pressure-purified inert atmosphere operation.

Items:

- 2×RF assemblies composed of five series inductor coils for equal power deposition.
- 1×RF assembly composed of five series inductor coils for variable power deposition with a ratio of 1, 2, and 4.
- 1×RF unit with a single inductor coil for constant power.
- Busswork to connect each RF assembly to an RF power supply.

Delivery: 12 to 16 wk ARO

Suppliers:

Vendor 1
Fluxtrol Manufacturing, Inc.
1388 Atlantic Boulevard
Auburn Boulevard
Auburn Hills, MI 48326–1572 USA
POC: Robert Goldstein
Tel: 248–393–2000

Vendor 2
Inductoheat, Inc.
32251 North Avis Drive
Madison Heights, MI 48071
POC: Michael R. Doerr
Tel: 724–327–5700

Vendor 3
Ajax-Tocco Inc.
1506 Industrial Blvd.
Boaz, AL 35957
POC: Houston Lee
Sales: 256–840–2339

Source: Full and open competitive (not planning on using a sole source); final selection shall be based on lowest cost technically acceptable.

J.2 Radio Frequency Induction Coil and Network Specifications

It is required that four RF inductive coil assemblies be designed and fabricated for long-duration (3 yr), continuous operation exposed to a high-temperature Mo-Re alloy tube (up to 1,400 K) in a vacuum or low-pressure-purified inert gas environment. The general pentagonal layout for three of the four assemblies was shown in figure 6. The fourth assembly is a single inductive coil. The vendor shall have sufficient RF inductive heating system design experience and two-dimensional electromagnetic modeling capabilities to thoroughly detail the performance of these assemblies for both nominal and off-nominal operations. Prior to initiating fabrication, the performance estimates and two-dimensional modeling (with assumptions) shall be provided to MSFC for review and approval. Once approved, the vendor may proceed with manufacturing and test evaluation of the RF coil assemblies. The vendor shall state relevant experience, capability, and manufacturing specifications/guidelines in their response.

(1) Geometry—The general layout of a single heated tube element with characteristic dimensions is provided in figure 38. These inductive coil elements shall be arranged to form the pentagonal configuration with a distance between centers ranging from 3 to 4 in. The design objective shall be to set gap and turn sizing to maximize coil to tube coupling efficiency while minimizing heat loss and the potential for voltage breakdown.

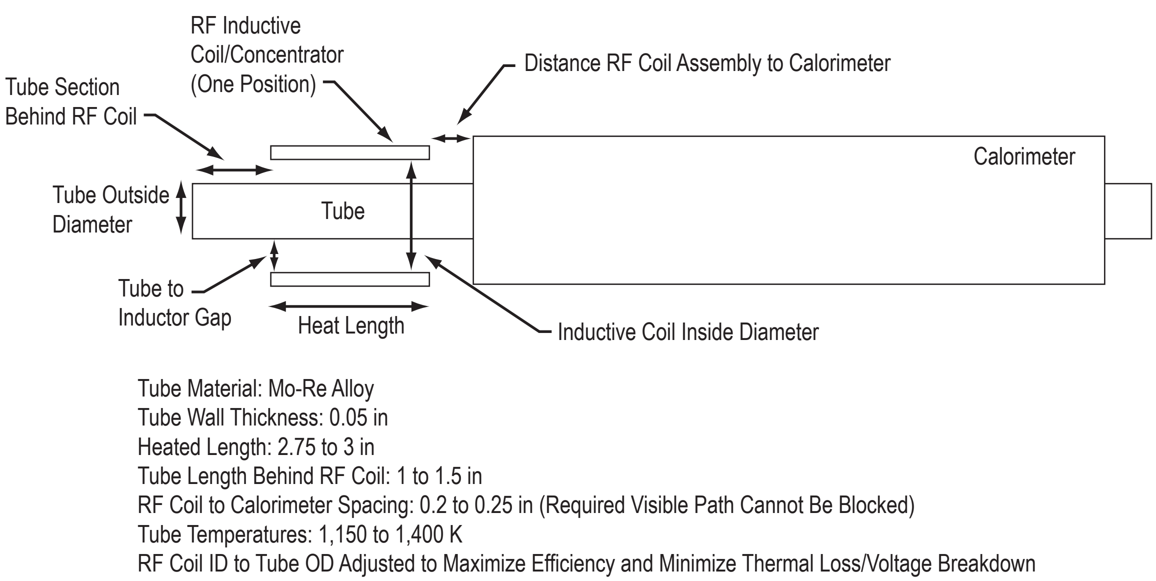

Figure 38. General dimensional layout of a single RF inductive coil position.

(2) Power—The RF inductive coil assemblies shall be designed to supply power in the manner specified in table 22 (refer to fig. 6). Radio frequency coil assemblies 1 and 2 have uniform power on all five elements in each series string. Radio frequency coil assembly 3 has three specified levels of power on the coils requiring a design assessment of the turn ratio. Radio frequency coil assembly 5 is a single inductive coil with no neighboring coils. During operation, the power variation between the coil assemblies (1 and 2) should be minimal and not exceed 10% regardless of the actual power being dissipated; i.e., if the combined series coil assembly is set at 12,500 or 20,000 W, the dissipation per coil is

Table 22. Required RF power induced in the part without thermal losses.

RF Coil Assembly	Position 1 (W)	Position 2 (W)	Position 3 (W)	Position 4 (W)	Position 5 (W)
1	3,000	3,000	3,000	3,000	3,000
2	3,000	3,000	3,000	3,000	3,000
3	1,000	2,000	2,000	4,000	4,000
4	5,000				

constant and one-fifth of the total. Likewise, for coil assembly 3, during operation, there should be minimal variation between like positions not exceeding 10%, and the power ratio should be maintained regardless of the actual power level the assembly is operated at.

(3) Open position performance—Periodically, it will be necessary to operate a cluster with 1, 2, 3, or 4 of its positions empty (no tube located inside to heat). The RF coil assemblies and distribution network should be designed such that the positions that are filled still maintain the required power levels with tolerance, as specified in (2) Power above.

(4) Busswork—All busswork and test chamber feedthroughs shall be designed and manufactured for maximum efficiency. The power supplies shall be located approximately 6 to 12 ft away from the test chambers.

(5) Efficiency—The RF inductive coil assemblies and busswork shall be designed to be as efficient as possible in coupling to the heated element and in making use of available power to satisfy the required applied power levels. The available frequency range for the RF power supplies for this application is zero to 50 kHz.

(6) Uniformity of heated region—Each RF coil shall provide a uniform and symmetric heated zone under its full length with variations in power along its length targeting 5% to 10%. That means there should be no power tilting from front to back of the inductive coil and that it should be symmetric about the full circumference of the heated tube element.

(7) Mutual inductance and interference—The RF inductive coils shall make use of flux concentrators to minimize “cross talk” with neighboring coils within the cluster and structural elements that will adversely affect the uniformity of the applied power to the surface of the heated part. Additionally, the design and use of flux concentrators shall reduce coupling to adjacent components, such as calorimeters, to minimize the heating to tens of watts or less. Any flux concentrators shall be assembled of materials that comply with the vacuum requirement, bake-out requirement, and cooling, as necessary.

(8) Materials and environment—The RF inductive coil assemblies shall be used in a test chamber with either a high vacuum or low-pressure-purified inert gas atmosphere. Contamination is a significant concern, therefore only materials suitable for high vacuum are acceptable. The manufacturing process must be orchestrated so as to eliminate the potential for trapped impurities or gas pockets that will continually outgas (create virtual leaks) during operation. Also, the final manufactured RF coil assemblies shall be capable of withstanding a thermal vacuum bake-out to a temperature of 150 to 250 °C.

(9) Thermal environment—The RF coil shall be capable of continuous operation exposed to a hot tube surface (1,400 K) with duration of operation estimated at 3 yr. The final design shall dictate the final gap width between the heated surface and the inner diameter of the inductive coil. This design shall place the coil as far from the heated surface as possible to minimize thermal losses yet sufficiently close to achieve acceptable inductive coupling.

(10) Applied voltage—The final operating voltage for the complete RF inductive coil assembly should not exceed one-half that of the Paschen breakdown voltage for the geometry—the product of the minimum distance between the coil and any ground in centimeters with the ambient pressure in torr. (See fig. 39.) This requirement is to prevent a potential discharge that could damage either the heated test specimen or the RF coil. The test atmosphere shall be inert He at an absolute pressure of 10 to 100 torr.

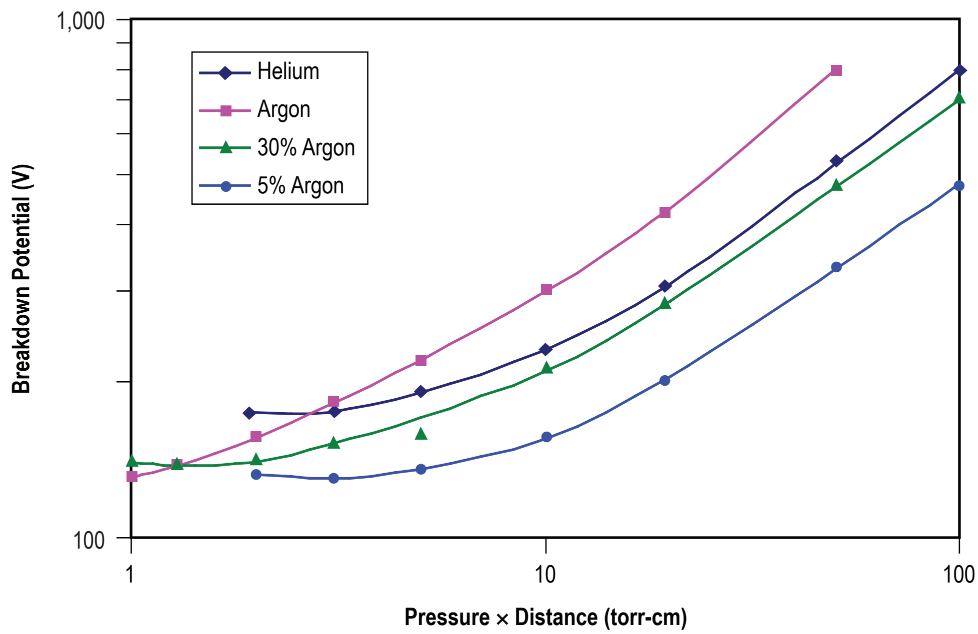

Figure 39. Direct current breakdown voltages in pure He, Ar, and mixtures (Paschen curves).

(11) Cooling—The RF inductive coil system and busswork shall make use of cooling water supplied at the RF power supply. (Water supply is not part of this procurement.) All mechanical connection on the RF power busswork and inductive coils must be made external to the test chamber. No leaks can be tolerated within the test chamber, therefore, all connections must be welded or brazed. The final assembly should be configured such that the temperature of the RF inductive coils should not exceed 350 K during normal operations.

(12) Leak checking—No leaks can be tolerated within the test chamber; therefore, all connections must be welded or brazed. These assemblies shall be checked with a He mass spectrometer leak detector with a sensitivity capable of detecting leaks rates of 1×10^{-10} std-cc/s of He or lower.

(13) Cleaning—During final assembly, all RF inductive coil components and busswork that is located within the test chambers shall be maintained in a clean environment so as to not trap contaminates within the structure/materials that will outgas or create virtual leaks. These assemblies shall be cleaned (to degrease) as necessary using PF solvent and pure ethyl alcohol rinses and wiped down with lint-free material. The parts should be cleaned and packaged appropriately to protect them from contamination and damage due to handling. If the vendor has procedures to be used during the assembly process, provide them to MSFC for review and approval.

(14) Final acceptance and packaging—Documentation shall be generated regarding the design performance with results of two-dimensional analysis, hardware layout, hookup, and operation and provided to MSFC for final review/acceptance. The complete RF inductive coil assemblies, test chamber feedthroughs, and the power supply to chamber busswork and sensors shall be packaged in a manner to prevent damage or contamination and shipped to MSFC.

APPENDIX K—GAS PURIFICATION SUBSYSTEM PROCUREMENTS

Table 23 provides a summary of the primary hardware needs for buildup of the gas mixing and purification system for the heat pipe life tests. Some hardware can presently be borrowed from other projects to allow rapid buildup of the system; however, due to the extent of the heat pipe life tests (continuous testing for 3 yr), borrowed components will need to be replaced. Therefore, specifications and quotes are currently being collected for all items in the gas purification system, even if an item is available inhouse for temporary use.

Table 23. General hardware for gas purification subsystems (large/small chambers).

Item	Model No.	Specifications	Quantity Needed
Monotorr phase II 3000 heated getter purifier for rare gases SAES Pure Gas, Inc.	PS4-MT3-R-1	Max flow rate: 50 slpm Operating temp: 400 °C Max pressure: 100 psig	2
Monotorr ambient temperature purifier for rare gases SAES Pure Gas, Inc.	PS11-MC200-R	Max flow rate: 50 slpm Nominal flow rate: 5 slpm Max pressure: 150 psig	2
Monotorr ambient temperature purifier for rare gases SAES Pure Gas, Inc.	PS11-MC500-R	Max flow rate: 100 slpm Nominal flow rate: 12 slpm Max pressure: 150 psig	1
Turbopump unit Varian Vacuum Inc.	V301 Navigator Part No. 9698829	300-L/min unit with built-in controller	1
Turbopump unit Varian Vacuum Inc.	V70LP Part No. 9698829	70-L/min unit with built-in controller	1
Rough pump unit Alcatel Vacuum Tech.	ACP 40 multistage scroll Part No. V4SACA	600-L/min unit with long life	2
Swagelock stainless bellows valve	SS-4H	Stainless steel, ¼-in tube fittings Max temp: 315 °C Max pressure: 1,000 psig	20
Swagelock stainless all weld bellows valve	SS-8BW	Stainless steel, ½-in tube fittings	20
Cyl-Tec, H-bottle*	Model 220, DOT spec./ rating 3AA-2015	Steel, rated to 2,015 psi, 9-in OD ×51-in length, 43.4 L water Contact: Paul O'Neill, 630–844–8800	2
Pressure gauge, dial	TBD	0–150 psig	3
Pressure gauge, dial	TBD	0–1,000 torr	3
Regulator for K-bottle	TBD	0–150 psi	3
Vacuum pressure relief valve	TBD	120 psig	6
Vacuum pressure relief valve	TBD	20 psia	8
Flow meter	Mass flow type	0–20 slpm	3
Gas pump Senior Aerospace Metal Bellows Division (possible use)	Manuf No.: MB601DC	Model MB-601 double containment, high-pressure pump, aluminum O-rings, ½-in female VCR connections, max pressure rating: 100 psi, max flow: 20 slpm, 110 VAC, 60-Hz motor	1
Gas pump diaphragm type	TBD	0–20 slpm operation at 10 to 760 torr	2

* Additional cleaning request will include an internal shot blast and treatment in 300 °F furnace. Cylinder will be valved immediately after treatment and shipped with a low-pressure gas fill.

APPENDIX L—WATER-COOLING SUBSYSTEM INSTRUMENTATION

Table 24 provides a summary of the general instrumentation requirements (various types) to monitor the facility coolant flow, the recirculation subsystem flow, and the calorimeter temperatures. This does not include instrumentation for the RF power supply recirculation cooling subsystem. That equipment will be provided separately with that subsystem when it is procured.

Table 24. General instrumentation options for water-cooling system.

Item	Model No.	Specification	Qty
Weber Sensor Inc. Programmable flow-captor inline flow and temperature meter	Type 4411.3	Flow repeatability: <1% of FS Flow accuracy: <3% of FS Fluid temperature range: –20 to 100 °C Temperature repeatability: 1% Temperature accuracy: ±1 K Connections: tube 0.47-in OD with 0.039-in wall Flow range: 0 to 4 gpm Material: 316 stainless steel	17
Sponsler Lo-Flo Precision turbine flow meter	MF150-CB-PH-A-4X-V	Repeatability: ±0.25% of reading Fluid temperature range: –267 to 204 °C Connections: ¾-in MNPT Flow range: 0.1 to 2 gpm Max pressure: 5,000 psig Material: 304 stainless steel Rotor: 17-4 PH stainless steel Bearings: Cryogenic ball (other options available) Includes 20-point NIST certification for water	17
Proteus Industries Flow (paddle wheel), temperature and pressure meter	04004SN2-TP	Fluid temperature range: –40 to 140 °C Connections: ¼-in FNPT Max pressure: 250 psi Output: User selected 0–5 VDC, 0–10 VDC, or 4–20 mA Flow range: 0.2 to 2.5 gpm Body: stainless steel Rotor: PPS O-ring: Silicone rubber Rotor shaft: 316 stainless steel Accuracy (flow, temp, & press): ±3% of FS (cal. points to ±1%) Linearity (flow, temp, & press): ±1% of FS Repeatability (flow, temp, & press): ±0.5% of FS	17
Omega Engineering Low flow turbine meter	FTB9511	Accuracy: ±½% of reading with linearization Repeatability: ±0.25% of reading Fluid temperature range: –268 to 232 °C Connections: ½-in MNPT std Flow range: 0.106 to 2.11 gpm Freq range: 40 to 1,050 Hz Max pressure: 5,000 psig Includes 20-point NIST certification for water	17

Table 24. General instrumentation options for water-cooling system (Continued).

Item	Model No.	Specification	Qty
Omega Engineering Economical ball bearing liquid turbine flow meter	FTB-905	Accuracy: ±½% of reading Repeatability: ±0.05% Body: 304 stainless steel Rotor: 17-4 pH SS Bearings: 440 °C stainless steel Fluid temperature range: –200 to 200 °C Connections: ¾-in MNPT std Linear range: 2.5 to 29 gpm Nominal K-factor: 1,035 pulses per gallon (43.125 to 500.25 Hz) Max pressure: 5,000 psi NIST certificate supplied	3
Sponsler Precision Turbine flow meter	SP(3/4-in)-CB-PHL-A-4X	Repeatability: ±0.5% Premium Repeatability: ±0.2% (over a specific range) Linearity: ±0.1% Premium linearity: ±0.2% (over a specific range) Fluid temperature range: –267 to 232 °C Connections: ¾-in MNPT Flow range: 2.5 to 29 gpm Max pressure: Accommodates unlimited pressure depending on the end fittings Material: 304 stainless steel Rotor: 17-4 PH stainless steel Bearings: Cryogenic ball (other options available) Includes 10-point NIST certification for water	3
Flow measurement remote indicator/totalizer (option to consider for signal conditioning)	IT400-DC-TRL-X	Operating temperature: –30 to 75 °C Input voltage: 48 VDC Signal input: Frequency: 0–3 kHz Amplitude: 50 mVmin Analog output: 4–20 mA Analog output accuracy: 0.025% F/S @ 20 °C Digitial output: RS-232 optional (RS_485 not avail.) Digital output accuracy: ±0.01% reading (rate) or ±1 count (total)	19
Moore Industries PC-programmable frequency-to-DC transmitter with display (option to consider for signal conditioning)	FDY/PRG/4-20MA/ 12-42DC/-CALIB [DN]	Operating temperature: –40 to 85 °C Input voltage: 12 to 42 VDC Signal input: Frequency: 0.005 Hz to 25 kHz Amplitude: 50 mVmin Accuracy: Typical accuracy is ±0.01% of reading with up to 5 yr between scheduled calibrations	19
Omega Engineering Signal conditioners for turbine flow meters	FLSC-61	Operating temperature: –40 to 85 °C Input voltage: 12–28 VDC, 50 mA MAX Signal input: Frequency: 0–10 kHz Amplitude: 50 mV–35 V Sine or square wave impedance: 10 kohms Analog output: 0 V @ 0 Hz, 5 or 10 V @ desired full-scale frequency Full-scale range: 75 Hz–10 kHz selectable Response time: 95% of change in 1 s Linearity: 0.3% F/S Tempco: <2% of reading over entire temperature range Minimum load resistance: 250 ohms	19

Table 24. General instrumentation options for water-cooling system (Continued).

Item	Model No.	Specification	Qty
Omega Engineering Miniature, quick-disconnect thermocouples Probes at calorimeter inlets	KMQSS-125G-6	Type: K Sheath diameter: 0.125 in Sheath material: 304 SS Connector body: Rated to 220 °C Junction type: Grounded Length: 6 in Mating connector, cable clamp, and locking clip included	4
Omega Engineering Miniature, high-temperature, quick-disconnect thermocouples Probes at calorimeter exit	SCASS-062G-6-SHX	Type: K Sheath diameter: 0.062 in Sheath material: 304 SS Connector body: Ceramic, rated to 650 °C Junction type: Grounded Length: 6 in Mating connector, cable clamp, and locking clip included	17

APPENDIX M—MASS AND VOLUMETRIC FLOW METERS FOR LOW-PRESSURE HELIUM/ARGON MIXTURES

M.1 Thermal Mass Flow-Type Meters

This thermal mass flow type of sensor has two elements—an RTD to measure the gas temperature and a heated element that maintains a constant temperature difference with respect to the flow temperature. As gas molecules remove heat from the heated element, power must be supplied to maintain a constant temperature difference. This power is directly proportional to the mass flow. The model 10A thermal flow meter from Fox Thermal Instruments can be factory calibrated for a specific gas or gas mixture. All calibrations are NIST traceable. The instrument can be factory configured to provide a 4- to 20-mA output that is proportional to either the mass flow or the internal thermal sensor's actual voltage reading. The gas in the gas circulation system will be a He/Ar mixture. However, the exact mixture ratio will not be known until testing begins. (It may need to be adjusted to achieve the required heat pipe thermal coupling.) Therefore, the meter cannot be calibrated ahead of time for the exact gas mixture. The test chambers will include an RGA from which the actual gas mixture ratio can be obtained in real time. To solve the problem, it is proposed that the instrument would be configured to provide a 4- to 20-mA output proportional to the thermal sensor's actual voltage reading, and have two calibrations performed—one for pure He and the other for pure Ar. The results are two calibration curves for converting voltage into mass flow as given by

$$\dot{m}_{\mathrm{He}} = f_{\mathrm{He}}(V_{\mathrm{He}}) \ , \tag{30}$$

and

$$\dot{m}_{\mathrm{Ar}} = f_{\mathrm{Ar}}(V_{\mathrm{Ar}}) \ , \tag{31}$$

where $\dot{m}_{\mathrm{He}}$ and $\dot{m}_{\mathrm{Ar}}$ are the mass flow rate, and V_{He} and V_{Ar} are the sensor voltage readings for He and Ar, respectively. Since the system will be operated at a pressure range of 50 to 100 torr, the two gas species will behave very much like ideal gases with virtually no interaction between them. Also, the thermal sensor's reading is proportional to the amount of heat taken away by gas molecules impinging on the sensor as the gas flows past it. Consequently, each gas's contribution to the sensor's voltage reading is independent of the other and can be written as

$$V = V_{\mathrm{He}} + V_{\mathrm{Ar}} \ , \tag{32}$$

where V_{He} and V_{Ar} are the contribution to the sensor's voltage reading (V) for He and Ar, respectively. A mass ratio can be expressed as

$$\frac{\dot{m}_{\mathrm{He}}}{\dot{m}_{\mathrm{Ar}}} = \frac{\chi_{\mathrm{He}} \cdot M_{\mathrm{He}}}{\chi_{\mathrm{Ar}} \cdot M_{\mathrm{Ar}}} \ , \tag{33}$$

where χ_{He} and χ_{Ar} are the mole fractions of He and Ar, respectively, and M_{He} and M_{Ar} are the molecular weights of He and Ar, respectively. The voltage (V) is obtained from the sensor reading, and χ_{He} and χ_{Ar} are obtained from the RGA. With these four equations and four unknowns, it is straightforward to calculate $\dot{m}_{He}$ and $\dot{m}_{Ar}$, with the total mass flow given by

$$\dot{m} = \dot{m}_{He} + \dot{m}_{Ar} \quad . \tag{34}$$

For a sanity check, the instrument could be calibrated for a 50/50 He/Ar mixture and a checkout test performed to compare calculated results with the calibration curve. The cost of each calibration was quoted as $500 by the vendor.

M.2 Laminar Volumetric-Type Flow Meters

The alternate flow meter option to consider is a laminar volumetric-type flow meter that measures volumetric flow by using an internal restriction to create a pressure drop where laminar flow is established along the restriction. For laminar flow, the relationship between flow and pressure drop is linear and is described by the Poiseuille equation:

$$Q = \frac{(P_1 - P_2)\pi \cdot r^4}{8\eta L} \quad , \tag{35}$$

where

Q = volumetric flow rate
P_1 = static pressure at the inlet
P_2 = static pressure at the outlet
r = radius of the restriction
η = dynamic viscosity of the fluid
L = length of the restriction.

With known geometry, pressure drop, and gas viscosity, the device is able to calculate the volumetric flow rate. The gas viscosity is dependent on pressure and temperature. For the ranges of these meters, the viscosity changes very little with pressure and no corrections for pressure variations are required. However, changes in temperature do significantly affect viscosity. Internally, these devices measure the temperature and correct for variations in the viscosity. As a result, these devices can also provide a pressure and temperature reading in addition to the flow rate. The mass flow rate can be calculated from this information.

To use the laminar flow meter, a calibration—similar to that for the mass flow meter—relevant to the gas system He/Ar mixture ratios will need to be assessed. However, if the volumetric flow meter's onboard signal processing provides signal outputs access for the internally measured pressure drop and temperature, this information along with the He/Ar mixture viscosity relationship can be use by the NI LabVIEW interface to construct the actual flow rate, without the need to calibrate the sensor for specific He/Ar mixtures.

APPENDIX N—TWO-BAND OPTICAL PYROMETER SPECIFICATIONS

Table 25 lists general specifications for two optical pyrometer units, available from manufacturers Mikron and Ircon.

Table 25. Optical pyrometer specifications.

	Mikron MI-SQ5	Ircon Modline 5R
Spectral region	0.70–1.15 µm; 0.97–1.15 µm	0.75–1.05 µm; 1–1.1 µm
Accuracy	<2,732 °F±0.5% of the measured value in °F±3.6 °F	0.5% of reading, plus 2 °C @ 25 °C
Response time	<10 ms, adjustable up to 10 s	10 ms, adjustable to 60 s
Resolution	<1 K	1 K
Temperature dependence	±0.25 K per K deviation of ambient temperature	Not listed
E-slope range	(ε_1/ ε_2): 0.800 ... 1.250	0.800–1.200
Repeatability	0.2% of the measured value in °F±3.6 °F	@ 25 °C 0.1% of full scale, plus 1 digit
Sighting	Through-the-lens or laser (optional)	Through-the-lens or laser (optional)
Analog output	4–20 mA or 0–20 mA	0–20 mA, 4–20 mA with 600 Ω max load (optional)
Digital interface	RS 232 or RS 485 addressable, half duplex, baud rate up to 38.4 kBd	RS-485 (user selectable, 57.6K max)
Power supply	24 VDC±25%, stabilized, ripple <50 mV	24 VDC±5%, 8 W max
Operating temperature	32...158 °F at housing	0 to 55 °C, 32 to 130 °F (without cooling)
Weight	19.4 oz	3.1 lb
Spot size @ 13 in	<0.25 in	<0.25 in

APPENDIX O—VACUUM GAUGING SPECIFICATIONS

Tables 26 and 27 provide manufacture details for vacuum measurement components suitable for use on the test chambers supporting bake-out, gas conditioning/loading, and normal test operations.

Table 26. Kurk J. Lesker multigauge box system with control boards.

Item	Model No.	Quantity
KJLC multigauge controller from Kurt J. Lesker	VL8350302	1
Capacitance manometers sensor board × 2	VL6491301	1
Convection gauges sensor board × 4	VL6496301	1
Cold cathode gauge sensor board (option 1) × 1	VL6433301	2

Table 27. Vacuum pressure sensors for the multigauge box.

Item	Model No.	Specifications	Quantity
MKS capacitance manomber	662A13TBD	Range: 1 to 1,000 torr Resolution: 1% of indicated decade Accuracy: ±0.15% Operating temperature: 0–50 °C Connection: 8 (½-in) VCR®-F	2
MKS convection pirani sensor tube	103170012	Range: 10^{-3} to 1,000 torr Resolution: 1% of indicated decade Operating temperature: 0–50 °C Connection: 8 (½-in) VCR®-F	2
MKS cold cathode sensor tube	104210005	Range: 10^{-11} to 10^{-2} torr Resolution: 1% of indicated decade, except 10% below 10^{-3} torr and above 100 torr Operating temperature: 0–50 °C Connection: 8 (½-in) VCR®-F	2

APPENDIX P—DISTRIBUTED FIELDPOINT INPUT/OUTPUT COMPONENT SPECIFICATIONS

Table 28 provides a listing of general electronic hardware components needed to make up the real-time control system. Some of the quantities are currently to be determined (TBD), depending on the final test chamber configuration and hardware selection for other subsystems.

Table 28. FieldPoint I/O components.

Item	Model No.	Quantity
Thermocouple module	FP-TC-120	7
Analog input module	FP-AI-110	TBD
Analog current output module	FP-AO-200	TBD
Analog voltage output module	FP-AO-210	TBD
Combination analog input/current output module	FP-AIO-600	TBD
Combination analog input/voltage output module	FP-AIO-610	TBD
Relay module	FP-RLY-420	TBD
Relay module	FP-RLY-422	TBD
Digital output module	FP-DO-401	TBD
General-purpose terminal base	FP-TB-1	TBD
Isothermal terminal base	FP-TB-3	7
Four-port ethernet device server for RS-485	ENET-485/4	1
Four-port ethernet device server for RS-232	ENET-232/4	1
Ethernet network interface for FieldPoint	FP-1601	1
Real-time controller	FP-2010	1

TBD=Quantity will depend on the final system configuration.

REFERENCES

1. Martin, J.J.; Reid, R.S.; and Bragg-Sitton, S.M.: "Design of Refractory Metal Life Test Heat Pipe and Calorimeter," *NASA/TP—2010–216435*, 2010.

2. "Standard Practice for Liquid Sodium Corrosion Testing of Metals and Alloys," ASTM G68-80, ASTM International, West Conshohocken, PA, 1980.

3. Deming, S.N.; and Morgan, S.L.: *Experimental Design*: *A Chemometric Approach*, Elsevier, New York, 1987.

4. ASME Boiler and Pressure Vessel Code, Section VIII, Division I, Section UG-28, American Society of Mechanical Engineers, 2001 Edition With 2003 Addenda.

5. Dortwegt, R.: "Low-Conductivity Water Systems for Accelerators," *Proceedings of PAC-2003*, Portland, OR, Vol. 1, pp. 630–634, 2003.

6. Pellegrino, L.: "Experience With Long Term Operation with Demineralized Water Systems at DA$_{\Phi}$NE," *Proceedings of EPAC 2004*, Lucerne, Switzerland, pp. 2080–2082, 2004.

7. ASTM International, "Standard Specification for Reagent Water," ASTM D1193-99$^{\varepsilon 1}$, February 10, 1999.

8. Dow Chemical Company, "Product Information, DOWTHERM 4000, Inhibited Ethylene Glycol-based Heat Transfer Fluid," <http://www.dow.com/heattrans>, November 2001.

9. Dow Chemical Company, "HVAC Overview Guide, DOWHERM, DOWFROST, and DOWCAL, Heat Transfer Fluids," <http://www.dow.com/heattrans>, May 1998.

10. Majumdar, A.K.; Bailey, J.W.; Schallhorn, P.A; and Steadman, T.E.: "Generalized Fluid System Simulation Program," United States Patent No. 6748349, 2004.

11. Verma, M.P.: "Steam Tables for Pure Water as an ActiveX Component in Visual Basic 6.0," *Computers & Geosciences*, Vol. 29, pp. 1155–1163, 2003.

12. Furukawa, M.: "Empirical Expressions Selected as a Common Basis of Heat-Transfer and Pressure-Drop Calculations," *Transactions of the Japan Society for Aeronautical and Space Sciences*, Vol. 36, No. 113, pp. 188–208, November 1993.

13. "Flow of Fluids Through Valves, Fittings and Pipe," Technical Paper No. 410, Crane Company, 1988.

14. Incropera, F.P.; and De Witt, D.P.: *Fundamentals of Heat and Mass Transfer,* 2nd Ed., John Wiley & Sons, 1985.

15. Weston, G.F.: “Glow-Discharge Characteristics of Helium-Argon Mixtures,” *British Journal of Applied Physics*, Vol. 11, pp. 305–306, July 1960.

16. Park, J.; Henins I.; Herrmann, H.; and Selwyn G.: “Gas Breakdown in an Atmospheric Pressure Radio-Frequency Capacitive Plasma Source,” *Journal of Applied Physics*, Vol. 89, No. 1, pp. 15–19, January 2001.

17. Loeb, L.B.: *Fundamental Processes of Electrical Discharges in Gases*, John Wiley and Sons, Inc., New York, 1939.

18. Goldstein, R.: “Radio Frequency Analysis Performed Using a General Concentric Tube/Inductor Layout,” Fluxtrol Inc., December 2004/January 2005.

19. Fox R.W.; and McDonald, A.T.: *Introduction to Fluid Mechanics*, 4th Ed., John Wiley & Sons, 1992.

20. Roth, A.: *Vacuum Technology*, 3rd Ed.—Updated and Enlarged, North-Holland, Elsevier, 1990.

21. Edwards, D.: “An Upper Bound to the Outgassing Rate of Metal Surfaces,” *Journal of Vacuum Science and Technology*, Vol. 14, p. 1030, 1977.

22. Odaka, K.; Ishikawa, Y.; and Furuse, M.: “Effect of Baking Temperature and Air Exposure on the Outgassing Rate of 316L Stainless Steel,” *Journal of Vacuum Science and Technology*, Vol. A 5(5), pp. 2902–2906, September 1987.

23. Foust, O.J.: *Sodium-NaK Engineering Handbook*, Gordon and Breach Science Publishing, Ltd., New York, 1980.

24. Advanced Technology in Refractory Metal and Custom Fabrication, <www.rembar.com>, January 2005.

REPORT DOCUMENTATION PAGE						Form Approved OMB No. 0704-0188

1. REPORT DATE *(DD-MM-YYYY)*
01–02–2011

2. REPORT TYPE
Technical Publication

3. DATES COVERED *(From - To)*

4. TITLE AND SUBTITLE
Design of Refractory Metal Heat Pipe Life Test Environment Chamber, Cooling System, and Radio Frequency Heating System

5a. CONTRACT NUMBER

5b. GRANT NUMBER

5c. PROGRAM ELEMENT NUMBER

6. AUTHOR(S)
J.J. Martin, S.M. Bragg-Sitton, R.S. Reid, E.T. Stewart, and J.D. Davis

5d. PROJECT NUMBER

5e. TASK NUMBER

5f. WORK UNIT NUMBER

7. PERFORMING ORGANIZATION NAME(S) AND ADDRESS(ES)
George C. Marshall Space Flight Center
Marshall Space Flight Center, AL 35812

8. PERFORMING ORGANIZATION REPORT NUMBER
M–1305

9. SPONSORING/MONITORING AGENCY NAME(S) AND ADDRESS(ES)
National Aeronautics and Space Administration
Washington, DC 20546–0001

10. SPONSORING/MONITOR'S ACRONYM(S)
NASA

11. SPONSORING/MONITORING REPORT NUMBER
NASA/TP—2011–216456

12. DISTRIBUTION/AVAILABILITY STATEMENT
Unclassified-Unlimited
Subject Category 20
Availability: NASA CASI (443–757–5802)

13. SUPPLEMENTARY NOTES
Prepared by the Propulsion Systems Department, Engineering Directorate

14. ABSTRACT
A series of 16 Mo-44.5%Re alloy/sodium heat pipes will be experimentally tested to examine heat pipe aging. To support this evaluation, an environmental test chamber and a number of auxiliary subsystems are required. These subsystems include radio frequency (RF) power supplies/inductive coils, recirculation water coolant loops, and chamber gas conditioning. The heat pipes will be grouped, based on like power and gas mixture requirements, into three clusters of five units each, configured in a pentagonal arrangement. The highest powered heat pipe will be tested separately. Test chamber atmospheric purity is targeted at <0.3 ppb oxygen at an approximate operating pressure of 76 torr (≈1.5 psia), maintained by active purification (oxygen level is comparable to a 10^{-6} torr environment). Treated water will be used in two independent cooling circuits to remove ≈85 kW. One circuit will service the RF hardware while the other will maintain the heat pipe calorimetry. Initial procedures for the startup and operation of support systems have been identified. Each of these subsystems is outfitted with a variety of instrumentation, integrated with distributed real-time controllers and computers. A local area network provides communication between all devices. This data and control network continuously monitors the health of the test hardware, providing warning indicators followed by automatic shutdown should potentially damaging conditions develop. During hardware construction, a number of checkout tests—many making use of stainless steel prototype heat pipes that are already fabricated—will be required to verify operation.

15. SUBJECT TERMS
alkali metals, sodium, heat pipes, refractory metals, molybdenum, rhenium, radio-frequency heating, fission power systems, life testing

16. SECURITY CLASSIFICATION OF: a. REPORT	b. ABSTRACT	c. THIS PAGE	17. LIMITATION OF ABSTRACT	18. NUMBER OF PAGES	19a. NAME OF RESPONSIBLE PERSON
U	U	U	UU	116	STI Help Desk at email: help@sti.nasa.gov
					19b. TELEPHONE NUMBER *(Include area code)* STI Help Desk at: 443–757–5802

Standard Form 298 (Rev. 8-98)
Prescribed by ANSI Std. Z39-18

National Aeronautics and
Space Administration
IS20
George C. Marshall Space Flight Center
Marshall Space Flight Center, Alabama
35812